# ASYMPTOTICS OF THE TURAEV-VIRO INVARIANTS AND q-HYPERBOLIC MANIFOLDS

Ву

Joseph M. Melby

## A DISSERTATION

Submitted to Michigan State University in partial fulfillment of the requirements for the degree of

Mathematics—Doctor of Philosophy

2023

#### ABSTRACT

We study asymptotic properties of the Turaev–Viro invariants and build on their conjectured connections to the geometry of 3-manifolds. Our focus is a conjecture of Chen and Yang [16] asserting that the exponential growth rate of the Turaev–Viro invariants coincides with the hyperbolic volume of the manifold.

We begin by studying the variation of the invariants of a manifold with toroidal boundary under the operation of attaching a (p,q)-torus knot cable space, establishing that the Chen–Yang conjecture is stable under this operation and generalizing results of Detcherry [21]. In doing so, we make heavy use of the SO(3)-Reshetikhin–Turaev TQFTs and their relationship to the Turaev–Viro invariants.

Next we introduce an infinite family of link complements, constructed from gluings of elementary hyperbolic manifolds inspired by work of Agol [4], satisfying the Chen-Yang volume conjecture. We show the asymptotics of the Turaev-Viro invariants of these manifolds are additive under the gluings of the elementary pieces, giving the first examples satisfying the conjecture which have an arbitrary number of hyperbolic pieces.

Lastly, we study a weak form of the Chen–Yang conjecture known as the Exponential Growth Conjecture, which asserts that the exponential growth rate of the Turaev–Viro invariants is positive. We construct the first infinite families of knots in  $S^3$  satisfying this conjecture using Dehn surgery methods. Detcherry and Kalfagianni [22] show the Exponential Growth Conjecture implies a conjecture of Andersen, Masbaum, and Ueno [5]. Using this, we construct an infinite family of mapping classes acting on surfaces of any genus and one boundary component satisfying the conjecture of [5] which correspond to fibered knots in  $S^3$ .

Copyright by JOSEPH M. MELBY 2023 Dedicated to Mike Melby

#### ACKNOWLEDGEMENTS

I would like to thank my advisor, Effie Kalfagianni, for her consistent guidance and support throughout my time at Michigan State. My growth as a mathematician is a reflection of her dedication to advising and support of future mathematical scientists.

I am grateful to Bob Bell, Matt Hedden, and Ben Schmidt for providing their insight, professional advice, and opportunities to learn throughout my graduate education. Additionally, thank you to Renaud Detcherry, Dave Futer, and Tian Yang for their comments, suggestions, and insight on some of the results presented in this work.

I would also like to thank my collaborators Sanjay Kumar, Hitesh Gakhar, and Jose Perea. It was wonderful learning, exploring, and writing with all of you. In addition, I appreciate all of the research, teaching, and career mentorship I have received from Chris Atkinson and Barry McQuarrie in Morris, as well as from Tsveta Sendova and Andy Krause here at MSU.

Moreover, I am incredibly thankful to my mom and Rita for their guidance and love, as well as the rest of my family and friends for their support throughout the past 6 years.

Finally, I would like to thank Tiffany for being my anchor and for her kindness and love.

The research contained here was partially supported by a Herbert T. Graham Scholarship through the Department of Mathematics at Michigan State University and the NSF grants DMS-1708249 and DMS-2004155.

## TABLE OF CONTENTS

CHAPTER 1 INTROD	OUCTION	1
1.1 Dissertation Org	ganization	4
	ro Invariant Volume Conjecture	4
	ions and Main Results of Chapter 3	7
	v	10
1.5 $q$ -hyperbolic Kn	nots in $S^3$ and Main Results of Chapter 5	11
CHAPTER 2 PRELIM	IINARIES	16
		16
		26
		$\frac{20}{30}$
		37
2.1 Quantum Repre	socionations of Mapping Class Groups	01
CHAPTER 3 TURAEV	V-VIRO INVARIANTS AND CABLING OPERATIONS	41
3.1 Introduction		41
3.2 The Witten–Rea	shetikhin–Turaev TQFTs and Cable Spaces	44
3.3 Bounding the Ir	nvariant Under Cabling	46
-		49
3.5 Further Direction	ons	64
CHAPTER 4 ASYMPT	TOTIC ADDITIVITY FOR AN INFINITE FAMILY	66
		66
		69
	·	73
	<u>-</u>	82
, <u> </u>	v	<i>ـ</i>
CHAPTER 5 $q$ -HYPEI	RBOLIC KNOTS IN $S^3$	94
5.1 Introduction		94
5.2 q-hyperbolic do	uble twist knots	97
		02
5.4 An application	to quantum representations	13
5.5 Low crossing kn	nots and low volume 3-manifolds	17
RIBLIOGR A PHV		23
DIDLIOGIMII III		ں ے
APPENDIX: FURTHER DI	ETAILS ON LINEAR OPERATORS OF CHAPTER 3 1	29

#### CHAPTER 1

#### INTRODUCTION

The field of quantum topology originated in the 1980s with work motivated by ideas from quantum physics, beginning with the discovery of the Jones polynomial [42, 43] of knots in  $S^3$  in 1984, establishing deep connections between physics, algebra, and low-dimensional topology. Soon after its introduction, Kauffman gave a formulation of the Jones polynomial in terms of combinatorial properties of knot and link diagrams [48].

This gave rise to the field of quantum topology and quantum invariants motivated similarly by quantum physics to the Jones polynomial. In the late 1980s, Witten [81, 82] gave an interpretation of the Jones polynomial in terms of path integrals, providing the first physical example of a family of (2+1)-dimensional Topological Quantum Field Theories (TQFTs) relating the Jones polynomial and Chern-Simons theory. These TQFTs were defined at a physical level of rigor, but an axiomatic interpretation of them was given by Atiyah [6] soon after their introduction. This family of TQFTs also provided a sequence of complex-valued invariants of closed 3-manifolds. Witten's work motivated predictions that quantum invariants related to the Jones polynomial have deep connections with the geometric properties of 3-manifolds.

In the years following Witten's work, Reshetikhin and Turaev [70] constructed a sequence of complex valued 3-manifold invariants with the same properties as those of Witten. Their approach, which was based on the representation theory of quantum groups, was the first mathematically rigorous construction of a (2 + 1)-dimensional TQFT consistent with the axiomatic framework of [6], and it is widely considered to be the mathematical formulation of Witten's theory. The work of Reshetikhin and Turaev in [70] also gave rise to a generalization of the Jones polynomial, known as the *colored Jones invariants*, which are a family of polynomial invariants of links in  $S^3$  parameterized by a positive integer n. The construction of Reshetikhin and Turaev's 3-manifold invariants begins with a surgery presentation for the manifold along a link in  $S^3$  [49], followed by an evaluation of the colored Jones polynomials

of the link at certain roots of unity. The resulting complex-valued invariants are known as the Witten–Reshetikhin–Turaev invariants.

While the constructions of Witten suggested connections between Jones-type invariants and the geometry of 3-manifolds, this connection is more difficult to establish from perspective of representations of quantum groups taken by Reshetikhin and Turaev. Nevertheless, interest in the relationship between the geometric properties, such as hyperbolic volume, and quantum invariants, such as the colored Jones invariants, of 3-manifolds became a central theme of quantum topology in the 1990s.

In 1997, Kashaev [45, 46] introduced an infinite family of complex-valued invariants of links in 3-manifolds defined using the quantum dilogarithm function and the combinatorics of a triangulation of the link complement. These invariants, like the colored Jones invariants, are parameterized by a positive integer  $n \in \mathbb{N}$ . Kashaev observed that the n-asymptotic growth of these invariants determined the hyperbolic volume of the complements of three knots in  $S^3$ :  $4_1, 5_2$ , and  $6_1$ , and conjectured in that this occurs for any hyperbolic knot [47]. In particular, Kashaev's conjecture asserted that for a hyperbolic link in  $S^3$ , the modulus of the invariants grows exponentially as  $n \to \infty$  with growth rate given by the hyperbolic volume of the link complement. Later, Murakami and Murakami built on the work of Kashev by showing that Kashaev's invariants coincide with evaluations of colored Jones polynomials at a certain root of unity [63]. This allowed them to reformulate Kashev's conjecture in terms of the colored Jones polynomials, as well as generalize it to all inks in  $S^3$  by considering the simplicial volume, an invariant of all link complements which is closely related to hyperbolic volume. This reformulated conjecture, known as the volume conjecture, is important to both knot theory and a more widespread framework of connections conjectured to exist between hyperbolic geometry and quantum invariants of 3-manifolds. Given the relationship between the colored Jones invariants and other quantum invariants discussed in this work, we state the conjecture here.

Conjecture 1.0.1. [47][63, Conjecture 5.1] For a link  $L \subset S^3$ , let  $J_n(L;q)$  be its n-th colored

Jones polynomial evalued at q. Then

$$\lim_{n \to \infty} \frac{2\pi}{n} \log |J_n(L; e^{\frac{2\pi\sqrt{-1}}{n}})| = v_{tet}||M_L||,$$

where  $M_L = \overline{S^3 \setminus n(L)}$  is the complement of L in  $S^3$ ,  $||\cdot||$  is the simplicial volume, and  $v_{tet} \approx 1.0149$  is the volume of a regular idea tetrahedron.

We refer the interested reader to the surveys of the volume conjecture given by Murakami [62] and Dimofte and Gukov [26] for further details on the historical context and development of this conjecture.

Analogous conjectures have been proposed which relate the growth rates of other quantum invariants to hyperbolic and simplicial volume. Two such families of quantum invariants which are studied throughout this work are the Reshetikhin–Turaev invariants, discussed briefly above, and the *Turaev-Viro invariants* [79]. These 3-manifold invariants, defined by Turaev and Viro using a triangulation of the manifold and certain building blocks from the representation theory of quantum groups studied by Kirillov and Reshetikhin in [50], turn out to coincide with the square of the modulus of the Reshetikhin–Turaev invariants [10, 71, 78]. This also establishes a deep connection between the Turaev–Viro invariants and the colored Jones invariants. Throughout this work, we will investigate a similar conjecture to Conjecture 1.0.1, which was originally stated by Chen and Yang [16], and asserts that the asymptotics of the Turaev–Viro invariants also capture hyperbolic data of a manifold. Details of this conjecture can be found in Section 1.2.

A portion of this work concerns another conjecture relating hyperbolic geometry and quantum invariants of 3-manifolds known as the Andersen-Masbaum-Ueno (AMU) conjecture [5]. The AMU conjecture asserts that the geometry of mapping tori associated to elements of surface mapping class groups, which are governed by the Nielsen-Thurston classification [27, Theorem 13.2] are detected by projective representations, known as quantum representations, arising from the Witten-Reshetikhin-Turaev TQFTs. We refer to Subsection 1.5.1 for the details, but briefly, the Nielsen-Thurston classification partitions the

mapping class group of a surface into finite and infinite-order elements, and the mapping tori associated to certain infinite-order mapping classes are known to be hyperbolic 3-manifolds. The AMU conjecture asserts that for these mapping classes, there is an associated quantum representation of infinite order.

Consideration of both the Turaev–Viro invariant volume conjecture and the AMU conjecture is a neural direction for this work since the former was shown to imply the latter by Detcherry and Kalfagianni [22].

## 1.1 Dissertation Organization

An introduction to the Turaev–Viro invariant volume conjecture is given in Section 1.2. We then summarize the main results of Chapters 3, 4, and 5 in Sections 1.3, 1.4, and 1.5, respectively. In addition, we discuss applications of the main results of Chapter 5 to the AMU conjecture in Subsection 1.5.1.

In Chapter 2, we present the necessary background underlying this work. This includes preliminaries on 3-manifolds, the Witten–Reshetikhin–Turaev invariants, the Turaev–Viro invariants, and quantum representations of mapping class groups. We investigate the behavior of the Turaev–Viro invariants under torus knot cabling operations on manifolds with torus boundary components in Chapter 3. Next, in Chapter 4, we introduce an infinite family of 3-manifolds satisfying Chen and Yang's Turaev–Viro invariant volume conjecture [16]. Finally, in Chapter 5, we introduce the first infinite families of knots and links in  $S^3$  satisfying a weaker version of the Chen–Yang conjecture.

## 1.2 The Turaev–Viro Invariant Volume Conjecture

In this section, we introduce the Turaev–Viro invariant volume conjecture.

Originally constructed in the early 1990s by Turaev and Viro [79], the Turaev–Viro invariants  $TV_r(M;q)$  of a compact 3-manifold M are a family of real-valued invariants parameterized by an integer  $r \geq 3$  and dependent on a 2r-th root of unity q. The precise definition of the r-th Turaev–Viro invariant is given in Section 2.3. Since their introduction, the Turaev–Viro invariants have been shown to be closely related to other quantum

invariants, including the Reshetikhin–Turaev and colored Jones invariants, and conjectured to recover geometric data in their r-asymptotics.

Chen and Yang [16] conjectured that the exponential growth rate of the Turaev–Viro invariants of hyperbolic 3-manifolds coincides with hyperbolic volume. They also provide extensive computational evidence for the conjecture for both closed and cusped hyperbolic manifolds in [16].

Conjecture 1.2.1 ([16], Conjecture 1.1). Let  $TV_r(M;q)$  be the r-th Turaev-Viro invariant of a hyperbolic 3-manifold M, and let vol(M) be the hyperbolic volume of M. For r running over odd integers and  $q = e^{\frac{2\pi\sqrt{-1}}{r}}$ ,

$$\lim_{r \to \infty} \frac{2\pi}{r} \log |TV_r(M;q)| = vol(M).$$

Detcherry and Kalfagianni [23] restated this conjecture in terms of the simplicial volume ||M|| of a manifold which is not necessarily hyperbolic. The simplicial volume of a 3-manifold M, roughly speaking, encodes the hyperbolic content of M. When M is hyperbolic, its hyperbolic and simplicial volumes are related by

$$vol(M) = v_{tet}||M||,$$

where  $v_{tet} \approx 1.0149$  is the volume of a regular ideal hyperbolic tetrahedron. We refer the reader to Section 2.1.2 for details on simplicial volume. This leads to a natural extension of Conjecture 1.2.1:

Conjecture 1.2.2 ([23], Conjecture 8.1). Let M be a compact orientable 3-manifold with empty or toroidal boundary. Then for  $q = e^{\frac{2\pi\sqrt{-1}}{r}}$ ,

$$LTV(M) := \limsup_{r \to \infty, \ r \ odd} \frac{2\pi}{r} \log |TV_r(M;q)| = v_{tet}||M||,$$

where  $v_{tet} \approx 1.0149$  is the volume of a regular ideal hyperbolic tetrahedron and  $||\cdot||$  is the simplicial volume.

Here the limit from Conjecture 1.2.1 is replaced by an upper limit since the Turaev–Viro invariants are known to vanish for certain manifolds. We will colloquially refer to both Conjectures 1.2.1 and 1.2.2 as the Turaev–Viro invariant volume conjecture since the manifolds in much of this work are not necessarily hyperbolic, so only the extended version of the conjecture applies. We also note that the full limit is obtained, rather than just the upper limit, in multiple results presented in this work.

These conjectures, which are similar in spirit to Conjecture 1.0.1, may be contrasted with conjectures associated to other roots of unity. Notably, Witten's Asymptotic Expansion Conjecture asserts that the asymptotics of the colored Jones invariants, and by extension the Turaev–Viro invariants, are bounded polynomially when evaluated at the root of unity  $q = e^{\frac{\pi \sqrt{-1}}{r}}$ .

Conjecture 1.2.2 has been verified for multiple examples and a few infinite families, though it remains wide open currently. These examples include the figure-eight knot and Borromean ring complements by Detcherry, Kalfagianni, and Yang [25], the Whitehead chains by Wong [84], the fundamental shadow links by Belletti, Detcherry, Kalfagianni, and Yang [9], a family of hyperbolic links in  $S^2 \times S^1$  by Belletti, and a large family of octahedral links in  $S^3$  by Kumar [51]. In addition, manifolds obtained by all but finitely-many Dehn-fillings on the figure-eight knot complement in  $S^3$  were shown to satisfy the conjecture by work of Ohtsuki [64] as well as Wong and Yang [87].

The results presented in this work add to the growing body of progress toward Conjectures 1.2.1 and 1.2.2.

#### 1.2.1 Asymptotic Additivity of the Turaev–Viro Invariants

An important property of a compact, irreducible, orientable 3-manifold is that it can be decomposed along tori into a unique collection of manifolds, known as its JSJ decomposition [40, 41]. Each of these manifolds are each either hyperbolic or Seifert fibered by Thurston's Geometrization Theorem [75], which was famously established rigorously by the work of Perelman [65, 66, 67]. We refer to Subsection 2.1.1 for further details of the JSJ

decomposition. For a 3-manifold M, the simplicial volume ||M|| coincides with the sum of the volumes of the hyperbolic pieces in this toroidal decomposition, and we naturally expect the asymptotics of the Turaev–Viro invariants to behave similarly due to Conjecture 1.2.2.

We say a manifold satisfies the asymptotic additivity property if the asymptotic growth rates of the Turaev-Viro invariants of its JSJ pieces are additive under the JSJ decomposition. This property is primarily concerned with the behavior of the Turaev-Viro invariants under gluing operations of 3-manifolds along surfaces such as tori, and it has been verified in a few cases. In particular, for a manifold M satisfying Conjecture 1.2.2, the asymptotic additivity property has been proven for the so-called invertible cablings of M by Detcherry and Kalfagianni [23] and (2n + 1, 2)-torus knot cablings of M by Detcherry [21]. Each of these results involve gluing a Seifert fibered manifold to M, which does not change simplicial volume. Additionally, the asymptotic additivity was verified by Wong for Whitehead chain cablings of the figure-eight knot, providing the first examples involving gluings of pairs of hyperbolic pieces.

The main results of Chapters 3 generalize the work of Detcherry [21] from (2n + 1, 2)torus knot cables of a manifold to establish the asymptotic additivity property to general (p,q)-torus knot cables of manifolds. In addition, the main results of Chapter 4 provide the first construction which glues several hyperbolic pieces to produce an infinite family of manifolds satisfying the asymptotic additivity property.

## 1.3 Cabling Operations and Main Results of Chapter 3

Here we summarize the main results of Chapter 3. We note that the results presented here are joint with Kumar and can be found in the preprint [53].

In Chapter 3, we study the behavior of the Turaev–Viro invariants under the gluing operation of attaching a (p,q)-torus knot cable space to a manifold with a nonempty torus boundary component. We call a manifold M' is obtained from M by attaching a cable space to one of its torus boundary components a (p,q)-cable of M. These cable spaces are Seifert fibered manifolds with two torus boundary components, so the cabling operation does not

increase the simplicial volume of the manifold, nor does it change the number of boundary tori of the manifold.

A natural question which arises is how the Turaev-Viro invariants change under the (p,q)cabling operation. Detcherry [21] first explored the variation of the Turaev-Viro invariants
under the (2n + 1, 2)-cabling operation, for  $n \in \mathbb{N}$ . He established that (2n + 1, 2)-cabling
changes the invariants by a factor which is at most polynomial in r, which means that the
exponential growth rate of the invariants is unchanged under (2n + 1, 2)-cabling and that
Conjecture 1.2.2 is stable under this cabling operation. This also provided some of the
earliest examples of the asymptotic additivity property discussed in Subsection 1.2.1.

The main result of Chapter 3 is the following, which generalizes Detcherry's result for (2n+1,2)-cablings [21, Theorem 1.5] to general (p,q)-cablings.

**Theorem 1.3.1.** Let M be a manifold with toroidal boundary, let p,q be coprime integers with q > 0, and let  $r \ge 3$  be an odd integer coprime to q. Suppose M' is a (p,q)-cable of M. Then there exists a constant C > 0 and natural number N such that

$$\frac{1}{Cr^N}TV_r(M) \le TV_r(M') \le Cr^NTV_r(M).$$

Theorem 1.3.1, analogously to Detcherry's bound in [21, Theorem 1.5], has applications to Conjecture 1.2.2. To the author's knowledge, in all of the proven examples of Conjecture 1.2.2, the stronger condition that the limit approaches the simplicial volume is verified, as opposed to only the limit superior. Notably, we have the following corollaries.

Corollary 1.3.2. Suppose for M we have

$$\lim_{r \to \infty, r \text{ odd}} \frac{2\pi}{r} \log |TV_r(M;q)| = v_{tet}||M||.$$

Then M satisfies Conjecture 1.2.2 and, for any p and q coprime, any (p,q)-cable M' also satisfies Conjecture 1.2.2.

Corollary 1.3.2 demonstrates a the stability of Conjecture 1.2.2 under general (p,q)cabling operations. Furthermore, in the case when  $q=2^n$  for  $n \in \mathbb{N}$ , we recover the full limit
automatically, as shown in the following corollary.

Corollary 1.3.3. Suppose M satisfies Conjecture 1.2.2. Then for any odd p and  $n \in \mathbb{N}$ , any  $(p, 2^n)$ -cable M' also satisfies Conjecture 1.2.2.

Corollaries 1.3.2 and 1.3.3 allow us to construct large families of manifolds satisfying Conjecture 1.2.2 from manifolds with torus boundary components for which Conjecture 1.2.2. These include an infinite family of manifolds constructed by Kumar and the author [52] introduced in Chapter 4.

The primary method we use to prove Theorem 1.3.1 follows the argument of Detcherry [21], which utilizes the relationship between the SO(3)-Reshetikhin–Turaev TQFTs and the Turaev–Viro invariants. We reserve the details for Chapter 3, but we briefly outline an important supporting result used to prove Theorem 1.3.1.

The SO(3)-Witten–Reshetikhin–Turaev TQFTs [11, 70] associate a linear operator on a finite-dimensional vector space to the (p,q)-torus knot cable spaces  $C_{p,q}$ , denoted  $RT_r(C_{p,q})$  for each odd integer  $r \geq 3$ . In [21], Detcherry proves that the linear operator  $RT_r(C_{2n+1,2})$  is nonsingular and that the operator norm of its inverse is bounded above polynomially in r. He then uses this bound in conjunction with the relationship between the Turaev–Viro and the Reshetikhin–turaev invariants to establish bounds on the Turaev–Viro invariants under cabling. We prove the analogous result for operators associated to general (p,q)-torus knot cable spaces.

**Theorem 1.3.4.** Let p be coprime to some positive integer q. Then  $RT_r(C_{p,q})$  is invertible if and only if r and q are coprime. Moreover, the operator norm  $|||RT_r(C_{p,q})^{-1}|||$  grows at most polynomially.

The argument for Theorem 1.3.4 is largely technical and comprises a majority of Chapter 3.

## 1.4 Asymptotic Addititvity and Main Results of Chapter 4

Here we introduce the main result of Chapter 4. The results presented here are included in joint work with Kumar published in the Journal of the London Mathematical Society [52].

The main theorem of Chapter 4 establishes the asymptotic additivity property for an infinite family  $\mathcal{M}$  of manifolds glued from several hyperbolic pieces. In particular, it implies that Conjecture 1.2.2 is preserved under gluings of toroidal boundary components for a family of 3-manifolds.

Our construction is inspired by a construction of Agol [4] of cusped 3-manifolds with well-understood geometric properties. Agol begins with an oriented  $S^1$ -bundle over a surface and systematically drills out curves to produce octahedral link complements. We refer to Section 4.2 for the details of Agol's construction. For our purposes, we focus on two hyperbolic manifolds which serve as elementary building blocks for the infite family  $\mathcal{M}$ .

We begin with a trivial  $S^1$ -bundle over the once-punctured torus  $\Sigma_{1,1}$  and use Agol's procedure to produce a hyperbolic link complement, which we call an S-piece, of volume  $2v_{oct}$ , where  $v_{oct} \approx 3.66$  is the volume of the regular ideal hyperbolic octahedron. Then we take a trivial  $S^1$ -bundle over the four-punctured sphere  $\Sigma_{0,4}$  and again use Agol's procedure to produce a hyperbolic link complement of volume  $4v_{oct}$  which we call an A-piece. Gluing k S-pieces and k k-pieces along their original torus boundary components produces a compact manifold  $M_L(k,l) \in \mathcal{M}$ , where k is the union of the link components of the k-and k-pieces.

The main result of Chapter 4 is the following.

**Theorem 1.4.1.** Let  $M_L(k,l) \in \mathcal{M}$ . Then for r running over odd integers and  $q = e^{\frac{2\pi\sqrt{-1}}{r}}$ ,

$$\lim_{r \to \infty} \frac{2\pi}{r} \log |TV_r(M_L(k, l); q)| = v_{tet} ||M_L(k, l)|| = 2(k + 2l)v_{oct}$$

where  $v_{\rm oct} \approx 3.66$  is the volume of the regular ideal hyperbolic octahedron.

Notably, Theorem 1.4.1 implies that the family  $\mathcal{M}$  satisfies the asymptotic additivity property as well as Conjecture 1.2.2. To the author's knowledge, this is also the first family of

manifolds satisfying the volume conjecture which may have an arbitrary number of hyperbolic pieces in their JSJ decomposition.

# 1.5 q-hyperbolic Knots in $S^3$ and Main Results of Chapter 5

Here we summarize the main results of Chapter 5. The results presented here are part of ongoing joint work with Kalfagianni and will be included in a forthcoming preprint.

As discussed above, the Turaev–Viro invariant volume conjecture holds for multiple particular examples, as well as a few infinite families with well-understood hyperbolic geometry [25, 64, 87, 86, 83, 51, 52, 53, 8, 9]. Despite this recent progress, Conjecture 1.2.2 is still wide open.

In Chapter 5, we consider the following weaker conjecture studied by Detcherry and Kalfagianni in [22, 23, 24], which asserts that the Turaev–Viro invariants of a manifold with hyperbolic JSJ pieces grow at least exponentially.

Conjecture 1.5.1. (Exponential Growth Conjecture) Let M be a compact orientable 3-manifold with empty or toroidal boundary. Then for  $q = e^{\frac{2\pi\sqrt{-1}}{r}}$ 

$$lTV(M) := \lim_{r \to \infty, r \text{ odd}} \inf_{r} \frac{2\pi}{r} \log |TV_r(M;q)| > 0$$

if and only if ||M|| > 0.

A manifold M with lTV(M) > 0 is called q-hyperbolic, and we will often refer to Conjecture 1.5.1 as the Exponential Growth Conjecture. The only hyperbolic knot complement in the 3-sphere for which the asymptotic behavior of the Turaev-Viro invariants has been explicitly understood is the figure-eight knot complement [25]. As discussed in Section 1.2, Conjecture 1.2.1 has been proved for all hyperbolic 3-manifolds that are obtained by Dehnfilling the figure eight knot complement in  $S^3$  [64, 87].

Chapter 5 is comprised of constructions of the first infinite families of q-hyperbolic knots in the 3-sphere. Our contructions combine the results of [64, 87] with a result of [23] about the behavior of the Turaev–Viro invariants under Dehn-filling, and with several Dehn surgery techniques. We refer to Section 2.1.3 for the details on Dehn-filling, surgery presentations

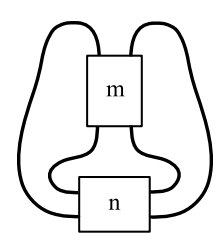


Figure 1.1 A double twist knot D(m, n) diagram with m vertical half-twists and n horizontal half-twists.

of manifolds, and Kirby calculus on surgery diagrams, which are important to many of the arguments of Chapter 5.

Briefly, a Dehn filling of the figure-eight knot complement, denoted  $M_{4_1}$ , is determined by a slope  $p/q \in \mathbb{Q}$ , where p, q are coprime, associated to the homological generators of the boundary torus of the knot complement. The result of Dehn-filling is a closed manifold, denoted  $M_{4_1}(p/q)$ . In general for a knot  $K \subset S^3$ , we denote its complement by  $M_K$ .

The families of knots corresponding to Dehn-fillings of  $M_{4_1}$  we consider in Chapter 5 belong to a family of knots known as the double twist knots. For  $m, n \in \mathbb{Z}$ , let the double twist knot D(m, n) with m vertical half-twists and n horizontal half-twists be as in Figure 1.1. For example, D(2, -2) is the figure-eight knot and D(2, 2) is the left-handed trefoil. The first main result of Chapter 5 is the following.

## **Theorem 1.5.2.** For any integer $n \neq 0, -1$ , the following are true:

- 1. The knots  $D_n := D(2n, -3)$  and  $D'_n := D(2n, -2)$  are q-hyperbolic.
- 2. The 3-manifolds  $M_n := M_{D_n}(4n+1)$  and  $M'_n := M_{D'_n}(1)$  are hyperbolic and q-hyperbolic.
- 3. We have

$$lTV(M_{D_n}) \ge vol(M_n), \quad and \quad lTV(M_{D'_n}) \ge vol(M'_n).$$

Using Theorem 1.5.2, we may conclude that many low-crossing knots are q-hyperbolic. We refer to Tables 5.1 and 5.2 in Section 5.5.

For the other families constructed in Chapter 5, we consider a type of slope known as a non-characterizing slope. This is a slope p/q for a knot  $K \subset S^3$  such that there is a knot K' that is not equivalent to K and such that  $M_K(p/q)$  is homeomorphic to  $M_{K'}(p/q)$ . In [2, 1, 3], the authors give constructions of knots that admit infinitely many non-characterizing slopes. Combining their techniques and results with Theorem 1.5.2, we are able to construct new infinite families of q-hyperbolic knots.

The first family is constructed from a particular knot,  $D_{-2} = D(-4, -3)$ , which is q-hyperbolic by Theorem 1.5.2 since  $M_{-2}(-7)$  is homeomorphic to  $M_{4_1}(-7/2)$ . Using Table 5.1 in Section 5.5, we see that  $D_{-2}$  is identified as the knot  $6_2$ . This knot admits a particular projection known as a good annulus presentation, defined in Section 3.3.1 of [1]. Knots admitting a good annulus presentation are shown in [1] to admit infinitely many non-characterizing slopes, so we apply these methods to produce such an infinite set for the knot  $6_2$  in the following theorem. See Section 5.3 for the details.

## **Theorem 1.5.3.** There is an an infinite set of knots K such that:

- 1. Every knot in K is q-hyperbolic.
- 2. For every  $K \in \mathcal{K}$ ,  $M_K(-7)$  is homeomorphic to  $M_{4_1}(-7/2)$  and it is q-hyperbolic.
- 3. No two knots in K are equivalent.

These techniques apply to any q-hyperbolic knot admitting a good annulus presentation, which allows use to state the following.

**Theorem 1.5.4.** Suppose that K is knot that admits a good annulus presentation and such that  $M_K(n)$  is q-hyperbolic for some  $n \in \mathbb{Z} \setminus \{0\}$ . Then there is an infinite family  $\{K_i\}_{i \in \mathbb{N}}$  of distinct q-hyperbolic knots, such that  $M_{K_i}(n) \cong M_K(n)$ , for any  $i \in \mathbb{N}$ .

The techniques of [1] also apply to the family of knots  $D'_n := D(2n, -2)$  to produce other families of q-hyperbolic knots in  $S^3$ . This is because they each admit a more general form

of knot projection known as an *annulus presentation*. However, in this case we don't know whether the resulting knots are necessarily distinct. This gives us the following result.

**Theorem 1.5.5.** For any |n| > 1, let  $D'_n := D(2n, -2)$ . There is a sequence of q-hyperbolic knots  $\{K_n^i\}_{i\in\mathbb{N}}$  such that for any  $i\in\mathbb{N}$  we have the following:

- 1. The knot  $K_n^i$  is q-hyperbolic.
- 2. The 3-manifold  $M_{K_n^i}(1)$  is homeomorphic to  $M_{D_n^i}(1)$  and it is q-hyperbolic.

## 1.5.1 Applications to the AMU Conjecture

Our results also have new applications to a conjecture of Andersen, Masbaum, and Ueno [5].

In order to state the conjecture, we will give a brief introduction to mapping class groups of surfaces and their associated quantum representations. For an oriented surface  $\Sigma_{g,n}$  of genus  $g \geq 0$  with  $n \geq 0$  boundary components, we denote its mapping class group, the group of orientation-preserving self-homeomorphisms of  $\Sigma_{g,n}$  which fix its boundary pointwise, by  $\operatorname{Mod}(\Sigma_{g,n})$ . The elements of  $\operatorname{Mod}(\Sigma_{g,n})$  are called mapping classes. Further details are given in Subsection 2.4.1.

There is a well-known classification of mapping class groups known as the Nielsen–Thurston classification [27, Theorem 13.2], which states that for any mapping class  $\phi \in \text{Mod}(\Sigma_{g,n})$ ,  $\phi$  is either *periodic*, meaning it has finite order, *pseudo-Anosov*, meaning it is irreducible and has infinite order, or it is *reducible*.

Now fix an odd integer  $r \geq 3$  called the *level*, and let  $I_r := \{0, 2, ..., r - 3\}$  be the set of non-negative even integers less than r - 2. For a 2r-th root of unity A and a coloring c of the boundary components of  $\Sigma_{g,n}$  by elements of  $I_r$ . The SO(3)-Reshetikhin–Turaev TQFTs [11, 70, 78] give rise to a projective representation

$$\rho_{r,c}: \operatorname{Mod}(\Sigma_{g,n}) \to \mathbb{P}\operatorname{Aut}(RT_r(\Sigma_{g,n})),$$

known as the SO(3)-quantum representation of  $Mod\Sigma_{g,n}$  at level r.

The AMU conjecture [5] asserts that the quantum representations detect the pseudo-Anosov mapping classes in their asymptotics.

Conjecture 1.5.6 (AMU Conjecture, [5]). Let  $\phi \in Mod(\Sigma_{g,n})$  be a pseudo-Anasov mapping class. Then for any big enough level r, there is a choice of coloring c of the components of  $\partial \Sigma_{g,n}$  such that  $\rho_{r,c}(\phi)$  has infinite order.

Conjecture 1.5.6 is closely related to conjectures stated earlier, namely the Exponential Growth conjecture (Conjecture 1.5.1) and the Turaev–Viro invariant Volume Conjecture (Conjecture 1.2.2). In particular, Detcherry and Kalfagianni [22] proved that if a mapping torus  $M_{\phi}$  with monodromy  $\phi$  is q-hyperbolic, then  $\phi$  satisfies the conclusion of the AMU conjecture.

We will see in Section 5.4 that the knots  $D_n = D(2n, -3)$  are fibered when  $n \leq -1$ . See Proposition 5.4.3 for the precise statement. In particular, for  $n \leq -1$  and g := -n, the knots  $D_n$  fiber over the surface  $\Sigma_{g,1}$  with monodromy  $\phi_g \in \operatorname{Mod}(\Sigma_{g,1})$ . We again refer to Section 5.4 for the precise definition of  $\phi_g$ . Since these knots  $D_n$  are q-hyperbolic, their monodromies  $\phi_g$  provide new examples of mapping classes satisfying Conjecture 1.5.6.

**Theorem 1.5.7.** For  $g \ge 1$ , the mapping classes  $\phi_g, \phi'_g \in Mod(\Sigma_{g,1})$  are pseudo-Anosov and they satisfy the AMU conjecture.

These are the first examples known to satisfy the AMU conjecture that are constructed as monodromies of fibered knots in  $S^3$ . The examples of [22] are coming from monodromies of fibered links of multiple components, while the examples [24] come from monodromies of fibered knots in closed q-hyperbolic 3-manifolds. In fact, the constructions presented here give rise to a framework for further examples to be discovered, as any fibered knot in  $S^3$  which can be shown to share a surgery with  $4_1$  has a monodromy satisfying the AMU conjecture.

#### CHAPTER 2

#### **PRELIMINARIES**

In this chapter, we will introduce the necessary background underlying the work presented in this dissertation. We begin with a discussion of 3-manifolds, their decompositions into elementary building blocks along surfaces, important geometric properties of 3-manifolds known as hyperbolic and simplicial volume, and the notion of surgery on a link in a 3-manifold in Section 2.1. We then define the Witten–Reshetikhin–Turaev invariants and the Witten–Reshetikhin–Turaev TQFTs 2.3. Finally, we discuss quantum representations of mapping class groups of surfaces in Section 2.4.

#### 2.1 Three-dimensional Manifolds

In this section, we will discuss 3-manifolds and some of their important characteristics. For further background on 3-manifolds, we refer the reader to [73, 35, 38]. We will focus on our attention on how 3-manifolds can be decomposed canonically along surfaces into elementary pieces. In this context, studying the geometry and topology of a 3-manifold involves studying properties of the elementary pieces that make up the manifold.

An n-manifold is an n-dimensional topological space  $X^n$  such that for any point  $x \in X^n$ , there is a neighborhood  $U \subset X^n$  of x which is homeomorphic to  $\mathbb{R}^n$ . We say that  $X^n$  is locally homeomorphic to  $\mathbb{R}^n$  in this case.

Restricting our attention to dimension 3, we say a 3-manifold M with boundary  $\partial M$  is compact if it is locally homeomorphic to  $\mathbb{R}^3$  in its interior and locally homeomorphic to the half space  $\{(x,y,z)\in\mathbb{R}^3|z\geq 0\}$  on its boundary. If  $\partial M=\emptyset$ , we say M is closed.

Every compact 3-manifold M has a double covering space called the orientable double cover. This double cover is connected if and only if M is non-orientable. We say a 3-manifold M is irreducible if every two-sphere  $S^2 \subset M$  bounds a three-ball  $B^3 \subset M$ . The connected sum of two 3-manifolds  $M_1$  and  $M_2$ , denoted  $M = M_1 \# M_2$ , is the 3-manifold constructed by removing a three-ball  $B^3$  from each of  $M_1$  and  $M_2$  and gluing the resulting pair of compact manifolds (with boundary  $S^2$ ) along their boundary components. Note that  $M \# S^3 = M$ .

We call a 3-manifold *prime* if  $M = M_1 \# M_2$  implies that either  $M_1 = S^3$  or  $M_2 = S^3$ . Throughout this work, we will be primarily concerned with compact irreducible 3-manifolds.

A link L with k components in a 3-manifold M is the image of an embedding  $\bigsqcup_{i=1}^k S^1 \hookrightarrow M$ , and we call a link with a single component a knot. Given a link  $L \subset M$ , we can consider the link complement

$$M_L := \overline{M \setminus n(L)},$$

where n(L) is a neighborhood of L in M. This is a compact 3-manifold bounded by a disjoint union of tori corresponding to each of the link components.

#### 2.1.1 Decompositions

Here we discuss how compact 3-manifolds can be decomposed into elementary pieces: the prime decomposition, and the JSJ decomposition. We refer the reader to [35, 38] for detailed accounts of these decompositions.

Let M be a 3-manifold,  $S \subset M$  be a properly embedded surface, and n(S) be an open tubular neighborhood of S in M. We do not assume S is connected and note that n(S) is an I-bundle over S that is trivial if and only if S is orientable. Define the 3-manifold obtained by splitting M along S by  $M|S:=M\setminus n(S)$ . The following prime decomposition of Kneser is one of the earliest general results on 3-manifolds.

**Theorem 2.1.1.** Let M be a compact, connected, orientable 3-manifold. Then there is a decomposition  $M = M_1 \# \cdots \# M_n$ , where each  $M_i$  is prime. Moreover, this decomposition is unique up to the connect sums of copies of  $S^3$ .

Kneser [39] established the existence of such a decomposition in 1928, and uniqueness was formally completed by Milnor in 1962 [59]. This decomposition along spheres into prime 3-manifolds is related to classifying compact orientable 3-manifolds in terms of irreducible ones, due to the following fact.

**Proposition 2.1.2.** The only orientable prime 3-manifold which is not irreducible is  $S^2 \times S^1$ .

Later, in the 1970s, a canonical decomposition of orientable compact irreducible 3-manifolds along embedded tori was introduced independently by Johannson [41] and Jaco-Shalen [40].

Let M be a compact 3-manifold. We say a properly embedded surface  $S \subset M$  is 2-sided if its normal I-bundle is trivial and 1-sided if its normal I-bundle is nontrivial.

**Definition 2.1.3.** A 2-sided surface S which contains no  $S^2$  or  $D^2$  components is *incompressible* if for each disk  $D \subset M$  satisfying  $D \cap S = \partial D$ , there is another disk  $D' \subset S$  with  $\partial D' = \partial D$ .

If no such disk  $D' \subset S$  exists, we refer to such a  $D \subset M$  as a compressing disk for S. The following is an important characterization of incompressibility for surfaces in 3-manifolds.

**Proposition 2.1.4.** A connected surface  $S \subset M$  is incompressible if and only if the inclusion map induces an injective homomorphism  $\pi_1(S) \to \pi_1(M)$ .

This leads to the following proposition, which characterizes incompressible tori in an irreducible 3-manifold.

**Proposition 2.1.5.** An embedded torus T in an irreducible 3-manifold M is compressible if and only if T is contained in a 3-ball in M or T bounds a solid torus.

A properly embedded surface  $S \subset M$  is  $\partial$ -parallel if it is isotopic to a subsurface of  $\partial M$ , and we say an irreducible 3-manifold M is atoroidal if every embedded torus in M is  $\partial$ -parallel.

The torus decomposition was introduced by Johannson [41] and Jaco-Shalen [40]. We refer to Hatcher's notes on 3-manifolds [35] for a proof of the following theorem.

**Theorem 2.1.6.** [41, 40] Let M be a compact irreducible 3-manifold. There exists a finite collection of disjoint incompressible tori  $T = T_1 \sqcup \cdots \sqcup T_n$  such that each component of M|T is either atoroidal or Seifert fibered. Moverover, there is a minimal such collection T which is unique up to isotopy.

This decomposition, known as the JSJ decomposition, is related to Thurston's Geometrization Conjecture [75], which asserts that compact irreducible manifolds can be decomposed into pieces which are either Seifert fibered or support a finite volume hyperbolic structure. Thurston established the conjecture for manifolds containing a 2-sided incompressible surface in [75], and the proof was famously completed following the work of Perelman [65, 66, 67]. Further detail on the Geometrization Conjecture can be found in Chapter 12 of Martelli's book [58].

## 2.1.2 Simplicial and Hyperbolic Volume

Here we introduce the simplicial volume, originally defined by Gromov [34], and its relationship to hyperbolic structures on 3-manifolds.

Gromov [34] originally defined simplicial volume as a homological invariant for manifolds of any dimension n, but we restrict our attention to orientable 3-manifolds. Details can be found in Section 6 of [74], though we provide relevant definitions and topological properties here.

**Definition 2.1.7.** [34, 74] Let M be a compact orientable 3-manifold with empty or toroidal boundary and let  $[M, \partial M] \in H_3(M, \partial M, \mathbb{R})$  be the fundamental class in singular relative homology. Consider a relative singular 3-cycle  $z = \sum c_i \sigma_i \in Z_3(M, \partial M, \mathbb{R})$  representing the fundamental class. Define its norm by  $||z|| = \sum |c_i| \in \mathbb{R}$ . The simplicial volume ||M|| is defined as follows.

(1) If  $\partial M = \emptyset$ , then

$$||M|| = \inf\{||z|| \mid [z] = [M]\}$$

.

(2) if  $\partial M \neq \emptyset$ , then  $[z] \in H_3(M, \partial M, \mathbb{R})$  determines a representative  $\partial z$  of the class  $[\partial M] \in H_2(\partial M, \mathbb{R})$ . Define

$$||M|| = \liminf_{\alpha \to 0} \bigg\{ ||z|| \ \bigg| \ [z] = [M, \partial M] \text{ and } ||\partial z|| \leq \alpha \bigg\}.$$

This limit is shown to exist in Section 6.5 of [75], so ||M|| is well-defined.

Remark 2.1.8. Simplicial volume is related to the *Gromov norm* in the literature. Throughout this dissertation, we take simplicial volume to be equivalent to the Gromov norm, but we note that some sources (see [30], for example) differentiate Gromov's original invariant from simplicial volume by a fixed proportionality constant. This distinction does knot change any of the results or arguments that follow.

Simplicial volume also encodes some of the hyperbolic content of a manifold through the pieces in its JSJ decomposition. This is realized by the relationship between simplicial and hyperbolic volume of 3-manifolds.

Let M be a compact irreducible 3-manifold and  $T \subset M$  be the collection of tori realizing its minimal JSJ decomposition. By Theorem 2.1.6 and Thurston's Geometrization Theorem, each component of M|T is either

- a Seifert manifold which does not support a finite volume hyperbolic structure, or
- a manifold whose interior admits a unique finite volume hyperbolic structure.

The volume of a hyperbolic 3-manifold M, denoted vol(M), is a topological invariant of M by Mostow-Prasad rigidity [61, 68], and Corollary 6.6.2 in Thurston's notes [74] implies that there are at most finitely many isometry classes of hyperbolic 3-manifolds of a given volume.

For example, the smallest volume closed orientable hyperbolic 3-manifold, known as the Weeks manifold, has volume approximately 0.9427, and the smallest volume cusped orientable hyperbolic 3-manifold, the figure-eight knot complement in  $S^3$ , has volume approximately 2.0299. Throughout this work, we denote the volume of the regular ideal hyperbolic tetrahedron by  $v_{tet} \approx 1.0149$  and the volume of the regular ideal hyperbolic octahedron by  $v_8 \approx 3.6638$ .

For more general manifolds with JSJ decompositions containing Seifert fibered pieces, the simplicial volume corresponds to the sum of the volumes of the hyperbolic pieces in the JSJ

decomposition. This means Seifert manifolds have simplicial volume zero while manifolds with hyperbolic JSJ components have positive simplicial volume. Simplicial volume also behaves well with respect to some topological operations.

**Theorem 2.1.9.** ([34, 74]) Let M be a compact orientable 3-manifold. The following are true:

- (1) ||M|| is additive under disjoint union and connected sums,
- (2) If M has a self-map of degree d > 1, then ||M|| = 0. In particular, the simplicial volume of a trivial circle bundle over a compact orientable surface vanishes.
- (3) If  $T \subset M$  is an embedded torus and M' is obtained from M by cutting along T, then

$$||M|| \le ||M'||,$$

with equality if T is incompressible in M.

(4) If M is obtained from M' by Dehn-filling along a torus boundary component of M', then

$$||M|| \le ||M'||.$$

(5) If M has a complete finite-volume hyperbolic structure, then

$$vol(M) = v_{tet}||M||.$$

(6) Let  $H_M$  denote the union if the hyperbolic components in the JSJ decomposition of M.

Then

$$vol(H_M) = v_{tet}||M||,$$

where  $vol(H_M)$  denotes the total volume of  $H_M$ .

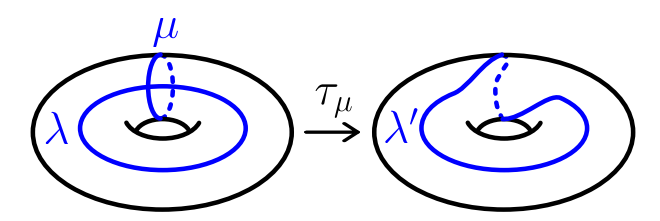


Figure 2.1 Dehn twist  $\tau_{\mu}$  along the meridian  $\mu$  of a torus.

## 2.1.3 Surgery Presentations

In this subsection, we discuss a method for encoding 3-manifolds using framed knots and links in  $S^3$ . These representations will aid in defining various quantum invariants in Section 2.2. We begin by defining certain homeomorphisms of surfaces.

Let  $\Sigma$  be a closed oriented surface. We will define the simplest example of an orientation-preserving homeomorphism of  $\Sigma$  which is not isotopic to the indentity map. Let  $\gamma \subset \Sigma$  be a non-separating simple closed curve, and let  $\gamma_1$  and  $\gamma_2$  be the two copies obtained by cutting  $\Sigma$  along  $\gamma$ . Fix  $\gamma_1$  and apply a full rotation by  $2\pi$  to  $\gamma_2$ . Now since each point on  $\gamma_2$  is in its original position, we may glue  $\gamma_1$  and  $\gamma_2$  back together via the identity map. This operation corresponds to a nontrivial self-homeomorphism of  $\Sigma$  called a *Dehn twist* along  $\gamma$ , denoted  $\gamma_2$ . For example, Figure 2.1 shows a Dehn twist along the meridian of a torus.

Dehn twists are particularly important to the classification of self-homeomorphisms of oriented surfaces, as evidenced by the following theorem.

**Theorem 2.1.10** (Dehn–Lickorish Theorem). Let  $\Sigma_g$  be a closed oriented surface of genus  $g \geq 0$ . Every orientation-preserving self-homeomorphism of  $\Sigma_g$  can be presented as a composition of Dehn twists and homeomorphisms isotopic to the identity.

Theorem 2.1.10 was originally established by Dehn, and Lickorish [54] later gave a simpler proof and an explicit set of generating curves along which the Dehn twists can be defined. Isotopy classes of self-homeomorphisms of surfaces actually form a group, but we will discuss the details of this group later in Section 2.4. For our purposes, we just note that the Dehn twist along a curve has an inverse, which we call the negative Dehn twist  $\tau_{\gamma}^{-1}$ .

This Dehn-Lickorish Theorem has important implications in the context of 3- and 4-

manifolds. In order to state these results, we start with a way to represent 3-manifolds using knots and links.

Consider the unknot  $U \subset S^3$ . Its neighborhood n(U) is a solid torus with  $\partial n(U) = T^2$ . As disussed in the beginning of this section, the complement of any knot in  $S^3$  is a compact 3-manifold with a single torus boundary component. In the case of the unknot U,  $M_U$  is homeomorphic to the solid tous. Rather than considering the complement obtained by removing n(U) from  $S^3$ , we may glue the solid torus back into along some homeomorphism of its boundary  $T^2$ . This operation, called *Dehn surgery*, results in a closed manifold which is determined by the choice of homeomorphism of  $T^2$ .

For example, consider the self-homeomorphism  $\tau_{\mu}: T^2 \to T^2$  corresonding to the Dehn twist along the meridian  $\mu$  of  $\partial n(U) = T^2$ . The associated Dehn surgery is performed by removing the solid torus  $n(U) = S^1 \times D^2$  and replacing it with a copy of  $D^2 \times S^1$ . It is encoded by labeling the knot diagram U with surgery coefficient 1, and is called the 1-surgery on U. The resulting closed manifold is denoted  $M_U(1)$ . Similarly, the manifold obtained by Dehn surgery with the negative Dehn twist along the meridian corresponds to a -1-surgery on U and is denoted  $M_U(-1)$ . In this case,  $M_U(\pm 1)$  is homeomorphic to  $S^3$ , but we will see below that this is a special case.

In general, we can perform Dehn surgery on any n-component framed link  $L \subset S^3$ . Since the link complement  $M_L$  has boundary  $\partial M_L = \bigsqcup_{i=1}^n T^2$ , the surgery involves removing a solid torus neighborhood of each component and gluing it back in via a specified homeomorphism on each torus.

In particular, let  $\mu$  and  $\lambda$  be the meridian and longitude of  $T^2$ , respectively. Consider the simple closed curve  $J_{p,q} := p\mu + q\lambda$  that wraps around the meridian p times and longitude q times. It is known that the isotopy classes of homeomorphisms of  $T^2$  correspond to the rational number r = p/q when p and q are coprime. In particular, each homeomorphism  $f: T^2 \to T^2$  is isotopic to a map of the form  $\mu \mapsto p\mu + q\lambda$ . This means that Dehn surgery on a link  $L \subset S^3$  is determined by specifying a set of rational surgery coefficients

 $\{r_1,\ldots,r_n\}$  corresponding to the torus components of  $\partial M_L$ . Performing Dehn surgery on  $L\subset S^3$  produces another closed 3-manifold, denoted  $M_L(r_1,\ldots,r_n)$ .

Remark 2.1.11. We note that the  $r = p/q = 1/0 = \infty$  surgery is allowed; this surgery corresponds to the identity map on  $T^2$  sending the meridian to itself, so it does not change the manifold. The surgery coefficient r = 0/1 = 0 corresponds to a *torus switch*, which interchanges the meridian and longitude.

**Example 2.1.12.** Let  $U \subset S^3$  be the unknot and  $M_U$  be its complement. The following manifolds  $M_U(r)$  are examples of r = p/q surgeries on U.

- (1)  $M_U(0)$  is homeomorphic to  $S^1 \times S^2$ .
- (2)  $M_U(p/q)$  is homeomorphic to the lens space L(p,q).
- (3)  $M_U(\pm 1/n)$  is homeomorphic to  $S^3$
- (4)  $M_K(1/0)$  is homeomorphic to  $S^3$  for any knot  $K \subset S^3$ .
- (5) If  $L = L_1 \sqcup L_2$  such that  $L_1$  and  $L_2$  are unlinked, then  $M_L(r_1, r_2)$  is homeomorphic to the connect sum  $M_{L_1}(r_1) \# M_{L_2}(r_2)$ .

The following result is due independently to Lickorish [54] and Wallace [80] and is a corollary of Theorem 2.1.10.

**Theorem 2.1.13** ([54, 80]). Any closed orientable 3-manifold can be obtained by performing Dehn surgery on a framed link in  $L \subset S^3$  with surgery coefficients  $\pm 1$  on each component. Moreover, each component of L can be assumed to be unknotted.

Theorem 2.1.13 allows us to present any 3-manifold M as a framed link in  $S^3$ . We call this a surgery presentation of M. Surgery presentations are not unique; there is no unique way of expressing a homeomorphism as a product of Dehn twists. A large volume of work in low-dimensional topology is focused on the understanding the relationship between the surgery presentations of a given manifold.

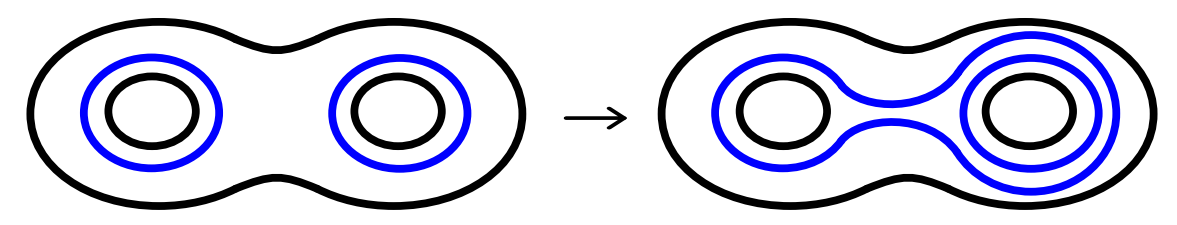


Figure 2.2 Kirby move of Type II.

When surgery along two framed links in  $S^3$  produce the same manifold, we say these surgeries are equivalent. For example, we saw above that for any  $n \in \mathbb{Z}$ , the (1/n)-surgery along the unknot in  $S^3$  is homeomorphic to  $S^3$ .

There is a systematic description of modifications of surgery on framed links which do not change the resulting manifold. In particular, one may modify a surgery presentation by certain combinatorial operations, known as Kirby calculus, to obtain another surgery presentation which produces the same 3-manifold. The details of Kirby calculus can be found in [72, 56, 69], but we state the main results used throughout this work here.

**Theorem 2.1.14** ([49]). Surgery along two framed links in  $S^3$  produces the same 3-manifold if and only if they are related by a sequence of moves of two types. A move of Type I involves adding/removing an  $(\pm 1)$ -framed unknotted component which is unlinked from the other components. In a move of Type II, any two components that are contained in a twice-punctured disk  $\Sigma_{0,2}$  can be modified as shown in Figure 2.2.

The moves of Type I and II are referred to as *Kirby moves*, and they are often described by the terms *blow up/blow down* and *handleslide*, respectively. They apply to framed links with integer surgery coefficients. Soon after Kirby's result [49], Fenn and Rourke [28] gave an equivalent construction which uses a single move to modify surgery presentations. This move, shown in Figure 2.3, turns out to be a combination of the Kirby moves.

Rolfsen [72] also gives a pair of similar surgery presentation modifications which do not change the resulting manifold. In addition, these moves extend those of Kirby to framed links with both integer and rational surgery coefficients. These moves are the following:

(1) Introduce or remove a component with surgery coefficient  $\infty$ ,

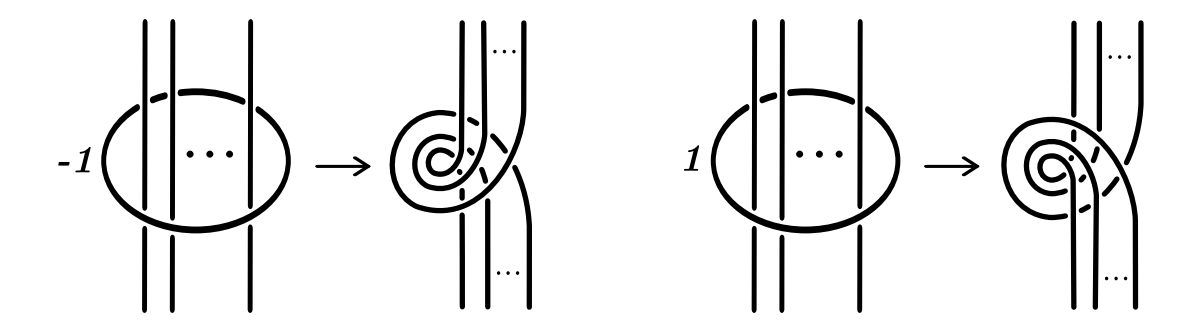


Figure 2.3 Fenn–Rourke moves, which correspond to Rolfsen's twist of the complement of an unknotted component. The positive twist is given on the left, and the negative twist on the right.

(2) Twist the complement of an unknotted component using a Fenn-Rourke move.

All combined, these operations on framed links consitute the Kirby–Rolfsen–Fenn–Rourke calculus. In the remainder of this work, we will use both Kirby and Fenn–Rourke/Rolfsen moves to modify surgery presentations, and we will leverage Theorems 2.1.10, 2.1.13 and 2.1.14 frequently to present homemorphisms and surgery descriptions of manifolds. This will be especially important in Sections 2.2 and 2.3 to define various quantum invariants of 3-manifolds.

#### 2.2 The Witten-Reshetikhin-Turaev Invariants

In this section, we discuss the Witten–Reshetikhin–Turaev invariants and the Topological Quantum Field Theories (TQFTs) they are a part of. We begin in Subsection 2.2.1 by introducing a version of these invariants for 3-manifolds containing framed links that is computed relative to a coloring of the link components. We then introduce the SO(3)-Witten–Reshetikhin–Turaev TQFTs and their relevant properties in Subsection 2.2.2. Both the relative invariants and the TQFT properties will be useful throughout this work.

#### 2.2.1 Relative Reshetikhin–Turaev Invariants

Here, we introduce the r-th relative Reshetikhin–Turaev invariants for manifolds containing framed links. We will follow the skein-theoretic framework given by Blanchet, Habegger, Masbaum, and Vogel [11] and Lickorish [55].

For a compact orientable 3-manifold M, odd  $r \geq 3$ , and 2r-th root of unity q, we define

the Kauffman bracket skein module  $K_r(M)$  of M to be the  $\mathbb{C}$ -module generated by the isotopy classes of framed links in M modulo the following relations:

(I) Kauffman bracket skein relation: 
$$\left\langle \middle{\searrow} \right\rangle = q^{\frac{1}{2}} \left\langle \middle{\searrow} \right\rangle + q^{-\frac{1}{2}} \left\langle \middle{\searrow} \right\rangle$$
.

(II) Framing relation: 
$$\langle L \sqcup \bigcirc \rangle = (-q - q^{-1}) \langle L \rangle$$
.

In the case when  $M = S^3$ , the Kauffman bracket skein module  $K_r(S^3)$  is 1-dimensional, and we obtain an isomorphism

$$\langle \cdot \rangle : K_r(S^3) \to \mathbb{C}$$

by sending the empty diagram to 1. For a link  $L \subset S^3$ , we call the image  $\langle L \rangle \in \mathbb{C}$  the Kauffman bracket of L.

We now consider the Kauffman bracket skein module  $K_r(S^1 \times [-1, 1]^2)$  of the solid torus. For any framed link  $L \subset S^3$  with k ordered components and  $b_1, b_2, \ldots, b_k \in K_r(S^1 \times [-1, 1]^2)$ , we define the  $\mathbb{C}$ -multilinear map

$$\langle \cdot, \dots, \cdot \rangle_L : K_r(S^1 \times [-1, 1]^2) \to \mathbb{C}$$

where  $\langle b_1, b_2, \ldots, b_k \rangle_L$  is the cabling of the components of L by  $b_1, b_2, \ldots, b_k$  followed by evaluating in  $K_r(S^3)$  using the Kauffman bracket. We refer to [11] for further details on cabling by an element of the skein module and note that these details are not necessary to the arguments that follow.

On  $K_r(S^1 \times [-1,1]^2)$ , there is a commutative multiplication induced by juxtaposition of annuli  $S^1 \times [0,1] \times \{pt\}$  making  $K_r(S^1 \times [-1,1]^2)$  a  $\mathbb{C}$ -algebra. By sending the core of the annuli to the indeterminate z, we obtain the isomorphism  $K_r(S^1 \times [-1,1]^2) \cong \mathbb{C}[z]$ .

We now construct specific elements of  $K_r(S^1 \times [-1, 1]^2)$  known as the Jones-Wenzl idempotents. For  $i \geq 0$ , define  $e_i(z)$  to be the *i*-th Chebychev polynomial, which is defined

recursively by

$$e_0(z) = 1$$
  
 $e_1(z) = z$   
 $e_i(z) = ze_{i-1}(z) - e_{i-2}(z)$ .

Define the n-th quantum integer [n] by

$$[n] := \frac{q^n - q^{-n}}{q - q^{-1}}.$$

Let  $I_r := \{0, 1, \dots, r-2\}$ . We define the Kirby coloring  $\omega_r \in K_r(S^1 \times [-1, 1]^2)$  by

$$\omega_r := \eta_r \sum_{i \in I_r} [i+1]e_i,$$

where

$$\eta_r := \frac{2\sin(\frac{2\pi}{r})}{\sqrt{r}}.$$

The  $e_i$  will correspond to colorings of our link by the (i-1)-th Jones-Wenzl idempotent, and the Kirby coloring  $\omega_r$  will allow us to define an invariant for a framed link in any closed oriented 3-manifold. We will now define the r-th relative Reshetikhin–Turaev invariants.

**Definition 2.2.1.** Let M be a closed oriented 3-manifold presented in  $S^3$  by surgery along the framed link L' with n' components, and let L be a framed link in  $S^3$  with n components. We consider the link  $L \sqcup L' \subset S^3$  with n+n' components where the first n components correspond to the components of L. For a coloring  $\gamma = (\gamma_1, \gamma_2, \ldots, \gamma_n) \in I_r^n$  of components of L, we define the r-th relative Reshetikhin-Turaev invariants as

$$RT_r(M, L, \gamma) = \mu_r \langle e_{\gamma_1}, \dots, e_{\gamma_n}, \omega_r, \dots, \omega_r \rangle_{L \sqcup L'} \langle \omega_r \rangle_{U_+}^{-\sigma(L')}$$

where  $U_+$  is the +1 framed unknot and  $\sigma(L')$  is the signature of the linking matrix of L'.

Reshetikhin and Turaev proved that this is indeed an invariant of the pair (M, L) relative to the coloring  $\gamma$  [70].

**Theorem 2.2.2.** [70] Let M be a closed oriented 3-manifold with surgery presentation along a link  $L' \subset S^3$ , and let  $L \subset S^3$  be an n-component framed link colored by  $\gamma \in I_r^n$ . Then  $RT_r(M, L, \gamma)$  is an invariant of the pair (M, L) relative to the coloring  $\gamma$ .

## 2.2.2 Witten-Reshetikhin-Turaev TQFTs

In this subsection, we introduce the Witten–Reshetikhin–Turaev TQFTs, which are functors from the category of (2+1)-dimensional cobordisms to finite-dimensional  $\mathbb{C}$ -vector spaces originally defined by Reshetikhin and Turaev in [70]. For odd r, the skein-theoretic approach of Blanchet, Habegger, Masbaum, and Vogel [11] and Lickorish [55] give rise this so-called  $SO_3$ -TQFT  $RT_r$ .

Fix an odd integer  $r \geq 3$  and primitive 2r-th root of unity A, and let  $\Sigma_{g,n}$  be a compact oriented surface of genus g with n boundary components. The SO(3)-Witten–Reshetikhin–Turaev TQFTs associate a complex vector space  $RT_r(\Sigma_{g,n})$  to  $\Sigma_{g,n}$ , and, for a 3-manifold M with  $\partial M \neq \emptyset$ ,  $RT_r(M) \in RT_r(\partial M)$  is a vector. For a closed 3-manifold M,  $RT_r(M) \in \mathbb{C}$  is known as the r-th Witten–Reshetikhin–Turaev invariant and coincides with Witten's original 3-manifold invariants [81, 82]. The main properties of the SO(3)-TQFT defined in [11] relevant to this work are the following.

**Theorem 2.2.3** ([11], Theorem 1.4). Let  $r \geq 3$  be an odd integer and A be a primitive 2r-th root of unity, and let  $\mathfrak{Cob}$  be the category of (2+1)-dimensional cobordisms. Then there is a (2+1)-dimensional TQFT functor

$$RT_r: \mathfrak{Cob} \to Vect(\mathbb{C})$$

satisfying:

- (1) For a closed oriented 3-manifold M,  $RT_r(M) \in \mathbb{C}$  is a topological invariant. Moreover, if  $\overline{M}$  is oppositely oriented to M, then  $RT_r(\overline{M}) = \overline{RT_r(M)}$ .
- (2)  $RT_r(S^3) = \eta_r \text{ and } RT_r(S^2 \times S^1) = 1.$
- (3)  $RT_r$  is multiplicative under disjoint unions.

(4) For connect sums, we have

$$RT_r(M\#N) = \eta_r^{-1}RT_r(M)RT_r(N).$$

(5) For a closed oriented surface  $\Sigma$ ,  $RT_r(\Sigma)$  is a finite dimensional  $\mathbb{C}$ -vector space, and there is a natural isomorphism

$$RT_r(\Sigma \sqcup \Sigma') \cong RT_r(\Sigma) \otimes RT_r(\Sigma').$$

(6) For a compact oriented 3-manifold M,  $RT_r(M) \in RT_r(\partial M)$  is a vector. Moreover, if  $M = M_1 \sqcup M_2$ , then

$$RT_r(M) = RT_r(M_1) \otimes RT_r(M_2) \in RT_r(\partial M_1) \otimes RT_r(\partial M_2).$$

(7) For a cobordism  $(M, \Sigma_1, \Sigma_2)$ ,  $RT_r(M) : RT_r(\Sigma_1) \to RT_r(\Sigma_2)$  is a linear map on  $\mathbb{C}$ -vector spaces.

We note that the use of notation  $RT_r$  for both the relative invariant and the TQFT is intentional. In particular, for closed M, if  $L = \emptyset$  or if the coloring  $\gamma = (0, ..., 0)$ , then the relative invariant  $RT_r(M, L, \gamma) = RT_r(M) \in \mathbb{C}$  coincides with the Witten–Reshetikhin–Turaev invariant.

#### 2.3 The Turaev–Viro Invariants

Turaev-Viro [79] defined a real-valued topological invariant on a triangulation of a compact 3-manifold for fixed r and a root of unity q using quantum 6j-symbols studied in [50]. We will define the SU(2)-version of the invariant for odd  $r \geq 3$  and  $q = e^{\frac{2\pi\sqrt{-1}}{r}}$ , following the conventions of [9]. We begin by introducing a building block for the Turaev-Viro invariant known as the quantum 6j-symbol.

## 2.3.1 Quantum 6*j*-symbols

Here we introduce the quantum integers, factorials, and quantum 6*j*-symbols.

Recall the *n*-th quantum integer is given by  $[n] = \frac{q^n - q^{-n}}{q - q^{-1}}$ , and define the quantum factorial by

$$[n]! = \prod_{k=1}^{n} [k]$$

where n is a positive integer. By convention, we also define [0]! = 1. Finally, let  $I_r = \{0, 1, 2, \ldots, r-2\}$ , to which we refer to as a *coloring set*. Throughout the paper, we use the convention that  $\sqrt{y} = \sqrt{|y|}\sqrt{-1}$  for any negative real number y.

Note that other than the use of [n] for the quantum integer rather than  $\{n\} := q^n - q^{-n}$ , the definitions introduced in this subsection largely follow the conventions and notation of [9]. In particular, our coloring set  $I_r$  is defined in terms of integers rather than the conventionally chosen half-integers used in [16, 79].

**Definition 2.3.1.** A triple  $(a_1, a_2, a_3)$  of integers in  $I_r$  is r-admissible if

- (i)  $a_1 + a_2 + a_3$  is even,
- (ii)  $a_1 + a_2 + a_3 \le 2(r-2)$ ,
- (iii)  $a_i + a_j a_k \ge 0$  for any  $i, j, k \in \{1, 2, 3\}$ .

We say a 6-tuple  $(a_1, \ldots, a_6)$  is r-admissible if the triples  $(a_1, a_2, a_3)$ ,  $(a_1, a_5, a_6)$ ,  $(a_2, a_4, a_6)$ , and  $(a_3, a_4, a_5)$  are r-admissible.

For an r-admissible triple  $(a_1, a_2, a_3)$ , define

$$\Delta(a_1, a_2, a_3) = \sqrt{\frac{\left[\frac{a_1 + a_2 - a_3}{2}\right]! \left[\frac{a_1 + a_3 - a_2}{2}\right]! \left[\frac{a_2 + a_3 - a_1}{2}\right]!}{\left[\frac{a_1 + a_2 + a_3}{2} + 1\right]!}}.$$

**Definition 2.3.2.** The quantum 6j-symbol of an r-admissible 6-tuple  $(a_1, \ldots, a_6)$  is the complex number

$$\begin{vmatrix} a_1 & a_2 & a_3 \\ a_4 & a_5 & a_6 \end{vmatrix} = \sqrt{-1}^{-\sum_{i=1}^6 a_i} \Delta(a_1, a_2, a_3) \Delta(a_1, a_5, a_6) \Delta(a_2, a_4, a_6) \Delta(a_3, a_4, a_5)$$

$$\sum_{k=\max\{T_i\}}^{\min\{Q_j\}} \frac{(-1)^k [k+1]!}{\prod_{i=1}^4 [k-T_i]! \prod_{j=1}^3 [Q_j - k]!} \in \mathbb{C},$$
(2.1)

where 
$$T_1 = \frac{a_1 + a_2 + a_3}{2}$$
,  $T_2 = \frac{a_1 + a_5 + a_6}{2}$ ,  $T_3 = \frac{a_2 + a_4 + a_6}{2}$ ,  $T_4 = \frac{a_3 + a_4 + a_5}{2}$ ,  $Q_1 = \frac{a_1 + a_2 + a_4 + a_5}{2}$ ,  $Q_2 = \frac{a_1 + a_3 + a_4 + a_6}{2}$ , and  $Q_3 = \frac{a_2 + a_3 + a_5 + a_6}{2}$ .

We remark that the value of the quantum 6j-symbol is either real or purely imaginary. A useful property of the quantum 6j-symbol is the following.

**Proposition 2.3.3.** For an r-admissible 6-tuple (i, j, k, l, m, n), the following symmetries follow directly from the definition of the quantum 6j-symbol at  $q = e^{\frac{2\pi\sqrt{-1}}{r}}$ :

$$\begin{vmatrix} i & j & k \\ l & m & n \end{vmatrix} = \begin{vmatrix} j & i & k \\ m & l & n \end{vmatrix} = \begin{vmatrix} i & k & j \\ l & n & m \end{vmatrix} = \begin{vmatrix} i & m & n \\ l & j & k \end{vmatrix} = \begin{vmatrix} l & m & k \\ i & j & n \end{vmatrix} = \begin{vmatrix} l & j & n \\ i & m & k \end{vmatrix}.$$
(2.2)

Deeper algebraic and geometric properties of the quantum 6*j*-symbols can be found in Kirillov-Reshetikhin [50], Turaev-Viro [79], and Turaev [77, 78], but properties relevant to the results of this work that follow are established directly from the above definitions and properties.

## 2.3.2 Invariant of a Triangulation

Here we define the r-th Turaev–Viro invariant as an invariant of a triangulation of a 3-manifold. We also include a result of [9, 25] relating them to the relative Reshetikhin–Turaev invariants.

We begin with a slightly generalized notion of a triangulation of a 3-manifold.

**Definition 2.3.4.** Let M be a compact orientable 3-manifold with boundary  $\partial M$ . We say  $\tau$  is a partially ideal triangulation of M if some vertices of the triangulation are truncated, and the faces of the truncated vertices form a triangulation of  $\partial M$ .

**Definition 2.3.5.** An r-admissible coloring of a tetrahedron T is a map assigning an r-admissible 6-tuple  $(a_1, \ldots, a_6) \in I_r^6$  to the edges of T. In particular, the triples  $(a_i, a_j, a_k)$  corresponding to each face of T must be r-admissible triples satisfying Definition 2.3.1. We say that a coloring of the edges of a triangulation  $\tau$  of a 3-manifold is r-admissible if each tetrahedron  $T \in \tau$  admits an r-admissible coloring.

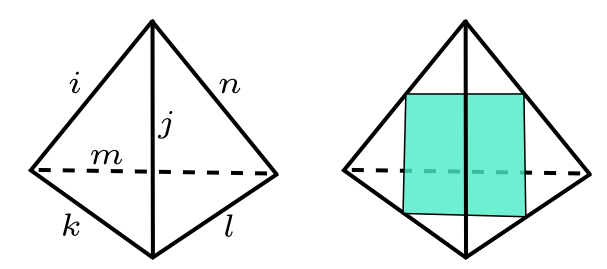


Figure 2.4 **Left:** A tetrahedron colored by a 6-tuple (i, j, k, l, m, n). **Right:** One of the three quadilaterals of a tetrahedron which separates pairs of vertices.

Let  $Adm(r,\tau)$  denote the set of r-admissible colorings of a partially ideal triangulation  $\tau$ . Denote the set of interior vertices of  $\tau$  by V and the set of interior edges of  $\tau$  by E. Given a coloring  $\gamma \in Adm(r,\tau)$ , and edge  $e \in E$ , and a tetrahedron  $T \in \tau$ , we define

$$|e|_{\gamma} := (-1)^{\gamma(e)} [\gamma(e) + 1],$$

and

$$|T|_{\gamma} := \left| \begin{array}{ccc} \gamma(e_1) & \gamma(e_2) & \gamma(e_3) \\ \gamma(e_4) & \gamma(e_5) & \gamma(e_6) \end{array} \right|,$$

where  $e_1, \ldots, e_6$  correspond to the edges of T.

Within this setting of an admissible coloring of a triangulation, the quantities  $T_i$ , i = 1, 2, 3, 4, in Definition 2.3.2 correspond to sums of colorings of the four faces of a tetrahedron and the quantities  $Q_j$ , j = 1, 2, 3, in Definition 2.3.2 correspond to sums of colorings of the three normal quadrilaterals of a tetrahedron. See Figure 2.4 for an example of a colored tetrahedron and a quadrilateral of a tetrahedron.

We are now ready to define the invariant.

**Definition 2.3.6.** Fix  $r \geq 3$  be odd and  $q = e^{\frac{2\pi\sqrt{-1}}{r}}$ . Let M be a compact orientable 3-manifold with boundary  $\partial M$ , and let  $\tau$  be a partially ideal triangulation of M. Then the r-th Turaev–Viro invariant at the root q is given by

$$TV_r(M,\tau;q) := \left(\frac{\sqrt{2}\sin\left(\frac{2\pi}{r}\right)}{\sqrt{r}}\right)^{2|V|} \sum_{\gamma \in Adm(r,\tau)} \left(\prod_{e \in E} |e|_{\gamma} \prod_{T \in \tau} |T|_{\gamma}\right). \tag{2.3}$$

Turaev-Viro [79] proved that  $TV_r(M, \tau; q)$  is independent of the choice of partially ideal triangulation  $\tau$ , so we may write the invariant as  $TV_r(M; q)$ . One particular implication of this for a link complement  $M_L$  is that  $TV_r(M_L; q)$  can be computed by summing over  $I_r$ -colorings of the link  $L \subset M$ .

Remark 2.3.7. For this dissertation, we will be concerned with the SU(2)-version of the Turaev-Viro invariants defined above, but we note that our results hold for the SO(3)-version, which was defined in [25] by Detcherry, Kalfagianni, and Yang. The distinction between these two versions of the Turaev-Viro invariants arises from the construction of the Reshetikhin-Turaev TQFTs by Blanchet, Habegger, Masbaum, and Vogel [11]. In the authors' work, the elements of the index set  $I_r$  correspond to the irreducible representations of SU(2). As SU(2) is a double-covering of SO(3), the authors remark that the SO(3) theory can be obtained as the restriction of the elements of  $I_r$  to elements with corresponding representations that lift to SO(3). This means the Turaev-Viro invariants can be defined to have an SU(2)-version and an SO(3)-version which are related to each other by Theorem 2.9 of [25]. For more details between these two versions of the Turaev-Viro invariants, we refer to Sections 2 and 3 of [25].

This state sum formulation of the invariant is not the only way to compute the Turaev–Viro invariants. These invariants are closely related to the Witten–Reshetikhin–Turaev invariants. The following identity was originally proven for closed 3-manifolds by Roberts [71] and then extended to compact manifolds with boundary by Benedetti and Petronio [10].

**Theorem 2.3.8** ([10, 71]). Let  $r \geq 3$  be an odd integer, and let q be a primitive 2r-th root of unity. Then for a compact oriented manifold M with toroidal boundary,

$$TV_r(M,q) = \left\|RT_r\left(M,q^{\frac{1}{2}}\right)\right\|^2$$

where  $\|\cdot\|$  is the natural Hermitian norm on  $RT_r(\partial M)$ .

We note that this identity holds more generally, but we have restricted to manifolds with toroidal boundary for simplicity. In addition, in [9] and [25], the authors prove that the r-th Turaev-Viro invariant of a link complement  $M_L$  can be computed via the r-th relative Reshetikhin-Turaev invariants of (M, L) in terms of a sum over colorings of the components of L.

**Proposition 2.3.9** ([9, 25]). Let M be a 3-manifold,  $L \subset M$  be a link with k components, and  $RT_r(M, L, \gamma)$  be the r-th relative Reshetikhin–Turaev invariant of (M, L) with the link L colored by  $\gamma \in I_r^k$ . Then the Turaev–Viro invariant of the complement  $M_L$  at  $q = e^{\frac{2\pi\sqrt{-1}}{r}}$  is given by

$$TV_r(M_L;q) = \sum_{\gamma \in I_r^k} |RT_r(M,L,\gamma)|^2.$$
(2.4)

## 2.3.3 The Turaev–Viro Invariant Volume Conjecture

While the Turaev–Viro invariants are difficult to compute in general, there is interest in the relationship between the r-asymptotic behavior and classical invariants of 3-manifolds such as hyperbolic volume. Chen and Yang [16] conjectured that the exponential growth rate of the Turaev–Viro invariants of hyperbolic 3-manifolds coincides with hyperbolic volume, which we stated in Conjecture 1.2.1. They provide computational evidence for this conjecture for multiple example manifolds, including the complements of the knots  $4_1, 5_2$ , and  $6_1$ , as well as closed manifolds obtained by some surgeries along  $4_1$  and  $5_2$ , in [16].

Detcherry and Kalfagianni [23] restated this conjecture in terms of the simplicial volume ||M|| of a manifold which is not necessarily hyperbolic. This work is primarily concerned with manifolds of this type. We define the following asymptotics of the Turaev–Viro invariants in order to restate the conjectures introduced in Chapter 1.

**Definition 2.3.10.** Define the following two asymptotics of the Turaev–Viro invariants for compact 3-manifolds as

$$lTV(M) := \liminf_{r \to \infty} \inf_{r \text{ odd}} \frac{2\pi}{r} \log \left| TV_r \left( M; q = e^{\frac{2\pi i}{r}} \right) \right|,$$

and

$$LTV(M) := \limsup_{r \to \infty, r \text{ odd}} \frac{2\pi}{r} \log \left| TV_r \left( M; q = e^{\frac{2\pi i}{r}} \right) \right|.$$

This leads to a natural extension of Conjecture 1.2.1, which we restate here.

Conjecture 1.2.2. Let M be a compact orientable 3-manifold with empty or toroidal boundary. For r running over the odd integers and  $q = e^{\frac{2\pi\sqrt{-1}}{r}}$ ,

$$LTV(M) = v_{tet}||M||,$$

where  $v_{tet} \approx 1.0149$  is the volume of a regular ideal hyperbolic tetrahedron and  $||\cdot||$  is the simplicial volume.

We may also consider the following weaker conjecture studied by Detcherry and Kalfagianni in [22, 23, 24]:

Conjecture 1.5.1. Let M be a compact orientable 3-manifold with empty or toroidal boundary. Then lTV(M) > 0 if and only if ||M|| > 0.

Recall from Section 1.5 that a manifold M with lTV(M) > 0 is called q-hyperbolic. We note that the "if" direction of Conjecture 1.5.1 follows from the main result of [23].

In [23], Detcherry and Kalfagianni proved that the growth rate of the Turaev–Viro invariants has properties reminiscent of simplicial volume. We summarize their results in the following theorem.

**Theorem 2.3.11** ([23]). Let M be a compact oriented 3-manifold, with empty or toroidal boundary.

- 1) If M is a Seifert manifold, then there exist constants B > 0 and N such that for any odd  $r \ge 3$ , we have  $TV_r(M) \le Br^N$  and  $LTV(M) \le 0$ .
- 2) If M is a Dehn-filling of M', then  $TV_r(M) \leq TV_r(M')$  and  $LTV(M) \leq LTV(M')$ .

3) If  $M = M_1 \bigcup_T M_2$  is obtained by gluing two 3-manifolds along a torus boundary component, then  $TV_r(M) \leq TV_r(M_1)TV_r(M_2)$  and  $LTV(M) \leq LTV(M_1) + LTV(M_2)$ .

While Conjectures 1.2.1, 1.2.2, and 1.5.1 differ slightly in generality and scope, each supports the notion that there is a deep relationship between the asymptotic behavior of the Turaev–Viro invariants and hyperbolic geometry of 3-manifolds.

### 2.4 Quantum Representations of Mapping Class Groups

In this section, we introduce the notion of the mapping class group of a surface, a classification of the elements of this group, and its relationship with quantum invariants of 3-manifolds. Additionally, we describe a conjecture of Andersen, Masbaum, and Ueno [5] relating this classification of elements of the mapping class group with its quantum representations.

### 2.4.1 Mapping Class Groups of Surfaces

Here we continue with our discussion on homeomorphisms of surfaces begun in Subsection 2.1.3. Let  $\Sigma_{g,n}$  be a compact oriented surface of genus g with n boundary components.

**Definition 2.4.1.** Let  $\operatorname{Homeo}^+(\Sigma_{g,n}, \partial \Sigma_{g,n})$  be the group of orientation-preserving homeomorphisms of  $\Sigma_{g,n}$  fixing  $\partial \Sigma_{g,n}$  pointwise. The mapping class group  $\operatorname{Mod}(\Sigma_{g,n})$  of  $\Sigma_{g,n}$  is the group

$$\operatorname{Mod}(\Sigma_{g,n}) = \pi_0 \left( \operatorname{Homeo}^+(\Sigma_{g,n}, \partial \Sigma_{g,n}) \right)$$
$$= \operatorname{Homeo}^+(\Sigma_{g,n}, \partial \Sigma_{g,n}) / \operatorname{Homeo}_0(\Sigma_{g,n}, \partial \Sigma_{g,n}),$$

where  $\text{Homeo}_0(\Sigma_{g,n}, \partial \Sigma_{g,n})$  is the connected component of the identity in the group of orientation-preserving homeomorphisms,  $\text{Homeo}^+(\Sigma_{g,n}, \partial \Sigma_{g,n})$ , which fix the boundary of  $\Sigma_{g,n}$ , pointwise.

The mapping class group of a compact oriented surface is the group of isotopy classes of self-homeomorphisms of the surface which restrict to the identity on the boundary. Its group operation corresponds to the composition of homeomorphisms, and we call its elements mapping classes. Theorem 2.1.10 implies that every mapping class of a closed oriented surface can be presented as a composition of Dehn twists up to isotopy. We note that this still holds for compact oriented surfaces with boundary, provided the boundary is fixed under the homeomorphism. For example, the mapping class group  $\text{Mod}(\Sigma_{0,2})$  of the annulus  $\Sigma_{0,2}$  is generated by the standard Dehn twist about its core curve.

## 2.4.2 The Nielsen-Thurston Classification

The Nielsen–Thurston classification of mapping class groups provides a geometric characterization of mapping classes of a given surface. Thurston completed the work of Nielsen four decades after his work studying the geometry of mapping classes using Teichmuller theory. We refer the reader to [27] for further details.

**Definition 2.4.2.** Let  $\Sigma_{g,n}$  be a compact oriented surface of genus g with n boundary components, and let  $\gamma \in \text{Mod}(\Sigma_{g,n})$  be a mapping class. We say

- (i)  $\gamma$  is periodic if some finite power of  $\gamma$  is isotopic to the identity on  $\Sigma_{g,n}$ .
- (ii)  $\gamma$  is reducible if there exists a nonempty set of simple closed curves in  $\Sigma_{g,n}$  which are fixed by  $\gamma$ . In such a case, we may cut  $\Sigma_{g,n}$  along this set of simple closed curves and consider the induced self-homeomorphisms on the resulting pieces.
- (iii)  $\gamma$  is pseudo-Anosov if it has infinite order in  $Mod(\Sigma_{g,n})$  and is not reducible.

The Nielsen–Thurston classification establishes that these are the only possibilities for elements of the mapping class group of a compact oriented surface:

**Theorem 2.4.3.** [27, Theorem 13.2](Nielsen-Thurston classification). For any  $g, n \geq 0$ , each element  $\gamma \in Mod(\Sigma_{g,n})$  is either periodic, reducible, or pseudo-Anosov.

As discussed earlier, this classification is closely related to the geometric properties of mapping classes. As such, a rich family of 3-manifolds is obtained by studying the mapping tori of mapping classes of compact oriented surfaces.

**Definition 2.4.4.** Let  $\gamma \in \text{Mod}(\Sigma_{g,n})$ . Define the mapping torus of  $\gamma$ , denoted  $M_{\gamma}$ , to be the 3-manifold

$$M_{\gamma} := \Sigma_{q,n} \times [-1,1]/(x,1) \sim (\gamma(x),-1),$$

where  $\gamma$  is called the monodromy of  $M_{\gamma}$ .

A well-known result of Thurston [76] establishes a deep connection between the Nielsen–Thurston classification mapping classes and the geometry of their associated mapping tori.

**Theorem 2.4.5** ([76]). A mapping class  $\gamma \in Mod(\Sigma_{g,n})$  is pseudo-Anosov if and only if its associated mapping torus  $M_{\gamma}$  is a hyperbolic 3-manifold.

## 2.4.3 Quantum Representations and the AMU Conjecture

Quantum invariants of 3-manifolds such as the Witten–Reshetikhin–Turaev invariants and the associated TQFT give rise to finite-dimensional representations of mapping class groups of surfaces. A natural question is what relationship these representations have with the Nielsen–Thurston classification of mapping classes.

Let  $\Sigma_{g,n}$  be the compact oriented surface of genus g with n boundary components. The SO(3)-Witten–Reshetikhin–Turaev TQFTs provide finite-dimensional projective representations of  $Mod(\Sigma_{g,n})$ .

Fix an odd integer  $r \geq 3$ , which we refer to as a level, and let  $I_r = \{0, 2, ..., r-3\}$ be the set of even integers less than r-2. Let A be a primitive 2r-th root of unity, and fix a coloring c of the components of  $\partial \Sigma_{g,n}$  by elements of  $I_r$ . Again following the skeintheoretic framework of Blanchet, Habegger, Masbaum, and Vogel [11], the SO(3)-TQFTs associate a finite-dimensional  $\mathbb{C}$ -vector space  $RT_r(\Sigma_{g,n})$  to  $\Sigma_{g,n}$  and give rise to a projective representation

$$\rho_{r,c}: \operatorname{Mod}(\Sigma_{g,n}) \to \mathbb{P}\operatorname{Aut}(RT_r(\Sigma_{g,n})),$$

which we call the SO(3)-quantum representation of  $\operatorname{Mod}(\Sigma_{g,n})$  at level r.

Andersen, Masbaum, and Ueno studied these representations for the sphere with four punctures  $\Sigma_{0,4}$  in [5]. There they established that the Nielsen–Thurston classification of mapping classes in  $\text{Mod}(\Sigma_{0,4})$  are determined by the quantum representations  $\rho_{r,c}$ . This is particularly useful for understanding pseudo-Anosov mapping classes of  $\Sigma_{0,4}$ . They conjectured that this is the case in general.

Conjecture 1.5.6. (AMU Conjecture, [5]) Let  $\gamma \in Mod(\Sigma_{g,n})$  be a pseudo-Anosov mapping class. Then for any big enough level r, there is a choice of coloring c of the components of  $\partial \Sigma_{g,n}$  such that  $\rho_{r,c}(\gamma)$  has infinite order.

We remark that the converse of Conjecture 1.5.6 is known: if  $\rho_{r,c}(\gamma)$  has infinite order, then  $\gamma$  is either pseudo-Anosov or reducible and induces a pseudo-Anosov map after cutting the surface along the curves fixed by the reducible map.

It is also worth noting that if a mapping class  $\gamma \in \text{Mod}(\Sigma_{g,n})$  satisfies the AMU conjecture, then any mapping class which is a power of a conjugate of  $\gamma$  also satisfies the conjecture.

Conjecture 1.5.6 is closely related to conjectures stated earlier, namely the Exponential Growth conjecture (Conjecture 1.5.1) and the original Turaev–Viro invariant Volume Conjecture (Conjecture 1.2.1). In particular, Detcherry and Kalfagianni [22] proved the following result.

**Theorem 2.4.6.** [22, Theorem 1.2] Let  $\gamma \in Mod(\Sigma_{g,n})$  be a pseudo-Anosov mapping class and let  $M_{\gamma}$  be its associated mapping torus. If  $lTV(M_{\gamma}) > 0$ , then  $\gamma$  satisfies the conclusion of the AMU conjecture.

This means that for 3-manifolds realized as mapping tori, the Exponential Growth Conjecture implies the AMU conjecture. Since Chen and Yang's original conjecture is a stronger assertion, we reach a similar conclusion for the Turaev–Viro invariant Volume Conjecture.

#### CHAPTER 3

#### TURAEV-VIRO INVARIANTS AND CABLING OPERATIONS

This chapter is based on joint work with Kumar in a paper published in the International Journal of Mathematics [53].

In this chapter, we study the variation of the Turaev-Viro invariants for 3-manifolds with toroidal boundary under the operation of attaching a (p,q)-cable space. We apply our results to the Turaev-Viro invariant volume conjecture. For p and q coprime, we show that Conjecture 1.2.2 is stable under (p,q)-cabling. We achieve our results by studying the linear operator  $RT_r$  associated to the torus knot cable spaces by the  $SO_3$ -Reshetikhin-Turaev Topological Quantum Field Theories (TQFTs), where the TQFT is well-known to be closely related to the desired Turaev-Viro invariants. In particular, our utilized method relies on the invertibility of the linear operator  $RT_r$  for which we provide necessary and sufficient conditions.

## 3.1 Introduction

Recall from Section 2.3, for a compact 3-manifold M, its Turaev–Viro invariants are a family of  $\mathbb{R}$ -valued homeomorphism invariants parameterized by an integer  $r \geq 3$  depending on a 2r-th root of unity q. We are primarily interested in the behavior of the invariants when r is odd and  $q = e^{\frac{2\pi\sqrt{-1}}{r}}$  under the attaching of a (p,q)-cable space.

**Definition 3.1.1.** Let V be the standardly embedded solid torus in  $S^3$ , and let V' be a closed neighborhood of V. For p,q coprime integers with q>0, let  $T_{p,q}\subset \partial V$  be the torus knot of slope p/q. The (p,q)-cable space, denoted  $C_{p,q}$ , is the complement of the torus knot  $T_{p,q}$  in V'. Let M be a 3-manifold with toroidal boundary. A manifold M' obtained from gluing a (p,q)-cable space  $C_{p,q}$  to a boundary component of M along the exterior toroidal boundary component of  $C_{p,q}$  is called a (p,q)-cable of M.

The main theorem of this chapter is the following.

**Theorem 1.3.1.** Let M be a manifold with toroidal boundary, let p, q be coprime integers

with q > 0, and let  $r \ge 3$  be an odd integer coprime to q. Suppose M' is a (p,q)-cable of M. Then there exists a constant C > 0 and natural number N such that

$$\frac{1}{Cr^N}TV_r(M) \le TV_r(M') \le Cr^NTV_r(M).$$

Theorem 1.3.1 has notable applications to Conjecture 1.2.2. A key property of the (p,q)cable spaces is that they have simplicial volume zero. Theorem 1.3.1 provides a way to construct new manifolds without changing the simplicial volume while controlling the growth of
the Turaev–Viro invariants. This leads to many examples of manifolds satisfying Conjecture
1.2.2.

To the authors' knowledge, in all of the proven examples of Conjecture 1.2.2, the stronger condition that the limit approaches the simplicial volume is verified, as opposed to only the limit superior. Theorem 1.3.1 implies the following corollaries. For more details, see Section 3.3.

Corollary 1.3.2. Suppose M satisfies Conjecture 1.2.2 and  $lTV(M) = v_{tet}||M||$ . Then for any p and q coprime, any (p,q)-cable M' also satisfies Conjecture 1.2.2.

Some examples which satisfy the hypothesis of Corollary 1.3.2 include the figure-eight knot and the Borromean rings by Detcherry-Kalfagianni-Yang [25], the Whitehead chains by Wong [83], the fundamental shadow links by Belletti-Detcherry-Kalfagianni-Yang [9], a family of hyperbolic links in  $S^2 \times S^1$  by Belletti [8], a large family of octahedral links in  $S^3$  by Kumar [51], and a family of link complements in trivial  $S^1$ -bundles over oriented connected closed surfaces by Kumar and the author of this work [52].

For general p and q coprime, Corollary 1.3.2 demonstrates that Conjecture 1.2.2 is preserved under the (p,q)-cabling operation. However, in the case when  $q=2^n$  for  $n \in \mathbb{N}$ , we recover the full limit as shown in the following corollary.

Corollary 1.3.3. Suppose M satisfies Conjecture 1.2.2. Then for any odd p and  $n \in \mathbb{N}$ , any  $(p, 2^n)$ -cable M' also satisfies Conjecture 1.2.2. Moreover, if  $|TV(M)| = v_3 ||M||$ , then  $|TV(M')| = |TV(M')| = v_3 ||M'||$ .

As a direct result of Corollaries 1.3.2 and 1.3.3, we extend the work of Detcherry [21] where the author considers the operation of attaching a (p, 2)-cable space. This allows us to construct manifolds satisfying Conjecture 1.2.2 from manifolds with toroidal boundary where the conjecture is already known. This includes all previously mentioned examples.

The general method of proof for Theorem 1.3.1 follows from the work of Detcherry [21]. Considering the cable space  $C_{p,q}$  as a cobordism between tori, recall from Section 2.2 the Reshetikhin–Turaev  $SO_3$ –TQFT at level r, denoted by  $RT_r$ , associates to it a linear operator

$$RT_r(C_{p,q}): RT_r(T^2) \to RT_r(T^2),$$

where  $RT_r(T^2)$  is a  $\mathbb{C}$ -vector space of dimension  $m = \frac{r-1}{2}$  which is a quotient of the Kauffman bracket skein module  $K_r(S^1 \times [-1,1]^2)$  of the solid torus. As discussed in Subsection 2.2.1, there exist elements  $e_i \in K_r(S^1 \times [-1,1]^2)$  known as the Jones-Wenzl idempotents which, under this quotient, correspond to basis elements for the vector space  $RT_r(T^2)$ .

For p odd and q=2, Detcherry presents  $RT_r(C_{p,2})$  using the basis  $\{e_1,e_3,\ldots,e_{2m-1}\}$ , which is equivalent to the orthonormal basis  $\{e_1,e_2,\ldots,e_m\}$  for  $RT_r(T^2)$  given in [11] under the symmetry  $e_{m-i}=e_{m+i+1}$  for  $0 \le i \le m-1$ . More details of the construction are given in Section 3.2. With this basis,  $RT_r(C_{p,2})$  can be presented as a product of two diagonal matrices and one triangular matrix. This allows the author to directly write the inverse of  $RT_r(C_{p,2})$ . From the inverse of this linear operator, Detcherry establishes a lower bound of the Turaev–Viro invariants under attaching a (p,2)-cable space.

For general p and q coprime,  $RT_r(C_{p,q})$  does not have as simple a presentation under the same basis, making it more difficult to conclude that  $RT_r(C_{p,q})$  is invertible. In order to resolve this, we present  $RT_r(C_{p,q})$  using a different basis for  $RT_r(T^2)$ , defined in Section 3.4, that allows us to also show directly that  $RT_r(C_{p,q})$  is invertible provided r and q are coprime. Following Detcherry's argument, the invertibility of  $RT_r(C_{p,q})$  is integral to finding the lower bound from Theorem 1.3.1; however, the invertibility of  $RT_r(C_{p,q})$  is constrained by the condition that r and q are coprime, as outlined by Theorem 1.3.4. **Theorem 1.3.4.** Let p be coprime to some positive integer q. Then  $RT_r(C_{p,q})$  is invertible if and only if r and q are coprime. Moreover, the operator norm  $|||RT_r(C_{p,q})^{-1}|||$  grows at most polynomially.

the discrepancy between recovering the limit superior in Corollary 1.3.2 versus the full limit in Corollary 1.3.3.

Remark 3.1.2. We can characterize the polynomial bound given in Theorem 1.3.4 on the operator norm  $|||RT_r(C_{p,q})^{-1}|||$  more explicitly: we will see later in the proof of Proposition 3.4.2 that this operator norm is actually linearly bounded in r. Using the relationship between the Turaev–Viro and Reshetikhin–Turaev invariants given by Theorem 2.3.8, this means the degree N of the polynomial in the bound of Theorem 1.3.1 is actually bounded above by  $N \leq 2$ .

As we will show in Section 3.3, the coprime condition between r and q leads to The chapter is organized as follows: We recall properties of the Reshetikhin–Turaev  $SO_3$ -TQFTs, the  $RT_r$  torus knot cabling formula, and relevant properties of the Turaev–Viro invariants in Section 3.2. In Section 3.3, we prove Theorem 1.3.1 assuming Theorem 1.3.4. In Section 3.4, the construction of the relevant basis for  $RT_r(T^2)$  and the proof of Theorem 1.3.4 are given. Lastly, we consider future directions in Section 3.5.

#### 3.2 The Witten-Reshetikhin-Turaev TQFTs and Cable Spaces

In this section, we will discuss the Witten–Reshetikhin–Turaev TQFTs in the context of the torus knot cable spaces and introduce a formula of Morton [60] governing the invariants associated to these spaces. For the remainder of this chapter, we fix odd  $r = 2m + 1 \ge 3$  and 2r-th root of unity A.

We will focus on the m-dimensional  $\mathbb{C}$ -vector space  $RT_r(T^2)$ , which can be considered as a quotient of the Kauffman skein module  $K_r(S^1 \times [-1,1]^2)$  of the genus 1 handlebody  $S^1 \times [-1,1]^2$  discussed in Subsection 2.2.1. We begin by coloring the core  $\{0\} \times S^1$  by the (i-1)-th Jones-Wenzl idempotent  $e_i \in K_r(S^1 \times [-1,1]^2)$ . Under the quotient  $K_r(S^1 \times [-1,1]^2)$ 

 $[-1,1]^2) \to RT_r(T^2)$ , the infinite family of idempotents  $\{e_i|i \in \mathbb{N} \cup \{0\}\}$  maps to a finite family  $\{e_1,\ldots,e_{2m-1}\}$  of vectors. Abusing notation slightly, we also refer to these vectors as  $e_i$ 's. These  $e_i$ 's provide a basis for  $RT_r(T^2)$ , as shown by the following result of [11].

**Theorem 3.2.1** ([11], Theorem 4.10). Let  $r = 2m + 1 \ge 3$ . Then the family  $\{e_1, \ldots, e_m\}$  is an orthonormal basis for  $RT_r(T^2)$ . Moreover, the relation  $e_{m-i} = e_{m+1+i}$  holds for  $0 \le i \le m-1$ .

The second part of the theorem implies that  $\{e_1, e_3, \ldots, e_{2m-1}\}$  is just a reordering of the basis  $\{e_1, \ldots, e_m\}$ .

We may now give an explicit description for the Reshetikhin–Turaev invariants of the torus knot cable spaces.

Let p,q be coprime integers where q>0, and let  $C_{p,q}$  be the (p,q)-cable space. These spaces are Seifert-fibered and therefore have simplicial volume zero. For  $r=2m+1\geq 3$ , we extend the vectors  $e_i\in RT_r(T^2)$  to all  $i\in\mathbb{Z}$  in the following way.

- Let  $e_{-i} = -e_i$  for any  $i \ge 0$ , and
- let  $e_{i+kr} = (-1)^k e_i$  for any  $k \in \mathbb{Z}$ .

Note this means that  $e_r = e_0 = 0$ .

Regarding the cable space  $C_{p,q}$  as a cobordism between tori, by Theorem 2.2.3, the Reshetikhin–Turaev  $SO_3$ -TQFT gives a linear map

$$RT_r(C_{p,q}): RT_r(T^2) \to RT_r(T^2).$$

The map  $RT_r(C_{p,q})$  sends the element  $e_i$  to the element of  $RT_r(T^2)$  corresponding to a (p,q)torus knot embedded in the solid torus and colored by the (i-1)-th Jones-Wenzl idempotent.

Morton [60] gives the following formula for the image of the basis elements under  $RT_r(C_{p,q})$ .

Theorem 3.2.2 ([60], Section 3, Cabling Formula).

$$RT_r(C_{p,q})(e_i) = A^{pq(i^2-1)/2} \sum_{k \in S_i} A^{-2pk(qk+1)} e_{2qk+1},$$

where  $S_i$  is the set

$$S_i = \left\{ -\frac{i-1}{2}, -\frac{i-3}{2}, ..., \frac{i-3}{2}, \frac{i-1}{2} \right\}.$$

As we discussed in Section 2.3, the Witten–Reshetikhin–Turaev TQFTs are closely related to the Turaev–Viro invariants of 3-manifolds. By using this relationship, the explicit formula given in Theorem 3.2.2 will allow us to obtain a lower bound on the Turaev–Viro invariants under the cabling operation.

#### 3.3 Bounding the Invariant Under Cabling

In this section, we will prove Theorem 1.3.1 with the assumption of a key theorem, and we reserve the technical details for Section 3.4. We remark that the major components of our argument follow from the work of Detcherry [21] where the case when p is odd and q = 2 was proven. For convenience, we will restate the main theorem.

**Theorem 1.3.1.** Let M be a manifold with toroidal boundary, let p,q be coprime integers with q > 0, and let  $r \ge 3$  be an odd integer coprime to q. Suppose M' is a (p,q)-cable of M. Then there exists a constant C > 0 and natural number N such that

$$\frac{1}{Cr^N}TV_r(M) \le TV_r(M') \le Cr^NTV_r(M).$$

We will now assume Theorem 1.3.4, which we also restate for convenience.

**Theorem 1.3.4.** Let p be coprime to some positive integer q. Then  $RT_r(C_{p,q})$  is invertible if and only if r and q are coprime. Moreover, the operator norm  $|||RT_r(C_{p,q})^{-1}|||$  grows at most polynomially.

Proof of Theorem 1.3.1. As mentioned previously, the case when p is odd and q = 2 was shown by Detcherry [21], and our approach follows closely in structure. We let M be a manifold with toroidal boundary, p an integer, q > 0 an integer coprime to p,  $r \ge 3$  odd and coprime to q, and M' a (p,q)-cable of M. We will proceed to prove Theorem 1.3.1 by showing the upper inequality of

$$\frac{1}{Cr^N}TV_r(M) \le TV_r(M') \le Cr^NTV_r(M)$$

followed by the lower inequality, where C > 0 and  $N \in \mathbb{N}$ . To obtain the upper inequality, we first remark that  $M' = C_{p,q} \bigcup_T M$ . By Theorem 2.3.11, this implies that

$$TV_r(M') \le TV_r(C_{p,q})TV_r(M).$$

Since  $C_{p,q}$  is a Seifert manifold, we have that

$$TV_r(C_{p,q}) \le C_1 r^{N_1}$$

for some  $C_1>0$  and  $N_1\in\mathbb{N}$  also by Theorem 2.3.11 . This leads to the upper inequality

$$TV_r(M') \le C_1 r^{N_1} TV_r(M).$$

For the lower inequality, we will use Theorem 1.3.4. From the properties of the Reshetikhin–Turaev  $SO_3$ -TQFT, we consider the linear map

$$RT_r(C_{p,q}): RT_r(T^2) \to RT_r(T^2).$$

If M only has one boundary component, then

$$RT_r(M') = RT_r(C_{p,q})RT_r(M)$$

by the properties of a TQFT. If M has other boundary components, then the invariant associated to any coloring i of the other boundary components may be computed as

$$RT_r(M',i) = RT_r(C_{p,q})RT_r(M,i).$$

By the invertibility of  $RT_r(C_{p,q})$  from Theorem 1.3.4, we have the inequality

$$||RT_r(M)|| \le |||RT_r(C_{p,q})^{-1}||| \cdot ||RT_r(M')||$$

where  $||\cdot||$  is the norm induced by the Hermitian form of the TQFT and  $|||\cdot|||$  is the operator norm. Since the operator norm grows at most polynomially by Theorem 1.3.4, we obtain the inequality

$$\frac{1}{C_2 r^{N_2}} ||RT_r(M)|| \le ||RT_r(M')||$$

for some  $C_2 > 0$  and  $N_2 \in \mathbb{N}$ . Lastly, by Theorem 2.3.8, the norm of the Reshetikhin–Turaev invariant is related to the Turaev–Viro invariant such that we arrive to the desired inequality

$$\frac{1}{C_3 r^{N_3}} TV_r(M) \le TV_r(M')$$

for some  $C_3 > 0$  and  $N_3 \in \mathbb{N}$ . This leads to

$$\frac{1}{Cr^N}TV_r(M) \le TV_r(M') \le Cr^NTV_r(M)$$

where C > 0 and  $N \in \mathbb{N}$ .

As discussed in Section 3.1, the following corollaries follow from Theorem 1.3.1.

Corollary 1.3.2. Suppose M satisfies Conjecture 1.2.2 and  $lTV(M) = v_{tet}||M||$ . Then for any p and q coprime, the (p,q)-cable M' also satisfies Conjecture 1.2.2.

Proof. By Theorem 2.3.11 part (1),  $LTV(C_{p,q}) \leq 0$ , and thus by Theorem 2.3.11 part (3),  $LTV(M') \leq LTV(M)$ . Since  $lTV(M) = LTV(M) = v_{tet}||M||$ , the limit exists, and any subsequence also converges to  $v_{tet}||M||$ . By Theorem 1.3.1 along odd r,

$$\lim \sup_{r \to \infty, \; (r,q)=1} \frac{2\pi}{r} \log |\mathrm{TV}_r\left(M'\right)| = \lim \sup_{r \to \infty, \; (r,q)=1} \frac{2\pi}{r} \log |\mathrm{TV}_r\left(M\right)| = LTV(M) = v_{tet}||M||,$$

where

$$\lim_{r \to \infty, (r,q)=1} \frac{2\pi}{r} \log |\text{TV}_r(-)|$$

is the limit superior of the subsequence along which r and q are coprime.

Since

$$v_{tet}||M|| = \limsup_{r \to \infty, (r,q)=1} \frac{2\pi}{r} \log|\mathrm{TV}_r(M')| \le LTV(M') \le LTV(M) = v_{tet}||M||,$$

we have

$$LTV(M') = v_{tet}||M|| = v_{tet}||M'||,$$

where the final equality follows from the fact that the simplicial volume does not change under (p,q)-cabling.

Corollary 1.3.3. Suppose M satisfies Conjecture 1.2.2. Then for any odd p and  $n \in \mathbb{N}$ , the  $(p, 2^n)$ -cable M' also satisfies Conjecture 1.2.2. Moreover, if  $|TV(M)| = v_{tet}||M||$ , then  $|TV(M')| = |TV(M')| = v_{tet}||M'||$ .

*Proof.* Since r is odd,  $(r, 2^n) = 1$  for any  $n \ge 1$ , which means Theorem 1.3.1 holds for any  $(p, 2^n)$ -cable of M provided p is odd. Since ||M|| = ||M'||, this implies that

$$LTV(M') = LTV(M) = v_{tet}||M|| = v_{tet}||M'||,$$

so M' also satisfies Conjecture 1.2.2.

Theorem 1.3.1 also implies that lTV(M') = lTV(M). In the case where  $lTV(M) = v_{tet}||M||$ , we recover the full limit

$$lTV(M') = lTV(M) = v_{tet}||M| = v_{tet}||M'|| = LTV(M').$$

## 3.4 Proof of the Supporting Theorem

In this section, we will provide a proof of Theorem 1.3.4, which we restate here for convenience. The argument involves presenting  $RT_r(C_{p,q})$  as a product of invertible matrices, such that each of their inverses have polynomially bounded operator norm.

**Theorem 1.3.4.** Let p be coprime to some positive integer q. Then  $RT_r(C_{p,q})$  is invertible if and only if r and q are coprime. Moreover, the operator norm  $|||RT_r(C_{p,q})^{-1}|||$  grows at most polynomially.

We will use the following supporting proposition for the proof of Theorem 1.3.4, which is given in Subsection 3.4.1. The proof of this proposition is given in Subsection 3.4.2. We also use a couple of technical lemmas which are subsequently proven in Subsection 3.4.3. We begin by constructing a basis over which  $RT_r(C_{p,q})$  admits a simpler expression.

By the cabling formula given by Theorem 3.2.2,

$$RT_r(C_{p,q})(e_i) \in Span\{e_1, e_{ql+1}, e_{ql-1}\}_{l=1}^{m-1}$$

where  $m = \frac{r-1}{2}$ . Let  $F_m := \{f_l\}_{l=0}^{m-1}$ , where

$$f_0 := e_1$$
  
 $f_l := e_{ql+1} - A^{2pl} e_{ql-1}$   $l = 1, ..., m$ .

Define  $\tilde{f}_l \in Span\{e_1, \dots, e_m\}$  to be the reduction of  $f_l$  under the quotient induced by the symmetries  $e_{-i} = -e_i$  for any  $i \geq 0$  and  $e_{i+nr} = (-1)^n e_i$  for any  $n \in \mathbb{Z}$ . Note that for each l,  $ql \pm 1 = kr + j$  for some non-negative integers k, j where  $0 \leq j < r$ . This means that up to sign, these symmetries imply

$$e_{al\pm 1} = e_{al-kr\pm 1} = e_j \qquad \text{for } 0 \le j \le m \tag{3.1}$$

$$e_{ql\pm 1} = e_{(k+1)r-ql\mp 1} = e_{r-j}$$
 for  $m+1 \le j < r$ . (3.2)

Finally, define  $\tilde{F}_m := {\{\tilde{f}_l\}_{l=0}^{m-1}}$ , and let  $R_m$  be the  $(m \times m)$ -matrix with columns corresponding to the reduced vectors  $\tilde{f}_l$ , for  $l = 0, \ldots, m-1$ . In particular,  $\tilde{f}_l$  corresponds to col(l+1) of  $R_m$ , and the rows of  $R_m$  correspond to the original orthonormal basis  $\{e_1, \ldots, e_m\}$  spanning  $RT_r(T^2)$ .

**Remark 3.4.1.** We note that  $F_m$ ,  $\tilde{F}_m$ , and  $R_m$  are also dependent on p and q, but these dependencies are suppressed to avoid unwieldy notation.

The following proposition will be used to prove Theorem 1.3.4.

**Proposition 3.4.2.** Let r = 2m + 1 be coprime to q. Then  $R_m$  is a change of basis from  $\tilde{F}_m \to \{e_1, \ldots, e_m\}$  and the operator norm  $|||R_m^{-1}|||$  grows at most polynomially in m. Moreover, for  $i \in \{1, \ldots, m\}$ ,

$$RT_r(C_{p,q})(e_i) = A^{\frac{qp}{2}(i^2-1)} \sum_{l \in T_i} A^{-p(\frac{q}{2}l^2+l)} \tilde{f}_l, \tag{3.3}$$

where  $T_i = \{0, 2, \dots, i-1\}$  for odd i and  $T_i = \{1, 3, \dots, i-1\}$  for even i.

The idea of the proof is to leverage symmetric properties of the  $\tilde{f}_l$  to give a presentation of  $R_m^{-1}$  and bound its operator norm. The assumption that (r,q)=1 is necessary for invertibility, as indicated by the following proposition.

**Proposition 3.4.3.** Suppose  $r \geq 3$  is odd and not coprime to q. Then  $R_m$  is singular.

The proofs of Propositions 3.4.2 and 3.4.3 will be given in Subsection 3.4.2.

#### 3.4.1 Proof of Theorem 1.3.4

We now can proceed with the proof of Theorem 1.3.4 assuming Proposition 3.4.2.

Proof of Theorem 1.3.4. We begin with the necessary condition. Suppose (r,q)=d>1. Then there are coprime q',r' such that q=dq' and r=dr'. We claim that row(nd) of  $RT_r(C_{p,q})$  consists of only zeros for each n. Suppose some  $e_{ql\pm 1}=e_{kr+j}$ , where  $0 \le j \le m$ , reduces to  $e_j=e_{nd}$ . Then by Equation (3.1),  $ql-kr\pm 1=nd$ , which means  $d(q'l-r'k-n)=\pm 1$ , which is a contradiction. Similarly, if  $e_{ql\pm 1}=e_{kr+j}$ , where  $m+1 \le j < r$ , reduces to  $e_{r-j}=e_{nd}$ . Then by Equation (3.2),  $d((1+k)r'-q'l-n)=\pm 1$ , which is also a contradiction. This means that  $row(nd)=[0,\ldots,0]$ , thus  $RT_r(C_{p,q})$  is singular.

For sufficiency, suppose (r,q) = 1. By Proposition 3.4.2, we can write  $RT_r(C_{p,q})$  as a product of two diagonal matrices with an upper-triangular matrix and the change of basis  $R_m$ :

$$RT_{r}(C_{p,q}) = R_{m} \begin{pmatrix} 1 & 0 & \dots & 0 \\ 0 & A^{-p\left((2-1)+\frac{q}{2}(2-1)^{2}\right)} & \ddots & \vdots \\ \vdots & & \ddots & & 0 \\ 0 & & \dots & & 0 & A^{-p\left((m-1)+\frac{q}{2}(m-1)^{2}\right)} \end{pmatrix} \times \begin{pmatrix} 1 & 0 & 1 & 0 & 1 & 0 & \dots \\ 0 & 1 & 0 & 1 & 0 & \dots & \\ 0 & 1 & 0 & 1 & 0 & \dots & \\ & & 1 & 0 & 1 & \dots & \\ \vdots & & & 1 & 0 & 1 & \dots \\ & & & & 1 & 0 & \\ & & & & \ddots & \\ 0 & & \dots & & 0 & 1 \end{pmatrix} \begin{pmatrix} 1 & 0 & \dots & 0 \\ 0 & A^{\frac{qp}{2}(2^{2}-1)} & \ddots & \vdots \\ \vdots & \ddots & \ddots & 0 \\ 0 & \dots & 0 & A^{\frac{qp}{2}(m^{2}-1)} \end{pmatrix}.$$

Note that the columns of the middle upper triangular matrix correspond to the index sets  $T_i$  of the sum in Equation (3.3). Inverting this product, we have

$$RT_{r}(C_{p,q})^{-1} = \begin{pmatrix} 1 & 0 & \dots & 0 \\ 0 & A^{\frac{qp}{2}(1-2^{2})} & \ddots & \vdots \\ \vdots & \ddots & \ddots & 0 \\ 0 & \dots & 0 & A^{\frac{qp}{2}(1-m^{2})} \end{pmatrix} \begin{pmatrix} 1 & 0 & -1 & 0 & \dots & 0 \\ 0 & 1 & 0 & -1 & 0 & \dots & 0 \\ & & 1 & 0 & -1 & 0 & \vdots \\ \vdots & & 1 & 0 & -1 & \dots & 0 \\ & & & 1 & \ddots & -1 \\ & & & \ddots & 0 \\ 0 & & \dots & & 0 & 1 \end{pmatrix}$$

$$\times \begin{pmatrix} 1 & 0 & \dots & 0 \\ 0 & A^{p((2-1)+\frac{q}{2}(2-1)^{2})} & \ddots & \vdots \\ \vdots & \ddots & \ddots & 0 \\ 0 & \dots & 0 & A^{p((m-1)+\frac{q}{2}(m-1)^{2})} \end{pmatrix} R_{m}^{-1}.$$

By Proposition 3.4.2,  $|||R_m^{-1}|||$  grows at most polynomially in m, so it is bounded polynomially in r. For the total bound, observe that both of the diagonal matrices are isometries, and

the upper triangular matrix has operator norm bounded above by a polynomial in r by the Cauchy-Schwartz inequality.

### 3.4.2 Proof of Propositions 3.4.2 and 3.4.3

We give proofs of Propositions 3.4.2 and 3.4.3 in this subsection. The following definitions and lemmas will be useful in the proofs.

By the symmetries  $e_{-i} = -e_i$  for any  $i \ge 0$  and  $e_{i+kr} = (-1)^k e_i$  for any  $k \in \mathbb{Z}$ , we may extend the definition of  $f_l$  to all  $l \in \mathbb{Z}$  using the following symmetries:

- $f_l = e_{1+ql} + A^{2pl}e_{1-ql}$  for any  $l \in \mathbb{Z}$ ,
- $f_{l+r} = (-1)^q f_l$  for any  $l \in \mathbb{Z}$ , and
- $f_l = A^{2pl} f_{-l}$ .

The following Lemma will be used to present  $R_m^{-1}$ .

**Lemma 3.4.4.** Let  $r=2m+1\geq 3$  be coprime to q, and let  $q^*$  be the inverse of q modulo r. Then for  $l\in\{0,\ldots,m-1\}$ ,

$$e_{l+1} = \begin{cases} f_0 & \text{if } l = 0 \\ f_{q^*} & \text{if } l = 1 \\ f_{q^*l} + \sum_{k=1}^{\lfloor l/2 \rfloor} A^{2pq^* \left(kl - \sum_{i=0}^{k-1} 2i\right)} f_{q^*(l-2k)} & \text{if } l > 1. \end{cases}$$

$$(3.4)$$

Moreover, for  $i, j \in \{0, \dots, r-1\}$ ,  $q^*i \equiv q^*j \mod r$  if and only if i = j.

*Proof.* Since (r,q) = 1, there is a unique  $q^* \in \mathbb{Z}_r$  such that  $qq^* \equiv 1 \mod r$ . Using the symmetries of  $f_l$  and substituting in  $q^*l$ , we have

$$e_{1+l} = f_{q^*l} - A^{2pq^*l} e_{1-l} = f_{q^*l} + A^{2pq^*l} e_{l-1} = f_{q^*l} + A^{2pq^*l} e_{1+(l-2)}.$$
 (3.5)

We can then apply Equation (3.5) iteratively to express the  $e_i$ 's in terms of the  $f_j$ 's.

$$e_{l+1} = f_{q^*l} + A^{2pq^*l} f_{q^*(l-2)} + A^{2pq^*(2l-2)} f_{q^*(l-4)} + \dots + A^{2pq^* \left( \lfloor l/2 \rfloor l - \sum_{i=0}^{\lfloor l/2 \rfloor - 1} 2i \right)} f_{q^*(l-2\lfloor l/2 \rfloor)}$$

for  $l \in \{2, ..., m-1\}$ . When l = 0, by definition,  $e_1 = f_0$ . When l = 1, Equation (3.5) yields that  $e_2 = f_{q^*}$ . For any  $l \in \{0, ..., m-1\}$ , the iterative use of Equation (3.5) to express  $e_{l+1}$  terminates when the final term is a scalar multiple of either  $e_1$  or  $e_2$ , depending on the parity of l.

For the final statement, note that  $(q^*, r) = 1$ . This means there is a group isomorphism between the cyclic groups  $\{q^*k \mod r | k \in \mathbb{Z}_r\}$  and  $\mathbb{Z}_r$  sending the indices  $q^*k \mod r$  in Equation (3.4) to distinct j for  $j \in \{0, 1, \ldots, r-1\}$ . Since  $q^*k \mod r$  are distinct for  $k \in \mathbb{Z}_r$ , this shows that  $q^*i \equiv q^*j \mod r$  if and only if i = j.

In order to prove Proposition 3.4.2, we will use the following lemma. The proof of this lemma is given in Subsection 3.4.3.

**Lemma 3.4.5.** Suppose  $r = 2m + 1 \ge 3$  is coprime to q. Then

$$\tilde{f}_m = \sum_{j=0}^{m-1} C_j f_j,$$

where  $C_j \in \mathbb{C}$  such that  $|C_j| = 1$  for  $j \in \{0, \dots, m-1\}$ .

Proof of Proposition 3.4.2. It suffices to show that  $R_m$  is nonsingular, in which case  $R_m$  corresponds to the basis transformation  $\tilde{F}_m \to \{e_1, \dots, e_m\}$ . To establish nonsingularity, we will give a presentation of  $R_m^{-1}$  by expressing  $e_i$ , for  $i \in \{1, \dots, m\}$ , in terms of  $f_j$  where  $j \in \{0, \dots, m-1\}$ .

By Lemma 3.4.4, each  $e_i$ , for  $i \in \{1, ..., m\}$ , can be written in terms of  $f_j$  where  $j \in \mathbb{Z}$ . These  $f_j$ 's reduce to  $f_l$ 's, where  $l \in \{0, ..., m\}$ , using the above symmetries. This means that  $Span\{e_1, ..., e_m\}$  of dimension m is contained in  $Span\{f_0, ..., f_m\}$ , a vector space of dimension at most m + 1.

Lemma 3.4.5 implies that  $\tilde{f}_m \in Span\{f_0, \dots, f_{m-1}\}$ , which means that

$$Span\{f_0, ..., f_{m-1}\} = Span\{f_0, ..., f_m\} \supseteq Span\{e_1, ..., e_m\}.$$

Since  $\{e_1, \ldots, e_m\}$  is a basis for the m-dimensional vector space  $RT_r(T^2)$ ,  $\{f_0, \ldots, f_{m-1}\}$  is a set of m vectors, and  $Span\{f_0, \ldots, f_{m-1}\} \supseteq Span\{e_1, \ldots, e_m\}$ , then

$$Span\{f_0, \dots, f_{m-1}\} = Span\{e_1, \dots, e_m\} = RT_r(T^2).$$

From this, we conclude that  $\{f_0, \ldots, f_{m-1}\}$  is also a basis for  $RT_r(T^2)$ . Since  $\{f_0, \ldots, f_{m-1}\}$  is a basis, this implies that  $R_m^{-1}$  is a change-of-basis matrix and is nonsingular, therefore,  $R_m$  is nonsingular.

In order to bound the operator norm  $|||R_m^{-1}|||$ , we study the presentation of  $R_m^{-1}$  more closely. By Lemma 3.4.4, we may express each  $e_i$  as

$$e_i = \sum_{j=0}^{r-1} B_j^i f_j,$$

where  $B_j^i$  is either zero or a root of unity and the summands correspond to the reduction of each index modulo r. We remark that since  $B_j^i$  is either zero or a root of unity,  $|B_j^i| \leq 1$ . Now after applying the symmetry  $f_l = A^{2pl} f_{-l} = A^{2pl} f_{r-l}$  for any l > m, we may express  $e_i$  as

$$e_i = \sum_{j=0}^{m} (B_j^i + A^{2p(r-j)} B_{r-j}^i) f_j = \sum_{j=0}^{m} D_j^i f_j,$$

where  $D_j^i = B_j^i + A^{2p(r-j)}B_{r-j}^i$  and  $|D_j^i| \le 2$ . Additionally, by Lemma 3.4.5, we know that the coefficient of any summand of  $f_m$  in terms of the basis  $\{f_0, \ldots, f_{m-1}\}$  is  $C_j^i$  with  $|C_j^i| = 1$ . This means we may write

$$e_{i} = \left(\sum_{j=0}^{m-1} D_{j}^{i} f_{j}\right) + D_{m}^{i} f_{m}$$

$$= \left(\sum_{j=0}^{m-1} D_{j}^{i} f_{j}\right) + D_{m}^{i} \left(\sum_{k=0}^{m-1} C_{k}^{i} f_{k}\right)$$

$$= \sum_{j=0}^{m-1} \left[D_{m}^{i} C_{j}^{i} + D_{j}^{i}\right] f_{j}.$$

$$= \sum_{j=0}^{m-1} E_{j}^{i} f_{j}$$

where  $E_j^i = D_m^i C_j^i + D_j^i$ . Note that since  $|D_j^i| \leq 2$  and  $|C_j^i| = 1$ , we have

$$|E_j^i| = |D_m^i C_j^i + D_j^i| \le |D_m^i C_j^i| + |D_j^i| = |D_m^i||C_j^i| + |D_j^i| \le 4.$$

Hence every entry of  $R_m^{-1}$  has modulus bounded above by 4. For any complex unit vector  $v = [v_0, \ldots, v_{m-1}]^T$  such that  $|v_i| \le 1$  for  $i \in \{0, \ldots, m-1\}$ , the Cauchy-Schwartz inequality implies that

$$||R_{m}^{-1}v|| = \left| \left| \left[ \sum_{i=0}^{m-1} E_{0}^{i} v_{i}, \dots, \sum_{i=0}^{m-1} E_{m-1}^{i} v_{i} \right]^{T} \right| \right|$$

$$= \left( \left| \sum_{i=0}^{m-1} E_{0}^{i} v_{i} \right|^{2} + \dots + \left| \sum_{i=0}^{m-1} E_{m-1}^{i} v_{i} \right|^{2} \right)^{\frac{1}{2}}$$

$$\leq \left( \sum_{i,j=0}^{m-1} |E_{j}^{i}|^{2} |v_{i}|^{2} \right)^{\frac{1}{2}} \leq \left( \sum_{i,j=0}^{m-1} |E_{j}^{i}|^{2} \right)^{\frac{1}{2}}$$

$$\leq \left( \sum_{i,j=0}^{m-1} 4^{2} \right)^{\frac{1}{2}} = \left( \sum_{i,j=0}^{m-1} 16 \right)^{\frac{1}{2}} = \left( 16m^{2} \right)^{\frac{1}{2}} = 4m.$$

This shows that

$$||R_m^{-1}v|| \le O(m),$$

so the operator norm  $|||R_m^{-1}|||$  is bounded polynomially.

Lastly, by the Cabling Formula in Theorem 3.2.2 and the definition of  $f_l$ , the coefficient of  $f_l$  in  $RT_r(C_{p,q})(e_i)$  is given by

$$RT_r(C_{p,q})(e_i) = A^{\frac{qp}{2}(i^2-1)} \sum_{l \in T_i} A^{-p(\frac{q}{2}l^2+l)} \tilde{f}_l,$$

where  $T_i = \{0, 2, \dots, i-1\}$  for odd i and  $T_i = \{1, 3, \dots, i-1\}$  for even i.

In order to prove Proposition 3.4.3, we establish the following definitions.

For  $1 \leq l \leq m$ , define  $f_l^{\pm} := e_{ql\pm 1}$ . Observe that  $f_l = f_l^+ - A^{2pl} f_l^-$  for  $1 \leq l \leq m$ . In addition, define  $\tilde{f}_l^{\pm}$  to be the quotient of  $f_l^{\pm}$  under the symmetries  $e_{-i} = -e_i$  for any  $i \geq 0$  and  $e_{i+kr} = (-1)^k e_i$  for any  $k \in \mathbb{Z}$ . We will use the convention that  $f_0^+ = f_0 = e_1$  and  $f_0^- = 0$ .

Recall that for each l,  $ql \pm 1 = kr + j$  for some non-negative integers k, j where  $0 \le j < r$ . This means that up to sign,

$$\tilde{f}_{l}^{\pm} = \begin{cases}
e_{j} = e_{ql-kr\pm 1} & 0 \le j \le m \\
e_{r-j} = e_{(k+1)r-ql\mp 1} & m+1 \le j < r.
\end{cases}$$
(3.6)

We can now prove Proposition 3.4.3.

Proof of Proposition 3.4.3. We will repeat the argument given in the proof of Theorem 1.3.4. Suppose (r,q)=d>1, then there are coprime q' and r' such that q=dq' and r=dr'. We claim that row(nd) of  $R_m$  consists of only zeros for each n. Suppose some  $\tilde{f}_l^{\pm}=e_j=e_{nd}$ , then  $ql-kr\pm 1=nd$ . This implies that  $d(q'l-r'k-n)=\mp 1$  which is a contradiction. Similarly, if  $\tilde{f}_l^{\pm}=e_{r-j}=e_{nd}$ , then  $d((1+k)r'-q'l-n)=\pm 1$  which is also a contradiction. This means that  $row(nd)=[0,\ldots,0]$ , thus  $R_m$  is singular.

#### 3.4.3 Proofs of Technical Lemmas

In this subsection, we provide a proof for Lemma 3.4.5. We use the notation introduced in Subsection 3.4.2.

Remark 3.4.6. For the following arguments, we use the convention that equalities between vectors  $e_i$  are necessarily taken up to sign. This ultimately has no effect on the arguments for Proposition 3.4.2 and Theorem 1.3.4.

Recall  $R_m$  is the  $(m \times m)$ -matrix with columns corresponding to  $\tilde{F}_m = \{f_0, \dots, f_{m-1}\}$ . We also define  $S_m$  to be the  $(m \times (m+1))$ -matrix obtained by appending the column corresponding to  $\tilde{f}_m$  to  $R_m$ . The following technical lemmas will be used in the proof of Lemma 3.4.5.

**Lemma 3.4.7.** Suppose  $r = 2m + 1 \ge 3$  is coprime to q, and let  $q^*$  be the multiplicative inverse of q in the ring  $\mathbb{Z}_r$ . Then

(i) Each column of  $S_m$  has at most two nonzero entries. Moreover, for each column with two nonzero entries, their corresponding row indices differ by at most 2.

(ii) Let

$$l^* := \begin{cases} q^* & \text{if } q^* \le m \\ r - q^* & \text{if } q^* > m. \end{cases}$$

Then in  $S_m$ ,  $col(1) = [1, 0, ..., 0]^T$  and  $col(l^* + 1) = [0, D_{l^*}, 0, ..., 0]^T$  where  $D_{l^*}$  is a root of unity. Moreover, every other column of  $S_m$  has exactly two nonzero entries which are roots of unity.

Proof. Part (i): Each column of  $S_m$  corresponds to the reduced vector  $\tilde{f}_l$ ,  $0 \le l \le m$ . Since  $f_l$  is a linear combination of at most two vectors in  $Span\{e_1, e_{ql+1}, e_{ql-1}\}_{l=1}^{m-1}$ , there are at most two nonzero entries in col(l+1).

Now suppose the index of  $f_l^+$  is ql+1=kr+j, where  $0 \le j < r$ . Then the index of  $f_l^-$  is ql-1=kr+j-2=k'r+j', where either (k',j')=(k-1,r+j-2) (for  $j \in \{0,1\}$ ) or (k',j')=(k,j-2) (for  $j \ge 2$ ). We split into cases:

- If j = 0, then j' = r 2,  $\tilde{f}_l^+ = e_0 = 0$ , and  $\tilde{f}_l^- = e_2$ .
- If j=1, then j'=r-1,  $\tilde{f}_l^+=e_{ql-kr+1}=e_1$ , and  $\tilde{f}_l^-=e_{(k+1)r-ql+1}=e_1$ . This implies that  $l=\frac{kr}{q}$ . Since  $l\in\mathbb{Z}$  and r,q are coprime, k=qn, for some  $n\geq 0$ . However, if  $n\geq 1$ , we have  $l\geq 1+r>m$ , which is a contradiction. Thus n=0, so l=0, corresponding to col(1).
- If  $2 \le j \le m$ , then  $\tilde{f}_l^+ = e_j \ne e_{j-2} = \tilde{f}_l^-$ .
- If j = m+1, then j' = m-1 and  $\tilde{f}_l^+ = e_m \neq e_{m-1} = \tilde{f}_l^-$ .
- If j = m + 2, then j' = m and  $\tilde{f}_{l}^{+} = e_{m-2} \neq e_{m} = \tilde{f}_{l}^{-}$ .
- If  $m+3 \le j < r$ , then  $\tilde{f}_l^+ = e_{r-j} \ne e_{r-j+2} = \tilde{f}_l^-$ .

This implies that the row indices of the nonzero entries in each column differ by at most two for every column except col(1). In particular, the only case where the row indices differ by exactly 1 occurs when j = m + 1.

**Part** (ii): Since  $e_{-i} = -e_i$ , we have  $f_l = e_{1+ql} + A^{2pl}e_{1-ql}$  for  $1 \le l \le m$ . Note that col(l+1) has exactly one nonzero entry if and only if one of the following occurs:

- (1) Either 1 + ql and 1 ql are equal or opposite modulo r.
- (2) Either 1 + ql or 1 ql vanishes modulo r.

Case (1) occurs if and only if l=0, corresponding to  $\tilde{f}_0=f_0=e_0$ . In this case,  $col(1)=[1,0,\ldots,0]^T$ .

Case (2) occurs if and only if either  $l = q^*$  or  $l = -q^*$  modulo r. Define

$$l^* := \begin{cases} q^* & \text{if } q^* \le m \\ r - q^* & \text{if } q^* > m. \end{cases}$$

Note that if  $ql \pm 1$  vanishes, then  $|ql \mp 1| = 2$ . Define  $D_{l^*}$  to be the coefficient of the vector  $e_{|ql \mp 1|} = e_2$  obtained from Equation (3.3). This means that  $col(l^* + 1)$  is the unique column with exactly one nonzero entry except for col(1).

Finally, the conclusion follows from the uniqueness of  $l^*$  and Part (i).

The second technical lemma makes use of Lemma 3.4.7 in its proof.

**Lemma 3.4.8.** (i) Each row of  $S_m$  has exactly two nonzero entries.

(ii) There is a unique l',  $1 \leq l' \leq m$ , such that  $col(l'+1) = [0, \ldots, 0, D_{l'}, E_{l'}]^T$ , where  $D_{l'}, E_{l'}$  are roots of unity.

The following lemma will be useful in the proof of Lemma 3.4.8.

**Lemma 3.4.9.** Suppose  $r \geq 3$  is coprime to q, and let  $g_l^{\pm} := ql - kr \pm 1$  and  $h_l^{\pm} = (1+k)r - ql \mp 1$ . Then for  $0 \leq l_1, l_2 \leq m$  with  $l_1 \neq l_2$ ,

- (i)  $g_{l_1}^{\pm} = g_{l_2}^{\pm}$ ,  $g_{l_1}^{\pm} = h_{l_2}^{\mp}$ , and  $h_{l_1}^{\pm} = h_{l_2}^{\pm}$  do not have integer solutions,
- (ii)  $g_{l_1}^{\pm} = g_{l_2}^{\mp}, \ g_{l_1}^{\pm} = h_{l_2}^{\pm}, \ and \ h_{l_1}^{\pm} = h_{l_2}^{\mp} \ may \ each \ have \ integer \ solutions.$

*Proof.* Note  $g_l^{\pm}$  and  $h_l^{\pm}$  encode the two families of indices of the reduced vectors  $\tilde{f}_l^{\pm}$  given in Equation (3.6). There are six equations relating pairs of expressions in  $\{g_l^+, g_l^-, h_l^+, h_l^-\}$ .

**Part** (i): This follows from the fact that (r,q) = 1 and the bounds on  $l_1$  and  $l_2$ . We show each case separately.

Case 1: Suppose  $g_{l_1}^{\pm} = g_{l_2}^{\pm}$  for distinct  $l_1, l_2 \in \{0, \dots, m\}$  and  $k_1, k_2 \in \mathbb{Z}$ . By definition, we have  $ql_1 - k_1r \pm 1 = ql_2 - k_2r \pm 1$ . This implies

$$k_1 - k_2 = \frac{q(l_1 - l_2)}{r} \in \mathbb{Z}.$$

Since  $l_1 \neq l_2$  and (r,q) = 1,  $l_1 - l_2$  must have a nontrivial factor of r, which contradicts the bounds on  $l_1$  and  $l_2$ .

Case 2: Suppose  $g_{l_1}^{\pm} = h_{l_2}^{\mp}$  for distinct  $l_1, l_2 \in \{0, \dots, m\}$  and  $k_1, k_2 \in \mathbb{Z}$ . By definition, we have  $ql_1 - k_1r \pm 1 = (k_2 + 1)r - ql_2 \pm 1$ . This implies

$$k_1 + k_2 + 1 = \frac{q(l_1 + l_2)}{r} \in \mathbb{Z}.$$

Since (r,q) = 1,  $l_1 + l_2$  must have a nontrivial factor of r, which similarly contradicts the bounds on  $l_1$  and  $l_2$ .

Case 3: Suppose  $h_{l_1}^{\pm} = h_{l_2}^{\pm}$  for distinct  $l_1, l_2 \in \{0, \dots, m\}$  and  $k_1, k_2 \in \mathbb{Z}$ . By definition, we have  $(k_1 + 1)r - ql_1 \mp 1 = (k_2 + 1)r - ql_2 \mp 1$ . This implies

$$k_1 - k_2 = \frac{q(l_1 - l_2)}{r} \in \mathbb{Z}.$$

Since  $l_1 \neq l_2$  and (r,q) = 1,  $l_1 - l_2$  must have a nontrivial factor of r, which contradicts the bounds on  $l_1$  and  $l_2$ .

Thus, these three equations do not have any integer solutions  $(l_1, l_2)$  satisfying  $l_i \in \{0, \ldots, m\}$ .

**Part** (ii): We have the following:

- $g_{l_1}^{\pm} = g_{l_2}^{\mp}$  if and only if  $q(l_1 l_2) = (k_1 k_2)r \mp 2$ ,
- $g_{l_1}^{\pm} = h_{l_2}^{\pm}$  if and only if  $q(l_1 + l_2) = (1 + k_1 + k_2)r \mp 2$ , and

•  $h_{l_1}^{\pm} = h_{l_2}^{\mp}$  if and only if  $q(l_1 - l_2) = (k_1 - k_2)r \mp 2$ .

All three of these equations may have integer solutions for  $l_1, l_2 \in \{0, \dots, m\}$ .

*Proof of Lemma 3.4.8.* We will use the same notation as in the proof of Lemma 3.4.7 and in Lemma 3.4.9.

Part (i): It is a corollary of Lemma 3.4.9 that every row of  $S_m$  has at most two nonzero entries. In particular, let  $(l_1, l_2)$  be an integral solution to one of the equations of Lemma 3.4.9 Part (ii). Suppose  $l_3 \in \{0, \ldots, m-1\}$  is such that  $(l_1, l_3)$  and  $(l_2, l_3)$  are both solutions to equations in Lemma 3.4.9 Part (ii). Then by Lemma 3.4.9 Part (i), either  $l_3 = l_1$  or  $l_3 = l_2$ .

Note that by Lemma 3.4.7,  $S_m$  has exactly 2m nonzero entries since there are two in each column other than col(1) and  $col(l^* + 1)$ , which each have exactly 1. This means that every row must have exactly 2 nonzero entries.

Part (ii): In the proof of Lemma 3.4.7 Part (i), we saw that the only value of j corresponding to a column with the nonzero row entry indices differing by 1 is j = m + 1. By Part (i), row(m) of  $S_m$  has exactly 2 nonzero entries. This implies that there are some  $l_1, l_2$  such that  $col(l_1 + 1)$  has nonzero entries in row(m) and row(m - 1) and  $col(l_2 + 1)$  has nonzero entries in row(m) and row(m - 2). Take  $l' = l_1$ . Finally, define  $D_{l'}$  and  $E_{l'}$  to be the coefficients of the vectors  $e_{m-1}$  and  $e_m$  defined by Equation (3.3), respectively.

Lastly, we are ready to prove Lemma 3.4.5.

Proof of Lemma 3.4.5. The last column col(m+1) of the matrix  $S_m$  represents the reduced vector  $f_m$  written in terms of the basis  $\{e_1, \ldots, e_m\}$ . We will prove Lemma 3.4.5 by showing that col(m+1) can be written as a linear combination of the first m columns. From this linear combination, we will see that the coefficients will have the required bounds from the statement.

We claim that col(m+1) of  $S_m$  can be written as a linear combination of elements in  $\{f_0, \ldots, f_{m-1}\}$ . From Lemma 3.4.7 Part (ii), either the col(m+1) has exactly one nonzero

entry, corresponding to the case  $l^* = m$ , or exactly two nonzero entries, corresponding to when  $l^* < m$ .

#### Case 1:

We first consider the case  $l^* = m$ . Here, the nonzero entry of col(m+1) lies in row(2). This implies that  $\tilde{f}_m \in Span\{e_1, \ldots, e_m\}$  has a scalar of  $e_2$  as a summand. By Lemma 3.4.8 Part (i), we know that there is exactly one other nonzero entry in row(2) in some column  $j_1$ . From the argument of Lemma 3.4.7 Part (i), there exists a nonzero entry in row(4) of  $col(j_1)$ . Lemma 3.4.8 Part (i) implies there exists a nonzero entry in some column  $j_2$  and row(4). From the argument of Lemma 3.4.7 Part (i), there exists a nonzero entry in row(6) of  $col(j_2)$ . Again, we pick the other nonzero entry of row(6) which lies in some column  $j_3$ . Note that  $col(j_3)$  cannot be equal to any of the previous columns. If it were a previous column, it would contradict our bound on the number of nonzero entries in a column. We continue this iteration until we reach either row(m-1) or row(m), depending on the parity of m.

If m-1 is even, by Lemma 3.4.8 Part (ii), the next corresponding row with a nonzero entry will be row(m) where m is odd. Similarly, if m is even, by Lemma 3.4.8 Part (ii), the next corresponding row with a nonzero entry will be row(m-1) where m-1 is odd. Now when we continue the algorithm, our subsequent row indices will be odd and decrease by 2 until we reach row(1). By Lemma 3.4.8 Part (i) and Lemma 3.4.7 Part (ii), there exists a nonzero entry in row(1) of col(1), and it is the only nonzero entry in col(1). Since every entry of our matrix is a root of unity by Lemma 3.4.7 Part (ii) and terminates at row(1), then scalars by roots of unity of the columns appearing in our sequence gives  $f_m$  as a linear combination of elements of  $\{f_0, \ldots, f_{m-1}\}$  where all coefficients are roots of unity.

## Case 2:

Now suppose col(m+1) has exactly two nonzero entries. We denote the row indices of these entries by  $i_1^-$  and  $i_1^+$ , where  $i_1^- < i_1^+$ . By Lemma 3.4.8 Part (i),  $row(i_1^-)$  has another nonzero entry in some other column  $j_1^-$ . Similarly,  $row(i_1^+)$  has another nonzero entry in

some column  $j_1^+$ . We make the following claim, which we prove at the end.

Claim:  $j_1^- \neq j_1^+$ .

We will proceed similarly to the first case. Consider the column  $col(j_1^+)$ , which has exactly two nonzero entries and cannot correspond to either col(1) or  $col(l^*+1)$  since  $i_1^+ > 2$ . By Lemma 3.4.8 Part (i) and the claim, there exists another nonzero entry in some  $row(i_2^+)$  of  $col(j_1^+)$  such that  $(i_2^+ - i_1^+) \in \{-1, 1, 2\}$ . The case when  $(i_2^+ - i_1^+) = -1$  corresponds to  $i_1^+ = m$ , and the case when  $(i_2^+ - i_1^+) = 1$  corresponds to  $i_1^+ = m - 1$ . We now implement the same argument as the case with one entry in col(m+1). Note that, in this procedure, we do not utilize any rows with index less than  $i_1^-$  with the same parity as  $i_1^-$ . If  $i_1^- = m - 1$  and  $i_1^+ = m$ , they will have different parities. In the other case,  $i_1^-$  will have the same parity of  $i_k^+$  until we have a k such that  $(i_k^+ - i_{k-1}^+) \in \{-1, 1\}$ . This implies that for all  $k' \geq k$ ,  $i_{k'}^+$  will have opposite parity to  $i_1^-$ .

We now follow the same algorithm beginning with  $row(i_1^-)$ . By the claim, the indices of our subsequent rows  $i_k^-$  must be decreasing. Otherwise, this would contradict Lemma 3.4.8 Part (i).

Since both cases in total utilize every row exactly once,  $f_m$  is given by a linear combination of elements of  $\{f_0, \ldots, f_{m-1}\}$  where, by Lemma 3.4.7 Part (ii), all coefficients are roots of unity.

# **Proof of Claim:**

It now suffices to prove that  $j_1^+ \neq j_1^-$ . By contradiction, let us assume that  $j_1^+ = j_1^-$ , and we will denote  $i_1 = i_1^+$ .

If  $i_1 = m$ , then either  $i_1^- = m - 1$  or  $i_1^- = m - 2$ . If  $i_1^- = m - 1$ , then since  $j_1^+ = j_1^-$ , we will have two columns with nonzero entries in the last two rows. This contradicts Lemma 3.4.8 Part (ii), which states that there is a unique such column. If  $i_1^- = m - 2$ , then there are two distinct columns with nonzero entries in row(m-2) and row(m). By Lemma 3.4.8 Part (ii), there must exist a different column with nonzero entries in row(m-1) and row(m), which contradicts there being at most 2 entries in row(m).

If  $i_1 = m - 1$ , then  $i_1^- < m - 1$ , and there are no other columns with nonzero entries in row(m-1) besides  $col(j_1^+)$  and col(m+1). By Lemma 3.4.8 Part (ii), there must exist a different column with nonzero entries in row(m-1) and row(m), which contradicts there being at most 2 entries in row(m-1).

In the general case, we assume  $i_1 \leq m-2$ , and we will define  $i_2 = i_1 + 2$ . Since  $j_1^+ = j_1^-$ ,  $col(j_1^+)$  and col(m+1) already have two nonzero entries. Since  $i_2 > 2$ , these entries cannot be in either col(1) or  $col(l^*+1)$  since they only have entries in the first two rows. This implies that the columns which correspond to nonzero entries in  $row(i_2)$  must have exactly two nonzero entries in some columns  $col(j_2^+)$  and  $col(j_2^-)$  such that  $j_2^+, j_2^- \notin \{j_1^+, m+1\}$ . Since  $row(i_1)$  has two nonzero entries in  $col(j_1^+)$  and col(m+1), the other nonzero entries in  $col(j_2^+)$  and  $col(j_2^-)$  must be in some  $row(i_3)$ , where  $i_3 - i_2 \in \{-1, 1, 2\}$ .

- If  $i_3 i_2 = -1$ , we have  $i_2 = m$  and  $i_3 = m 1$ . Here, we reach the same contradiction as when  $i_1 = m$  and  $i_1 = m 1$ .
- If  $i_3 i_2 = 1$ , then  $i_2 = m 1$  and  $i_3 = m$ . This gives the same contradiction as when  $i_1 = m$  and  $i_1^- = m 1$ .
- If  $i_3 i_2 = 2$  with  $i_2 = m 2$  and  $i_3 = m$ , then our argument is the same as when  $i_1 = m$  and  $i_1^- = m 2$ .

Finally, we consider when  $i_3 - i_2 = 2$  and  $i_3 \neq m$ . In this case, we can continue to iterate the same algorithm until we reach the same contradictions.

#### 3.5 Further Directions

The primary approach of this chapter utilizes the invertibility of the operator  $RT_r$  on the cable space  $C_{p,q}$  as well as a polynomial bound on its operator norm. The same methodology could apply in the context for the operator  $RT_r$  for other cable spaces.

Although the technique may apply in the case when the cable space has positive simplicial volume, a more natural approach would be to generalize our argument to other cable spaces with simplicial volume zero. For example, we may consider the manifold defined as follows. Let  $N = \Sigma_{g,2} \times S^1$  where  $\Sigma_{g,2}$  is a orientable compact genus g surface with 2 boundary components. Now let  $\{x_i\}_{i=1}^m \subset \Sigma_{g,2}$  such that  $\{x_i\}_{i=1}^m \times S^1$  is a collection of m vertical fibers in N. We define the Seifert cable space  $C(s_1, \ldots s_m)$  where  $s_i = \frac{p_i}{q_i} \in \mathbb{Q}$  to be the manifold obtained by performing  $s_i$ -Dehn surgery along the i-th vertical fiber in N.

If an analogous result to Theorem 1.3.4 holds for the Seifert cable space  $C(s_1, \ldots s_m)$ , the corresponding Theorem 1.3.1 will also follow as well as its applications to Conjecture 1.2.2. Similar to the constraint of Theorem 1.3.4 where r and q must be coprime, the analogous result for the Seifert cable space may require a related caveat. This leads to the following concluding question.

**Question 3.5.1.** Is  $RT_r(C(s_1, ... s_m))$  invertible when r is sufficiently large and coprime to every  $q_i$ ?

#### CHAPTER 4

#### ASYMPTOTIC ADDITIVITY FOR AN INFINITE FAMILY

This chapter is based on joint work with Kumar published in the Journal of the London Mathematical Society [52].

In this chapter, we introduce an infinite family of 3-manifolds with interesting geometric and combinatorial characteristics that satisfy an extended version of the Turaev-Viro invariant Volume Conjecture (Conjecture 1.2.2). In particular, we will show that the asymptotics of the Turaev-Viro invariants are additive under gluings of elementary hyperbolic cusped manifolds arising from a construction due to Agol [4]. These elementary hyperbolic cusped manifolds correspond to JSJ pieces in the resulting manifold, so they are additive with respect to the simplicial volume.

#### 4.1 Introduction

For this chapter, we will be concerned with the SU(2)-version of the Turaev–Viro invariants, for which Conjecture 1.2.1 was originally stated; however, the results hold for the SO(3)-version with minor changes.

In defining these two versions of the Turaev–Viro invariants, the distinction arises from the construction of the topological quantum fields theories of the Reshetikhin–Turaev invariants by Blanchet, Habegger, Masbaum, and Vogel [11]. In the authors' work, the elements of the index set  $I_r$  correspond to the irreducible representations of SU(2). As SU(2) is a double-covering of SO(3), we remark that the SO(3) theory can be obtained as the restriction of the elements of the index set to elements with corresponding representations that lift to SO(3). In addition to considering different roots of unity, this is realized as requiring that r is odd for SO(3) as opposed to any integer r for SU(2). By following the construction, the Turaev–Viro invariants can also be defined to have an SU(2)-version and an SO(3)-version. For more details between these two versions of the Turaev–Viro invariants, we refer to Sections 2 and 3 of [25] by Detcherry, Kalfagianni, and Yang where the SO(3) Turaev–Viro invariants are defined.

Recall that the simplicial volume of a manifold is the sum of the volumes of its hyperbolic JSJ pieces, and we say a manifold satisfies the asymptotic additivity property if the asymptotics of its Turaev–Viro invariants behave analogously, i.e. the sum of the asymptotics of the Turaev–Viro invariants of the JSJ pieces of a given manifold coincide with the asymptotics of the Turaev–Viro invariants of the manifold itself. This property has been proven for a few families of manifolds, see Subsection 1.4, but our construction is the first which glues several (> 2) hyperbolic pieces to produce infinite families of manifolds satisfying the asymptotic additivity property.

As the main result of this chapter, we restate Theorem 1.4.1, which establishes the asymptotic additivity property for an infinite family of manifolds glued from several hyperbolic pieces. Our construction is inspired by a construction of Agol [4] of cusped 3-manifolds with well-understood geometric properties. Agol begins with an oriented  $S^1$ -bundle over a surface and systematically drills out curves to produce octahedral link complements. This procedure depends on a path on the 1-skeleton of the pants complex of the surface. The hyperbolic building blocks for our family  $\mathcal{M}$  of manifolds are obtained as follows: We begin with a trivial  $S^1$ -bundle over the once-punctured torus and use Agol's procedure to drill out a 2-component link. This produces a hyperbolic manifold, which we call an S-piece, of volume  $2v_{oct}$ , where  $v_{oct} \approx 3.66$  is the volume of the regular ideal hyperbolic octahedron. Then we begin with a trivial  $S^1$ -bundle over the four-punctured sphere and use Agol's procedure to drill out a 2-component link, producing a hyperbolic manifold of volume  $4v_{oct}$  which we call an A-piece. Gluing k S-pieces and l d-pieces along their original boundaries produces a compact manifold  $M_L(k, l) \in \mathcal{M}$ , where L is the union of the link components of the S- and d-pieces.

The main result of this chapter is the following.

**Theorem 1.4.1.** Let  $M_L(k,l) \in \mathcal{M}$ . Then for r running over odd integers and  $q = e^{\frac{2\pi\sqrt{-1}}{r}}$ ,

$$\lim_{r \to \infty} \frac{2\pi}{r} \log |TV_r(M_L(k, l); q)| = v_{tet} ||M_L(k, l)|| = 2(k + 2l)v_{oct}.$$

In general, the asymptotic additivity property is difficult to prove. In order to simplify the calculation, the family  $\mathcal{M}$  was constructed to have several advantageous properties which help make our argument more tractable. We first remark that the Turaev–Viro invariants can be computed from the relative Reshetikhin–Turaev invariants by a result of Belletti, Detcherry, Kalfagianni, and Yang in [9]. In addition, our family  $\mathcal{M}$  can be described effectively from Turaev's shadow perspective [77, Section 3] which Turaev related to the relative Reshetikhin–Turaev invariants in [78, Chapter X]. Additionally, manifolds in the family  $\mathcal{M}$  have relative Reshetikhin–Turaev invariants which are comparably simple to manage as well as well-understood simplicial volumes.

We note that the consideration of the shadow perspective was taken from the following works. In [18], Costantino extended the colored Jones invariants to links in  $S^3\#_k(S^2\times S^1)$  and used the formulation of the invariant to prove a version of the volume conjecture for a family of links in  $S^3\#_k(S^2\times S^1)$  known as the fundamental shadow links. Furthermore in [9], Belletti, Detcherry, Kalfagianni, and Yang represented the Turaev–Viro invariants in terms of the relative Reshetikhin–Turaev invariants, which they used in combination with Costantino's formulation [17] to show the fundamental shadow links satisfy Conjecture 1.2.1. In [85], Wong and Yang also use this shadow viewpoint to study a version of the volume conjecture involving the relative Reshetikhin–Turaev invariants. In this chapter, we utilize the same approach to prove Theorem 1.4.1; however, we note that the form of the relative Reshetikhin–Turaev invariants we study here is more complicated.

Moreover, the Turaev–Viro invariants are related to a measure of complexity of a manifold called the *shadow complexity* derived from Turaev's shadow perspective for 3-manifolds. We refer to Costantino and Thurston [19] or Turaev [78] for more details. The shadow complexity  $c \in \mathbb{N}$  of a manifold gives a sharp upper bound for the growth rate of its Turaev–Viro invariants as stated in the following.

Corollary 4.1.1 ([9], Corollary 3.11). If M has shadow complexity c, then

$$lTV(M) \le LTV(M) \le 2cv_{oct}$$

where  $lTV(M) = \liminf_{r \to \infty} \frac{2\pi}{r} \log |TV_r(M;q)|$  and  $LTV(M) = \limsup_{r \to \infty} \frac{2\pi}{r} \log |TV_r(M;q)|$ . Furthermore, we have equalities for fundamental shadow links.

In a similar way, the manifolds  $M_L(k,l)$  have a shadow complexity based on the elementary pieces used in their construction such that they satisfy the same equalities as the fundamental shadow links as shown in Theorem 1.4.1. In terms of the shadow construction described in Subsection 4.3.2, the shadow complexity is the number of the shadow's vertices c = k + 2l.

The remainder of the chapter is organized as follows: We recall Agol's construction of cusped 3-manifolds and introduce the family of manifolds  $\mathcal{M}$  in Section 4.2. In Section 4.3, we introduce Turaev's shadow invariant and discuss its relationship with the relative Reshetikhin–Turaev and Turaev–Viro invariants. The precise definitions of the relative Reshetikhin–Turaev and Turaev–Viro invariants are not needed to understand the proof of Theorem 1.4.1, just their relationships to Turaev's shadow invariants, so we refer to Chapter 2 for those details. Finally, the proof of Theorem 1.4.1 comprises Section 4.4.

### 4.2 An Infinite Family of Octahedral Manifolds

In this section, we will construct the link family  $\mathcal{M}$ . We begin by recalling a construction of Agol [4] in Subsection 4.2.1. In Subsection 4.2.2, we use Agol's algorithm to construct the family of link complements  $\mathcal{M}$ .

# 4.2.1 Agol's construction of cusped 3-manifolds

Agol [4] introduced a method which uses the pants complex of a surface and links in bundles over that surface to construct compact manifolds with well-understood geometric characteristics. We outline the construction here.

**Definition 4.2.1.** Let  $\Sigma_{g,n}$  be a connected compact orientable surface of genus g with n boundary components and Euler characteristic  $\chi(\Sigma_{g,n}) = 2(1-g) - n$ . We denote the closed

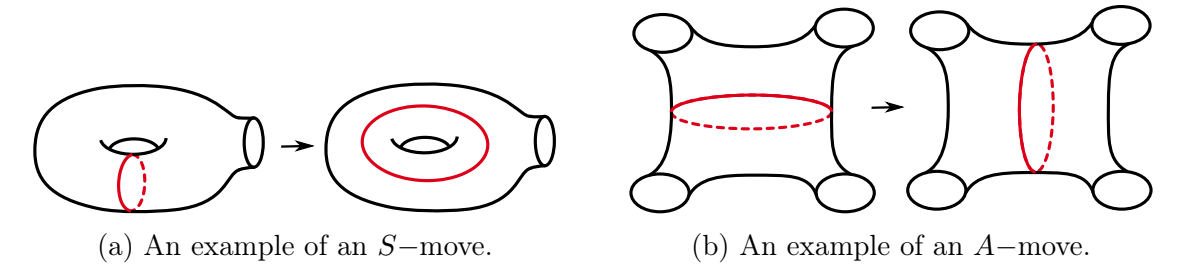


Figure 4.1 Examples of the elementary moves.

surface of genus g by  $\Sigma_g$ . For  $\chi(\Sigma_{g,n}) < 0$ , a pants decomposition is a maximal collection of distinct smoothly embedded simple closed curves on  $\Sigma_{g,n}$  which have trivial intersection pairwise. A pants decomposition  $\{\alpha_1, \ldots, \alpha_N\}$  consists of N = 3(g-1) + n curves, and cutting  $\Sigma_{g,n}$  along these curves produces  $-\chi(\Sigma_{g,n})$  pairs of pants  $\Sigma_{0,3}$ .

We note that the pants decompositions of a given surface are not unique.

**Definition 4.2.2.** Two pants decompositions  $P = \{\alpha_1, \ldots, \alpha_N\}$  and  $P' = \{\alpha'_1, \ldots, \alpha'_N\}$  of a surface  $\Sigma_{g,n}$  are said to differ by an elementary move if P' can be obtained from P by replacing one curve  $\alpha_i$  with another curve  $\alpha'_i$  such that  $\alpha_i$  and  $\alpha'_i$  intersect minimally in one of the following ways:

- If  $\alpha_i$  lies on a  $\Sigma_{1,1}$  in the complement of the other curves in P, then  $\alpha_i$  is on a single pair of pants and  $\alpha_i$  and  $\alpha'_i$  must intersect exactly once.
- If  $\alpha_i$  lies on a  $\Sigma_{0,4}$  in the complement of the other curves in P, then  $\alpha_i$  is the boundary between two pairs of pants and  $\alpha_i$  and  $\alpha'_i$  must intersect exactly twice.

We call a curve switch on  $\Sigma_{1,1}$  a *simple move*, or S-move, and a curve switch on  $\Sigma_{0,4}$  an associativity move, or A-move. Examples of the elementary moves are given in Figure 4.1.

**Definition 4.2.3.** [36] The pants decomposition graph  $\mathcal{P}(\Sigma_{g,n})^{(1)}$  of  $\Sigma_{g,n}$  is the graph with vertices corresponding to isotopy classes of pants decompositions of  $\Sigma_{g,n}$  and edges corresponding to pairs of isotopy classes which differ by a single elementary move.

The following theorem, originally stated at the end of [37], is proven by Hatcher, Lochak, and Schneps in Theorem 2 of [36].

**Theorem 4.2.4** ([36], Theorem 2). Let  $g, n \in \mathbb{N} \cup \{0\}$  and let  $\Sigma_{g,n}$  be a connected compact orientable surface with  $\chi(\Sigma_{g,n}) < 0$ . Then the pants decomposition graph  $\mathcal{P}(\Sigma_{g,n})^{(1)}$  is connected.

**Definition 4.2.5.** For a given homeomorphism  $f: \Sigma_{g,n} \to \Sigma_{g,n}$ , define the associated mapping torus by  $T_f = (\Sigma_{g,n} \times [0,1])/((x,0) \sim (f(x),1))$ .

In [4], Agol constructed cusped 3-manifolds from the mapping torus  $T_f$  and a path P on the pants decomposition graph  $\mathcal{P}(\Sigma_{g,n})^{(1)}$ . We outline the construction as follows:

- Let  $f: \Sigma_{g,n} \to \Sigma_{g,n}$  be a homeomorphism and  $P = \{P_i\}_{i=0}^m$  be a path such that each  $P_i$  is a vertex of the pants decomposition graph, each  $P_i$  and  $P_{i+1}$  are connected by an edge, and  $P_m = f(P_0)$ .
- For  $i \in \{1, ..., m\}$ , let  $\beta_i$  correspond to the simple closed curve in  $P_i$  obtained from performing a single elementary move on a simple closed curve in  $P_{i-1}$ . We assume there exists no curve  $\beta_j$  that is contained in all the pants decompositions  $P_i$ .
- Let  $B = \{B_i\}_{i=1}^m$  be the link in  $T_f$  such that  $B_i = \beta_i \times \{\frac{i}{m}\}$  is a link component, and we define the cusped 3-manifold  $M_P$  to be the complement of the link B in  $T_f$ .

Agol proves the following lemma in [4].

**Lemma 4.2.6** ([4], Lemma 2.3 and Corollary 2.4). Let  $M_P$  be the cusped 3-manifold obtained from Agol's construction for a homeomorphism  $f: \Sigma_{g,n} \to \Sigma_{g,n}$  and a path P on  $\mathcal{P}(\Sigma_{g,n})^{(1)}$ . Then  $M_P$  has a complete hyperbolic metric such that  $vol(M_P) = (|S| + 2|A|)v_{oct}$  where  $vol(M_P)$  is the hyperbolic volume, |S| and |A| are the number of S- and A-moves in P, respectively, and  $v_{oct} \approx 3.66$  is the volume of a regular ideal hyperbolic octahedron.

### 4.2.2 Manifold construction

Here we will discuss a family of links with octahedral complements in  $S^1$ -bundles over connected closed orientable surfaces.

Let  $\Sigma_g$  be a connected closed orientable surface of genus g constructed by gluing k copies of  $\Sigma_{1,1}$  and l copies of  $\Sigma_{0,4}$  along their boundary components. We glue each pair of  $S^1$  boundary components via identity maps. Since  $\Sigma_g$  has no boundary components, k must be even.

Consider the closed orientable 3-manifold  $T_{id} = \Sigma_g \times S^1$ . Note each gluing circle of  $\Sigma_g$  corresponds to a torus in  $T_{id}$ . This manifold can be decomposed into elementary pieces by cutting along these tori so that the resulting pieces are trivial  $S^1$ -bundles over k copies of  $\Sigma_{1,1}$  and l copies of  $\Sigma_{0,4}$ . We perform a pair of S-moves in each copy of  $\Sigma_{1,1}$  with  $P_0 = P_2$  on the pants complex of  $\Sigma_{1,1}$  to produce a two-component link  $L_S$ . By Lemma 4.2.6, the complement of  $L_S$  in  $\Sigma_{1,1} \times S^1$  has a complete hyperbolic metric with hyperbolic volume  $2v_{oct}$ . We call this complement an S-piece. Similarly, we perform a pair of A-moves in each copy of  $\Sigma_{0,4}$  with  $P_0 = P_2$  to produce a two-component link  $L_A$ . By Lemma 4.2.6, the complement of  $L_A$  in  $\Sigma_{0,4} \times S^1$  has a complete hyperbolic metric with hyperbolic volume  $4v_{oct}$ . We call this complement an A-piece.

Let  $L = \bigsqcup_{i=1}^k L_S^i \cup \bigsqcup_{j=1}^l L_A^j$  be the union of these two component links in  $\Sigma_g \times S^1$ . We denote the (2k+2l)-component link complement  $(\Sigma_g \times S^1) \setminus L$  by  $M_L(k,l)$ . We remark that  $M_L(k,l)$  is not hyperbolic since the gluing procedure produces essential tori. However, by Lemma 4.2.6, each S-piece and A-piece of  $M_L(k,l)$  contributes  $2v_{oct}$  and  $4v_{oct}$  to the simplicial volume, respectively, so  $v_{tet} ||M_L(k,l)|| = 2(k+2l)v_{oct}$ . Two examples of manifolds of type (2,2) are given in Figure 4.2. Figure 4.3 gives a decomposition of each example into their respective S- and A-pieces.

Let  $\mathcal{M} = \{M_L(k,l) \mid L \subset \Sigma_g \times S^1, g \geq 2, k, l \in \mathbb{N}, k \text{ even}\}$  be the family of compact orientable 3-manifolds constructed from k S-pieces and l A-pieces. In Section 4.4, we will prove Theorem 1.4.1 for manifolds in this infinite family.

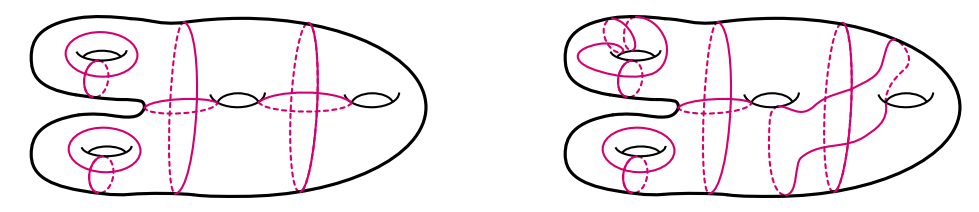


Figure 4.2 The projections of  $M_L(2,2)$  and  $M_{L'}(2,2)$  onto the base surface  $\Sigma_4$ , where L and L' are 8-component links in  $\Sigma_4 \times S^1$ .

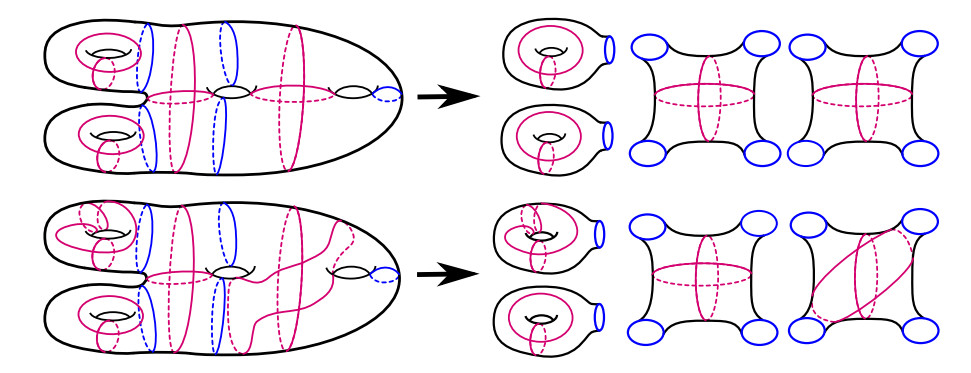


Figure 4.3 From cutting  $\Sigma_4$  along the blue curves which lift to essential tori in  $M_L(2,2)$  and  $M'_L(2,2)$ , we obtain two S-pieces and two A-pieces.

Remark 4.2.7. Note that since we only require that  $P_0 = P_2$  in the construction of the S- and A-pieces, we can take  $P_0$  to be an arbitrary vertex on the pants decomposition graph which gives rise to infinitely many choices for  $P_1$ . This implies that we also have infinitely many choices for the elementary pieces used in the construction of  $M_L(k,l)$ . That being said, because they are hyperbolic, Corollary 6.6.2 by Thurston [74] implies that there are at most finitely many elementary pieces up to homeomorphism.

# 4.3 The Turaev-Viro Invariants from the Shadow Perspective

In this section, we introduce Turaev's shadow theory of 3-manifolds. We begin by stating some useful asymptotic properties of the quantum 6j-symbols. Then we introduce Turaev's shadow state sum invariant for links in  $S^1$ -bundles over surfaces using quantum 6j-symbols and briefly discuss how Turaev's shadow construction can be generalized to all 3-manifolds. We then discuss the relationship between the relative Reshetikhin–Turaev invariants and the shadow state sum invariant. This will allow us to use the results of Belletti, Detcherry, Kalfagianni, and Yang [9] stated in Proposition 2.3.9 to compute the Turaev-Viro invariants

using the shadow state sum invariant.

For the rest of this chapter, let  $r \geq 3$  be an odd integer and  $q = e^{\frac{2\pi\sqrt{-1}}{r}}$ .

# 4.3.1 Properties of the Quantum 6*j*-symbols

In this subsection, we will give some relevant properties of the quantum 6j-symbols for the integer r and root q defined in Subsection 2.3.1 of Chapter 2. Deep algebraic and geometric properties of the quantum 6j-symbols are studied in Kirillov and Reshetikhin [50], Turaev and Viro [79], and Turaev [77, 78], but these particular results will be useful in the proof of Theorem 1.4.1.

Belletti, Detcherry, Kalfagianni, and Yang [9] give an upper bound for the growth rate of the quantum 6j-symbol, which we state in the following theorem. Related results on these growth rates are also due to Costantino [17].

**Theorem 4.3.1** ([9], Theorem 1.2 and Lemma 3.13). For any odd  $r \ge 3$  and any r-admissible 6-tuple  $(a_1, \ldots, a_6)$ ,

$$\frac{2\pi}{r} \log \left\| \begin{array}{ccc} a_1 & a_2 & a_3 \\ a_4 & a_5 & a_6 \end{array} \right|_{q=e^{\frac{2\pi\sqrt{-1}}{r}}} \le v_{oct} + O\left(\frac{\log(r)}{r}\right).$$
(4.1)

Moreover, this bound is sharp. If the sign is chosen such that  $\frac{r\pm 1}{2}$  is even, then

$$\frac{2\pi}{r} \log \left\| \frac{\frac{r\pm 1}{2} \frac{r\pm 1}{2} \frac{r\pm 1}{2}}{\frac{r\pm 1}{2} \frac{r\pm 1}{2}} \right\|_{q=e^{\frac{2\pi\sqrt{-1}}{r}}} = v_{oct} + O\left(\frac{\log(r)}{r}\right). \tag{4.2}$$

The authors of [9] also prove the following result of Costantino [17] for the root  $q = e^{\frac{2\pi\sqrt{-1}}{r}}$ . Let the summand of Equation (2.1) be given by

$$S_k = \frac{(-1)^k [k+1]!}{\prod_{i=1}^4 [k-T_i]! \prod_{j=1}^3 [Q_j - k]!}$$

where  $k \in \{\max\{T_i\}, \dots, \min\{Q_j\}\}\$  for i = 1, 2, 3, 4 and j = 1, 2, 3.

**Theorem 4.3.2** ([9], Theorem A.1). Let  $(a_1^{(r)}, \ldots, a_6^{(r)})$  be a sequence of admissible 6-tuples such that

(a) 
$$0 \le Q_j - T_i \le \frac{r-2}{2}$$
 for  $i = 1, 2, 3, 4$  and  $j = 1, 2, 3$ , and

(b) 
$$\frac{r-2}{2} \le T_i \le r-2$$
 for  $i = 1, 2, 3, 4$ .

Let 
$$\theta_i = \lim_{r \to \infty} \frac{2\pi a_i^{(r)}}{r}$$
 and let  $\alpha_i = |\pi - \theta_i|$ . Then

- (1) for each r, and for  $k \in \{\max\{T_i\}, \ldots, \min\{Q_j\}\}\$ , the sign of  $S_k$  is independent of k,
- (2)  $\alpha_1, \ldots, \alpha_6$  are the dihedral angles of an ideal or a hyperideal hyperbolic tetrahedron  $\Delta$ , see Remark 4.3.3, and
- (3) as r runs over the odd integers

$$\lim_{r \to \infty} \frac{2\pi}{r} \log \left\| \begin{array}{ccc} a_1^{(r)} & a_2^{(r)} & a_3^{(r)} \\ a_4^{(r)} & a_5^{(r)} & a_6^{(r)} \end{array} \right\|_{q=e^{\frac{2\pi\sqrt{-1}}{r}}} = vol(\Delta)$$

$$(4.3)$$

**Remark 4.3.3.** We refer to [7] for details on hyperideal hyperbolic tetrahedra. In particular, the numbers  $\alpha_1, \ldots, \alpha_6$  correspond to the dihedral angles of an ideal or hyperideal hyperbolic tetrahedron if and only if around each vertex,  $\alpha_i + \alpha_j + \alpha_k \leq \pi$  for  $i, j, k \in \{1, \ldots, 6\}$ .

The even integers can be written as the two sets  $\{\frac{r+1}{2} \mid r \equiv 3 \mod 4\}$  and  $\{\frac{r-1}{2} \mid r \equiv 1 \mod 4\}$  corresponding to the subsequences that achieve the sharp upper bound of Theorem 4.3.1 Equation (4.2). Another such pair of subsequences is  $(\frac{r-3}{2})$  and  $(\frac{r-1}{2})$ . The following is analogous to Lemma 3.13 of [9].

**Lemma 4.3.4.** If the sign is chosen such that  $\frac{r-2\pm 1}{2}$  is even, then

$$\frac{2\pi}{r} \log \left\| \frac{\frac{r-2\pm 1}{2}}{\frac{r-2\pm 1}{2}} \frac{\frac{r-2\pm 1}{2}}{\frac{r-2\pm 1}{2}} \frac{\frac{r-2\pm 1}{2}}{\frac{r-2\pm 1}{2}} \right\|_{q=e^{\frac{2\pi\sqrt{-1}}{r}}} = v_{oct} + O\left(\frac{\log(r)}{r}\right). \tag{4.4}$$

Proof. First note that the  $r \equiv 1 \mod 4$  case is covered by Equation (4.2). When  $r \equiv 3 \mod 4$ ,  $T_i = \frac{3(r-3)}{4}$  for all i = 1, 2, 3, 4 and  $Q_j = r - 3$  for j = 1, 2, 3, so the 6-tuple  $\left(\frac{r-3}{2}, \ldots, \frac{r-3}{2}\right)$  satisfies the assumptions of Theorem 4.3.2 for  $r \geq 5$ . Here the corresponding hyperideal truncated tetrahedron  $\Delta$  has dihedral angles  $\alpha_i = 0$  for all i, so  $\Delta$  is a regular

ideal hyperbolic octahedron and  $vol(\Delta) = v_{oct}$ . We refer to [17], Definition 2.1 for details. By part (3) of Theorem 4.3.2,

$$\lim_{r \to \infty} \frac{2\pi}{r} \log \left\| \frac{\frac{r-3}{2}}{\frac{r-3}{2}} \cdot \frac{\frac{r-3}{2}}{\frac{r-3}{2}} \right\|_{q=e^{\frac{2\pi\sqrt{-1}}{r}}} = v_{oct}.$$

### 4.3.2 Shadow state sum invariants

We now describe Turaev's state sum invariants for two-dimensional polyhedra representing links in  $S^1$ -bundles over surfaces. In an effort to construct analogous invariants to the colored Jones polynomial of links in  $S^3$ , Turaev [77, 78] introduces a technique to present links in  $S^1$ -fibrations over surfaces as loops on  $\Sigma_g$  with additional topological data given by the bundle. From this 2-dimensional presentation, we can build quantum invariants of the colored link.

We begin by recalling the construction of Turaev's shadow state sum invariant [77, 78] for  $S^1$ -bundles over surfaces, largely following the construction given in [77]. Let  $\Sigma_{g,n}$  be a compact orientable surface of genus g with n boundary components. Consider a finite collection of loops  $\{l_i: S^1 \to \Sigma_{g,n}\}$  on  $\Sigma_{g,n}$  with only double transversal crossings  $l_i \cap l_j$  for any i, j. Denote by  $\Gamma$  the 1-dimensional CW-complex consisting of the collection of loops  $\{l_i\}$  and crossing points  $\{l_i \cap l_j\}$ , and let P denote the pair  $(\Sigma_{g,n}, \Gamma)$ . We define the connected components  $X_t$  of  $\Sigma_{g,n} \setminus \Gamma$  to be the regions of P.

**Definition 4.3.5.** A shadow is a pair (P, gl) where  $gl : \{X_t\} \to \frac{1}{2}\mathbb{Z}$  is a map that assigns a half-integer to each region of P. This half-integer is called the *gleam* of the region. The total gleam of a shadow is defined to be

total gleam = 
$$\sum_{t} (gl(X_t)) - 2\#\{l_i \cap l_j\},$$

where  $\#\{l_i \cap l_j\}$  is the number of crossing points of P.

We will restrict our attention to shadows on closed surfaces. Suppose  $\Sigma_g$  is a closed orientable surface and  $\rho: M \to \Sigma_g$  is an oriented  $S^1$ -bundle over  $\Sigma_g$ . Let  $L \subset M$  be a link. We say that  $L \subset M$  is generic if it is transverse to the fibers with respect to  $\rho$  and the collection of immersed loops  $\rho(L) \subset \Sigma_{g,n}$  only have double transversal crossings. In [77], Turaev constructs a map which associates a shadow (P(L), gl) to  $L \subset M$ , where the gleams of each region of P(L) are determined by the Euler number of the 2-dimensional real vector bundle associated to the oriented circle bundle  $\rho$ . The construction of the map  $gl: \{X_t\} \to \frac{1}{2}\mathbb{Z}$  for general  $S^1$ -bundles over  $\Sigma_g$  will not be relevant to the arguments that follow, so we refer to Section 3(a) of [77] for further details. The following theorem of Turaev is a result of this construction.

**Theorem 4.3.6** ([77], Theorem 3.2). Let  $\rho: M \to \Sigma_g$  be an oriented circle bundle over a closed orientable surface  $\Sigma_g$ , and let  $L \subset M$  be a generic link with respect to  $\rho$ . Then there is a shadow (P(L), gl) with total gleam  $-\chi(p)$  associated to  $L \subset M$ , where  $\chi(p)$  is the Euler number of the bundle.

For our purposes, we restrict further to the special case where  $L \subset \Sigma_g \times S^1$  and  $\rho$ :  $\Sigma_g \times S^1 \to \Sigma_g$  is the trivial bundle. We can embed  $\Sigma_g \times [0,1] \hookrightarrow \Sigma_g \times S^1$  via the map

$$(x,t) \longmapsto \left(x, e^{2\pi\sqrt{-1}t}\right).$$

Now consider L as a subset of  $\Sigma_g \times [0,1]$ . It is a generic link with well-defined over- and under-crossings in the projection  $\rho|_{\Sigma_g \times [0,1]}(L)$  on  $\Sigma_g$ . This projection produces a shadow on  $\Sigma_g$  with gleams assigned as in Figure 4.4, where the gleam of each region is the sum of the associated 1's.

Note that  $L \subset \Sigma_g \times [0,1] \subset \Sigma_g \times S^1$  is a generic link with respect to  $\rho$ . The projection  $\rho|_{\Sigma_g \times [0,1]}(L)$  with gleams assigned using Figure 4.4 coincides with the shadow (P(L), gl) constructed using Theorem 4.3.6 with total gleam  $-\chi(\rho) = 0$ . As an elementary example, we consider the following example of Costantino and Thurston [19].

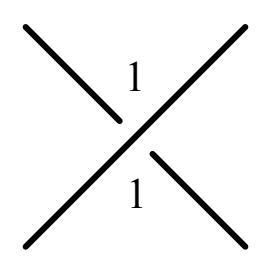


Figure 4.4 Gleam assignment for shadows of links in trivial bundles  $\Sigma_g \times [0,1]$ .

**Example 4.3.7** ([19], Example 3.5). Consider the shadow on  $\Sigma_0 = S^2$  with  $\Gamma = \emptyset$  and total gleam 0. This shadow corresponds to the empty link in the bundle  $\rho: S^2 \times S^1 \to S^2$ , where the triviality of the bundle is encoded by the zero gleam.

In order to define Turaev's shadow state sum invariant, we need to consider colorings of the link  $L \subset M$ .

**Definition 4.3.8.** Let M be a closed 3-manifold. An  $I_r$ -coloring of a link  $L \subset M$  assigns an element of  $I_r$  to each component of L. Similarly, an  $I_r$ -coloring of a shadow (P, gl) assigns an element of  $I_r$  to each loop of (P, gl).

If  $\rho: M \to \Sigma_g$  is a circle bundle over a closed surface  $\Sigma_g$ , an  $I_r$ -coloring  $\gamma$  of a link L in M descends to an  $I_r$ -coloring  $\gamma$  of the loops of the shadow (P(L), gl) constructed using Theorem 4.3.6.

**Definition 4.3.9.** Let  $(P, gl, \gamma)$  be an  $I_r$ -colored shadow with gleams gl and loops colored by  $\gamma$ . A surface-coloring  $\eta$  of  $(P, gl, \gamma)$  assigns an element of  $I_r$  to each region of  $(P, gl, \gamma)$ .

Suppose an edge e from a loop of  $(P, gl, \gamma)$  is adjacent to two regions X, X' of  $(P, gl, \gamma)$ . This edge has a fixed color  $\gamma(e)$ , and the regions X and X' are assigned colors  $\eta(X)$  and  $\eta(X')$ , respectively, by  $\eta$ .

**Definition 4.3.10.** A surface-coloring  $\eta$  of  $(P, gl, \gamma)$  is called *admissible* if for any edge e adjacent to two regions X, X' of  $(P, gl, \gamma)$ , the triple  $(\gamma(e), \eta(X), \eta(X')) \in I_r^3$  is r-admissible in the sense of Definition 2.3.1.

Figure 4.5 gives the local picture for admissibility. Let  $adm(P, gl, \gamma)$  denote the set of admissible surface-colorings of  $(P, gl, \gamma)$ .

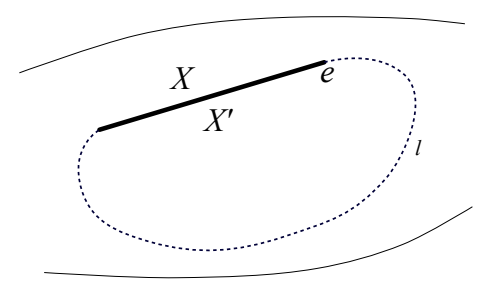


Figure 4.5 An edge e contained in a loop l of  $(P, gl, \gamma)$  and its two adjacent regions X and X'. An admissible surface-coloring assigns colors  $\eta(X)$  and  $\eta(X')$  for which  $(\gamma(e), \eta(X), \eta(X'))$  an r-admissible triple.

Suppose  $c_1, \ldots, c_p$  are the crossing points of P, each an intersection of two distinct loops or a self-crossing of a single loop of P. Suppose these loops have colors i and l, respectively. Then an admissible surface-coloring  $\eta \in \text{adm}(P, gl, \gamma)$  assigns colors j, k, m, n to the four regions incident at the crossing point  $c_s$  so that (i, j, k, l, m, n) forms an r-admissible 6-tuple. In particular, (i, j, k), (i, m, n), (j, l, n), and (k, l, m) are r-admissible triples. Figure 4.6 illustrates an admissible surface-coloring (j, k, m, n) around a crossing point of loops colored by i and l.

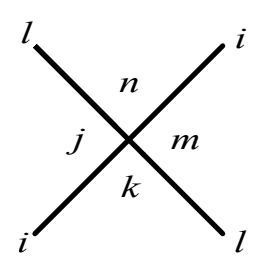


Figure 4.6 Admissible surface-coloring at a crossing.

Using Definition 2.3.2 of the quantum 6*j*-symbol, we let

$$|c_s|^{\eta} = \begin{vmatrix} i & j & k \\ l & m & n \end{vmatrix} \in \mathbb{C}.$$

Let  $X_1, \ldots, X_q$  be the regions of  $(P, gl, \gamma)$ , and let  $x_t, \chi_t$ , and  $z_t$  be the gleam, Euler characteristic, and number of corners of the region  $X_t$ , respectively. Define the modified

gleam of  $X_t$  by  $x'_t = x_t - z_t/2$ . For  $j \in I_r$ , let

$$u_j = \pi \sqrt{-1} \left(\frac{j}{2}\right) \left(1 - \frac{j+2}{r}\right), \quad v_j = (-1)^j [j+1].$$

Then for each admissible surface-coloring  $\eta$ , let

$$|(P,gl)|_{\gamma}^{\eta} = \prod_{s=1}^{p} |c_s|^{\eta} \prod_{t=1}^{q} ((v_{\eta(X_t)})^{\chi_t} \exp(2u_{\eta(X_t)}x_t')) \in \mathbb{C},$$
 (4.5)

where  $\eta(X_t)$  is the region color of  $X_t$  assigned by  $\eta$ .

Remark 4.3.11. Note that the gleams and the surface-colorings are independent of each other. The gleams encode topological data from the  $S^1$ -bundle  $\rho: M \to \Sigma_g$  and do not affect the quantum 6*j*-symbols in the first product of Equation (4.5), only the second product taken over the regions of (P, gl).

**Definition 4.3.12.** The *shadow state sum*  $|(P, gl)|_{\gamma}$  is defined by the following sum over all admissible surface-colorings  $\eta \in \text{adm}(P, gl, \gamma)$ .

$$|(P,gl)|_{\gamma} := \sum_{\eta \in \text{adm}(P,gl,\gamma)} |(P,gl)|_{\gamma}^{\eta} \in \mathbb{C}.$$

$$(4.6)$$

Turaev established the following theorem in [77] and generalized it in [78].

**Theorem 4.3.13** ([77], Theorem 5.1 and Corollary 5.2). Let  $(P, gl, \gamma)$  be an  $I_r$ -colored shadow. Then the shadow state sum  $|(P, gl)|_{\gamma}$  is a complex-valued regular isotopy invariant of colored shadows. Furthermore, this invariant gives rise to a complex-valued isotopy invariant of colored links in  $S^1$ -bundles over closed orientable surfaces.

Remark 4.3.14. The notion of regular isotopy invariance of colored shadows will not be relevant for our purposes since we only work with the projections arising from the construction of the links in Section 4.2. For details on the relationship between isotopy invariance of colored shadows and colored links in  $S^1$ -bundles over surfaces, we refer to [77] Sections 2, 3, and 4.

Turaev generalized the construction of colored shadows from the setting of colored links in  $S^1$ -bundles over closed surfaces [77] to colored links in closed 3-manifolds in [78], Chapters IX and X. While this general characterization is not relevant to the arguments that follow, we include a brief description. Turaev shows that any 3-manifold N which is the boundary of a 4-manifold W can be associated a shadow (P, gl). Roughly speaking, Turaev constructs the polyhedron P using dual cell subdivisions of a triangulation of N and equips gleams which encode the topology of the regular neighborhood of P in W. The details of this construction can be found in IX.1 of [78]. Further, if N contains a framed link T colored by  $\gamma$ , Turaev extended this construction to a colored shadow  $(P, gl, \gamma)$  associated to  $(N, T, \gamma)$ . In addition, we note this construction can be generalized to colored framed trivalent graphs contained in a 3-manifold N. We refer the reader to X.7.1 of [78] for details.

For simplicity, we consider the following alternative construction, which can be found in [19], to further support this more general notion of a shadow of a 3-manifold. The framed link  $L \subset S^3$  has a shadow  $(P_0, gl_0)$  constructed by gluing a disk to  $L \times [0, 1]$  along  $L \times \{0\}$ . Surgery along a component of L is equivalent to gluing the core of a 2-handle to  $P_0$ , and this gluing does not change the gleam of the capped region. Due independently to Lickorish [54] and Wallace [80], any 3-manifold N can be obtained by performing integer surgery on a link in  $S^3$ , meaning that every 3-manifold N has a shadow with gleams related to its surgery presentation. We refer the reader to Chapter 12 of [56] and Chapter 9 of [72] for more details on knot and link surgery.

### 4.3.3 Relating the quantum invariants

In this subsection, we state a result of Turaev [78] which establishes the relationship between the relative Reshetikhin–Turaev invariants and the shadow state sum invariant. We then discuss its implications in computing the Turaev–Viro invariants of a link complement using Proposition 2.3.9.

Turaev's constructions in IX and X of [78] establish a deep relationship between the r-th relative Reshetikhin–Turaev invariants and the generalized shadow state sum invariant.

Notably, one can study the r-th relative Reshetikhin–Turaev invariants of a colored framed link in a closed 3-manifold from the perspective of colored shadows. In [18], Costantino used this relationship to study the colored Jones invariants of links in  $S^3\#_k(S^2\times S^1)$  from the shadow perspective. We include Costantino's statement of Turaev's result from X.7.1 of [78] here.

**Theorem 4.3.15** ([18], Theorem 3.3). Let N be a closed 3-manifold and  $T \subset N$  a colored framed trivalent graph in N colored by  $\gamma$ . Let  $(P, gl, \gamma)$  be a colored shadow of (N, T). Then  $RT_r(N, T, \gamma) := C_r|(P, gl)|_{\gamma}$  is a complex-valued homeomorphism invariant of (N, T).

Remark 4.3.16. Theorem 4.3.15 is stated generally in terms of framed trivalent graphs (which are a generalization of framed links) to be consistent with the literature [18, 78]. The full generality of the result is not necessary for the arguments that follow since we only consider manifolds containing framed links.

**Remark 4.3.17.** Here, the factor  $C_r$  is considered a "normalization factor." See [18] for a precise formulation. In the case Turaev [77] studies, where N is homeomorphic to an  $S^1$ -bundle over a closed surface and T is a link in N, the factor  $C_r$  does not depend on T. It can therefore be ignored for our purposes.

Theorem 4.3.15, in combination with Proposition 2.3.9, provides a method for computing the Turaev–Viro invariants of manifolds in the family  $\mathcal{M}$  using their shadow state sum invariants. In particular, since  $M_L(k,l) \in \mathcal{M}$  the complement of a link in a trivial  $S^1$ -bundle over a closed oriented surface  $\Sigma$ , we may compute  $TV_r(M_L(k,l);q)$  by first coloring the link L with a fixed color  $\gamma$ , using Equation 4.6 to compute the r-th relative Reshetikhin–Turaev invariant  $RT_r(\Sigma \times S^1, L, \gamma)$ , and leveraging Proposition 2.3.9. In Section 4.4, we will see that this allows us to prove these manifolds satisfy the Turaev–Viro invariant volume conjecture.

# 4.4 Asymptotics of the Turaev-Viro Invariants for the Infinite Family

In this section, we prove Theorem 1.4.1 which we restate here.

**Theorem 1.4.1.** Let  $M_L(k,l) \in \mathcal{M}$ . Then for r running over odd integers and  $q = e^{\frac{2\pi\sqrt{-1}}{r}}$ ,

$$\lim_{r \to \infty} \frac{2\pi}{r} \log |TV_r(M_L(k, l); q)| = v_{tet} ||M_L(k, l)|| = 2(k + 2l)v_{oct}$$

where  $v_{oct} \approx 3.66$  is the volume of the regular ideal hyperbolic octahedron.

To do this, we first write a formula for the shadow state sum invariants  $|(P,gl)|_{\gamma}$  for the family  $\mathcal{M}$  of links in trivial  $S^1$ -bundles over surfaces constructed in Subsection 4.2.2. We will then state and prove Lemma 4.4.5 regarding the asymptotics of  $|(P,gl)|_{\gamma}$ . We complete the proof of Theorem 1.4.1 using Lemma 4.4.5 and the formulation of the Turaev–Viro invariants from Subsection 4.3.3 in terms of the r-th relative Reshetikhin–Turaev invariants.

Remark 4.4.1. Computing the relative Reshetikhin–Turaev invariants is difficult in general, but the family  $\mathcal{M}$  was constructed in order to simplify their calculation significantly from the shadow state sum perspective. In particular, shadows of these manifolds have simple gleams and topologically simple regions that allow us to reduce the proof of Theorem 1.4.1 to studying properties of quantum 6j-symbols. These manifolds also have well-understood simplicial volumes determined by k and l.

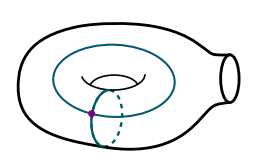
Let  $M_L(k,l) \in \mathcal{M}$  be the complement of a link L in a 3-manifold  $M = \Sigma_g \times S^1$  constructed as in Subsection 4.2.2. By Theorem 4.3.6,  $M_L(k,l)$  has a shadow (P,gl) associated to it.  $M_L(k,l)$  has an elementary decomposition into k S-pieces and l A-pieces. The shadow (P,gl) has a corresponding decomposition, so we also refer to these shadows on  $\Sigma_{1,1}$  and  $\Sigma_{0,4}$  as S-pieces and A-pieces, respectively. An S-piece has two loops which intersect at a single vertex. Let  $s_1, \ldots, s_k$  denote the intersection points on the k S-pieces. An A-piece has two loops which intersect at two vertices. Let  $(a_1^1, a_1^2), \ldots, (a_l^1, a_l^2)$  denote the intersection points on the l A-pieces.

We make the following observations about  $M_L(k, l)$ :

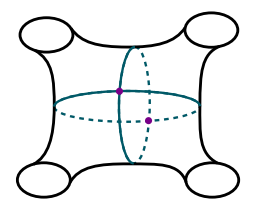
• Each S-piece of (P, gl) has two curves, one vertex, and one region X with z=4 corners as in Figure 4.7a. This region has gleam x=2 since gleams are assigned to

regions for trivial bundles as in Figure 4.4. Cutting  $\Sigma_{1,1}$  along one of the two curves produces a pair of pants such that the second curve becomes a simple arc connecting the two new boundary components. Cutting along this arc produces an annulus, so X has Euler characteristic  $\chi = 0$ . The modified gleam of the region of this shadow is x' = x - z/2 = 0.

• Each A-piece of (P, gl) has two curves, two vertices, and four regions X<sub>t</sub>, t = 1, 2, 3, 4, each with z<sub>t</sub> = 2 corners, as in Figure 4.7b. Again, using the gleam assignment from Figure 4.4, each of the four regions has gleam x<sub>t</sub> = 1. Cutting Σ<sub>0,4</sub> along one of the two curves separates Σ<sub>0,4</sub> into two pairs of pants such that the second curve is split into a simple arc on each pair of pants with endpoints on a single boundary component. Cutting the two pairs of pants along these arcs produces four annuli, so X<sub>t</sub> has Euler characteristic χ<sub>t</sub> = 0 for t = 1, 2, 3, 4. The modified gleam of each region of this shadow is x'<sub>t</sub> = x<sub>t</sub> - z<sub>t</sub>/2 = 0.



(a) Shadow corresponding to a pair of S—moves. The single region has gleam 2.



(b) Shadow corresponding to a pair of A-moves. Each region has gleam 1.

Figure 4.7 S- and A-pieces.

Remark 4.4.2. While the underlying surface of the shadow (P, gl) associated to  $M_L(k, l)$  is closed, the underlying surfaces of the S- and A-pieces have boundary. By the construction of  $M_L(k, l)$ , the annular regions of the S- and A-pieces are glued along their boundaries to form the regions of (P, gl). The gleam (resp. Euler characteristic) of a region X of (P, gl) is the sum of the gleams (resp. Euler characteristic) of the regions in the S- and A-pieces that are glued to form X.

Let  $\gamma \in I_r^{2k+2l}$  be an  $I_r$ -coloring of  $L \subset M$ . The loops of the associated shadow (P, gl) inherit this  $I_r$ -coloring  $\gamma$ . Let  $\eta \in \text{adm}(P, gl, \gamma)$  be an admissible surface-coloring of  $(P, gl, \gamma)$ . The S- and A-piece observations imply that for the state  $|(P, gl)|_{\gamma}^{\eta}$  defined in Equation (4.5),  $\chi_t = x_t' = 0$  for all regions  $X_t$ . This means

$$\prod_{t=1}^{q} \left( \left( v_{\eta(X_t)} \right)^{\chi_t} \exp \left( 2u_{\eta(X_t)} x_t' \right) \right) = 1.$$

Using this and Equation (4.5), we reformulate the state sum invariant of the  $I_r$ -colored shadow associated to  $M_L(k,l)$  in the following proposition.

**Proposition 4.4.3.** Let  $(P, gl, \gamma)$  be a colored shadow associated to  $M_L(k, l)$ . Then the shadow state sum invariant is given by

$$|(P,gl)|_{\gamma} = \sum_{\eta \in adm(P,gl,\gamma)} |(P,gl)|_{\gamma}^{\eta}$$

$$= \sum_{\eta \in adm(P,gl,\gamma)} \prod_{i=1}^{k} |s_{i}|^{\eta} \prod_{j=1}^{l} |a_{j}^{1}|^{\eta} |a_{j}^{2}|^{\eta}.$$
(4.7)

Since Equation (4.7) is a sum of products of quantum 6j-symbols, Proposition 4.4.3 allows us to use the explicit properties of quantum 6j-symbols discussed in Subsection 2.3.1. The following technical lemma will be used to prove Theorem 1.4.1.

**Remark 4.4.4.** We will use the abbreviation (n) := (n, ..., n) for tuples of colors throughout the rest of the chapter.

**Lemma 4.4.5.** Let  $M_L(k,l) \in \mathcal{M}$  and  $\gamma = (n_r) \in I_r^{2k+2l}$ , where  $n_r := \frac{r-1}{2}$  when  $r \equiv 1 \mod 4$  and  $n_r := \frac{r-3}{2}$  when  $r \equiv 3 \mod 4$ . Let  $(P, gl, \gamma)$  be the  $I_r$ -colored shadow representing  $M_L(k,l)$ . Then

$$\lim_{r \to \infty} \frac{4\pi}{r} \log ||(P, gl)|_{(n_r)}| = v_{tet} ||M_L(k, l)||, \tag{4.8}$$

where  $v_{tet}||M_L(k,l)|| = 2(k+2l)v_{oct}$  is the simplicial volume of  $M_L(k,l)$ .

The following two lemmas give properties of quantum 6j-symbols that will be leveraged to establish a lower bound for the limit in Equation (4.8) of Lemma 4.4.5.

**Lemma 4.4.6.** Let  $n_r := \frac{r-1}{2}$  when  $r \equiv 1 \mod 4$  and  $n_r := \frac{r-3}{2}$  when  $r \equiv 3 \mod 4$ . Suppose  $m_1, m_2, m_3, m_4 \in I_r$  and the tuple  $(n_r, m_1, m_2, n_r, m_3, m_4)$  is r-admissible. Then the quantum 6j-symbol

$$\begin{vmatrix}
 n_r & m_1 & m_2 \\
 n_r & m_3 & m_4
 \end{vmatrix}$$

is real-valued.

*Proof.* Let

$$n_r := \begin{cases} \frac{r-1}{2} & \text{if } r \equiv 1 \mod 4\\ \frac{r-3}{2} & \text{if } r \equiv 3 \mod 4 \end{cases}$$

Note that  $n_r$  is always even. Consider the quantum 6j-symbol associated to the tuple  $(n_r, m_1, m_2, n_r, m_3, m_4)$ . From Definition 2.3.2, the quantum 6j-symbol associated to the 6-tuple  $(a_1, \ldots, a_6)$  is either real or purely imaginary based on the value of the coefficient

$$\sqrt{-1}^{\left(-\sum_{i=1}^{6} a_i\right)} \Delta(a_1, a_2, a_3) \Delta(a_1, a_5, a_6) \Delta(a_2, a_4, a_6) \Delta(a_3, a_4, a_5), \tag{4.9}$$

since the sum in Equation (2.1) is real-valued.

For  $(n_r, m_1, m_2, n_r, m_3, m_4)$ , the first factor is given by

$$(\sqrt{-1})^{-(n_r+m_1+m_2+n_r+m_3+m_4)} = (\sqrt{-1})^{m_1+m_2+m_3+m_4} = \pm 1.$$

The first equality holds because  $n_r$  is even, so  $2n_r$  has a factor of 4. The second equality is due to the admissibility conditions which require that each of the sums  $m_1 + m_2$ ,  $m_3 + m_4$ ,  $m_1 + m_4$ , and  $m_2 + m_3$  are even. Notice in the case of  $(n_r, m, m, n_r, m, m)$ , the factor becomes

$$(\sqrt{-1})^{-(2n_r+4m)} = 1.$$

For the other factors of Equation (4.9), suppose  $(n_r, m, m')$  is an r-admissible triple and without loss of generality, assume  $m \ge m'$ . Then

$$\Delta(n_r, m, m') = \sqrt{\frac{\left[\frac{n_r + m - m'}{2}\right]! \left[\frac{m' + n_r - m}{2}\right]! \left[\frac{m + m' - n_r}{2}\right]!}{\left[\frac{n_r + m + m'}{2} + 1\right]!}}.$$

By the admissibility conditions,  $\frac{n_r+m-m'}{2} \leq n_r < \frac{r}{2}$ ,  $\frac{n_r+m'-m}{2} \leq \frac{n_r}{2} < \frac{r}{2}$ , and  $\frac{m+m'-n_r}{2} \leq r-2-n_r < \frac{r}{2}$ . Since [n]>0 for  $0\leq n<\frac{r}{2}$ , the numerator of  $\Delta(n_r,m,m')$  is real-valued. This implies the numerator of  $\Delta(n_r,m_1,m_2)\Delta(n_r,m_3,m_4)\Delta(m_1,n_r,m_4)\Delta(m_2,n_r,m_3)$  is also real-valued. In addition, the admissibility conditions imply that  $\frac{r-1}{2}\leq n_r+1\leq \frac{n_r+m+m'}{2}+1\leq r-1$ , so the sign of  $\left[\frac{n_r+m+m'}{2}+1\right]!$  is given by

$$(-1)^{\frac{n_r+m+m'}{2}+1-\frac{r-1}{2}}$$
.

This means the denominator of  $\Delta(n_r, m_1, m_2)\Delta(n_r, m_3, m_4)\Delta(m_1, n_r, m_4)\Delta(m_2, n_r, m_3)$  is some real-valued multiple of

$$\sqrt{(-1)^{2n_r+4-2(r-1)+m_1+m_2+m_3+m_4}} = \pm 1,$$

where equality holds because  $2n_r + 4 - 2(r - 1)$  contains a factor of 4 and  $m_1 + m_2 + m_3 + m_4$  is even. Hence, the coefficient given by Equation (4.9) is real-valued. This implies that the quantum 6*j*-symbol associated to the 6-tuple  $(n_r, m_1, m_2, n_r, m_3, m_4)$  is real-valued. Notice in the case of  $(n_r, m, m, n_r, m, m)$ , the coefficient given by Equation (4.9) is positive.

**Lemma 4.4.7.** Let  $n_r := \frac{r-1}{2}$  when  $r \equiv 1 \mod 4$  and  $n_r := \frac{r-3}{2}$  when  $r \equiv 3 \mod 4$ . Let  $m \in I_r$  and suppose that the tuple  $(n_r, m, m, n_r, m, m)$  is r-admissible. Then the sign of

$$\left| egin{array}{ccccc} n_r & m & m \\ n_r & m & m \end{array} \right|$$

is independent of m. Moreover, it is positive when  $r \equiv 3 \mod 4$  and negative when  $r \equiv 1 \mod 4$ .

*Proof.* Consider the quantum 6*j*-symbol associated to the 6-tuple  $(n_r, m, m, n_r, m, m)$ . By Lemma 4.4.6, this quantum 6*j*-symbol is real-valued. The admissibility conditions imply that  $\frac{n_r}{2} \leq m \leq r - 2 - \frac{n_r}{2}$ . By Definition 2.3.2,

$$\begin{vmatrix} n_r & m & m \\ n_r & m & m \end{vmatrix} = \Delta (n_r, m, m)^4 \left( \sum_{k=m+\frac{n_r}{2}}^{\min\{m+n_r, 2m\}} S_{m,k} \right)$$
(4.10)

where

$$S_{m,k} = \frac{(-1)^k [k+1]!}{\left[k - \left(m + \frac{n_r}{2}\right)\right]!^4 [m + n_r - k]!^2 [2m - k]!}.$$

Suppose  $r \equiv 1 \mod 4$ . By the admissibility conditions, the 6-tuple  $(\frac{r-1}{2}, m, m, \frac{r-1}{2}, m, m)$  satisfies assumptions (a) and (b) of Theorem 4.3.2. In the case that  $r \equiv 3 \mod 4$ , the admissibility conditions of the 6-tuple  $(\frac{r-3}{2}, m, m, \frac{r-3}{2}, m, m)$  imply it satisfies assumptions (a) and (b) of Theorem 4.3.2 for all admissible region colors except  $m = \frac{n_r}{2} = \frac{r-3}{4}$  and  $m = r - 2 - \frac{n_r}{2} = \frac{3r-5}{4}$ . We will consider these cases separately.

#### General Case:

Suppose either  $r \equiv 1 \mod 4$  or  $r \equiv 3 \mod 4$  with  $\frac{r-3}{4} < m < \frac{3r-5}{4}$ . Then by part (1) of Theorem 4.3.2, the sign of  $S_{m,k}$  is independent of k. We now show that the sign of  $S_{m,k}$  is independent of the region color m. Without loss of generality, consider the case  $k = m + \frac{n_r}{2}$ :

$$S_{m,m+\frac{n_r}{2}} = \frac{(-1)^{m+\frac{n_r}{2}} [m + \frac{n_r}{2} + 1]!}{\left[\frac{n_r}{2}\right]!^2 [m - \frac{n_r}{2}]!}.$$

Since the quantum integer [n] is real-valued, we only need to consider the signs of  $[m+\frac{n_r}{2}+1]!$  and  $[m-\frac{n_r}{2}]!$ . By assumption (a) of Theorem 4.3.2 and the assumption that  $m < r-2-\frac{n_r}{2}$ , we know  $0 \le m - \frac{n_r}{2} \le \frac{r-2}{2}$ , so  $[m-\frac{n_r}{2}]! > 0$  for all region colors m. By assumption (b) of Theorem 4.3.2 and the assumption that  $m > \frac{n_r}{2}$ , we know  $\frac{r-2}{2} \le m + \frac{n_r}{2} \le r - 2$ , so  $[m+\frac{n_r}{2}+1] < 0$  for all region colors m. Note that  $\left[\frac{r-1}{2}\right]! > 0$ , so  $[m+\frac{n_r}{2}+1]! = [m+\frac{n_r}{2}+1] \cdots [\frac{r+1}{2}][\frac{r-1}{2}]!$  has sign

$$(-1)^{m+\frac{n_r}{2}+1-\frac{r-1}{2}}$$
.

Then the sign of  $S_{m,m+\frac{n_r}{2}}$  is

$$(-1)^{m+\frac{n_r}{2}+m+\frac{n_r}{2}+1-\frac{r-1}{2}} = (-1)^{-\frac{r-3}{2}}, (4.11)$$

which is independent of the region color m. By part (1) of Theorem 4.3.2 and Equation (4.10), the sign of the quantum 6j-symbol associated to  $(n_r, m, m, n_r, m, m)$  is independent of the region color m, provided  $m \neq \frac{r-3}{4}, \frac{3r-5}{4}$  in the case  $r \equiv 3 \mod 4$ .

# **Special Cases:**

If  $m = \frac{r-3}{4}$ , we have  $\max T_i = \frac{r-3}{2} = \min Q_j$ , so

$$\begin{vmatrix} \frac{r-3}{2} & \frac{r-3}{4} & \frac{r-3}{4} \\ \frac{r-3}{2} & \frac{r-3}{4} & \frac{r-3}{4} \end{vmatrix} = \Delta \left( \frac{r-3}{2}, \frac{r-3}{4}, \frac{r-3}{4} \right)^4 \left( \frac{(-1)^{\frac{r-3}{2}} \left[ \frac{r-3}{2} + 1 \right]!}{\left[ \frac{r-3}{4} \right]!^2} \right) > 0.$$

Positivity follows because  $n_r = \frac{r-3}{2}$  is even and  $0 < \frac{r-3}{2} + 1 < \frac{r}{2}$ .

If  $m = \frac{3r-5}{4}$ , we have  $\max T_i = r-2$  and  $\min Q_j = r-2+\frac{r-3}{4}$ . However, since [k+1]! = 0 for k > r-2,

$$\begin{vmatrix} \frac{r-3}{2} & \frac{3r-5}{4} & \frac{3r-5}{4} \\ \frac{r-3}{2} & \frac{3r-5}{4} & \frac{3r-5}{4} \end{vmatrix} = \Delta \left( \frac{r-3}{2}, \frac{3r-5}{4}, \frac{3r-5}{4} \right)^4 \left( \frac{(-1)^{r-2} [r-1]!}{\left[\frac{r-3}{4}\right]!^2 \left[\frac{r-1}{2}\right]!} \right) > 0.$$

Positivity follows because the denominator is positive and the numerator is given by the product  $(-1)^{r-2}[r-1][r]\cdots \left[\frac{r+1}{2}\right]\left[\frac{r-1}{2}\right]!$ , which has sign

$$(-1)^{r-2+\left(r-1-\frac{r-1}{2}\right)} = (-1)^{\frac{3r-5}{2}} = 1.$$

Thus the sign of the quantum 6j-symbol associated to  $(n_r, m, m, n_r, m, m)$  is independent of m. Moreover, by Equation (4.11), this 6j-symbol is negative when  $r \equiv 1 \mod 4$  and positive when  $r \equiv 3 \mod 4$ .

We now prove Lemma 4.4.5.

Proof of Lemma 4.4.5. From Subsection 4.2.2, the link complement  $M_L(k,l)$  is a compact orientable 3-manifold with simplicial volume  $v_{tet}||M_L(k,l)|| = 2(k+2l)v_{oct}$ . We proceed by bounding the limit in Equation (4.8) above and below by  $v_{tet}||M_L(k,l)||$ .

# Step 1: The upper bound

For the upper bound, note that each summand in Equation (4.7) is a product of k + 2l quantum 6j-symbols. By Theorem 4.3.1, the growth rate of a single summand of Equation (4.7) is bounded above sharply by  $(k + 2l)v_{oct}$ . Let  $B_r = \#adm(P, gl, \gamma)$  be the number of r-admissible surface-colorings of  $(P, gl, \gamma)$ . The term  $B_r$  grows at most polynomially with

r since  $B_r$  is bounded above by the total number of r-admissible 6-tuples corresponding to well-defined quantum 6j-symbols. Thus, we obtain the following upper bound:

$$\limsup_{r \to \infty} \frac{4\pi}{r} \log ||(P, gl)|_{\gamma}| \le \limsup_{r \to \infty} \frac{4\pi}{r} \log \left| B_r \max_{\eta \in adm(P, gl, \gamma)} |(P, gl)|_{\gamma}^{\eta} \right|$$

$$= 2 \limsup_{r \to \infty} \frac{2\pi}{r} \log \left| \max_{\eta \in adm(P, gl, \gamma)} |(P, gl)|_{\gamma}^{\eta} \right|$$

$$\le 2(k+2l)v_{oct},$$

where the last inequality is due to Theorem 4.3.1.

We remark that this upper bound holds for any  $I_r$ -coloring  $\gamma$ , which implies the required upper bound for the limit in Equation (4.8).

# Step 2: The lower bound

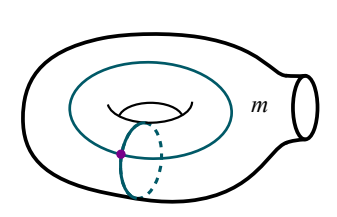
Let  $n_r := \frac{r-1}{2}$  when  $r \equiv 1 \mod 4$  and  $n_r := \frac{r-3}{2}$  when  $r \equiv 3 \mod 4$ . We will prove the lower bound for the  $(n_r)$ -colored link.

For the lower bound, it suffices to show that summands of Equation (4.7) do not cancel with each other when  $\gamma = (n_r)$ . In particular, we will show that, for fixed r, the sign of every summand of Equation (4.7) is independent of the surface-coloring  $\eta \in \text{adm}(P, gl, (n_r))$ . This means that the absolute value of any individual summand is a lower bound for  $||(P, gl)||_{(n_r)}|$ . We now make some observations about  $\prod_{i=1}^k |s_i|^{\eta} \prod_{j=1}^l |a_j^1|^{\eta} |a_j^2|^{\eta}$ .

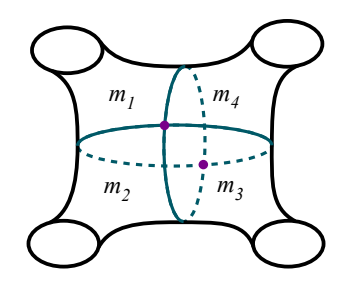
- The surface-coloring of each S-piece is given by Figure 4.8a. This means each factor  $|s_i|^{\eta}$  is the quantum 6j-symbol associated to the 6-tuple  $(n_r, m, m, n_r, m, m)$ .
- The surface-coloring of each A-piece is given by Figure 4.8b. Using the symmetries of the quantum 6j-symbol in Equation (2.2), each factor  $|a_j^i|^{\eta}$ , for i = 1, 2, is the quantum 6j-symbol associated to the 6-tuple  $(n_r, m_1, m_2, n_r, m_3, m_4)$ .

Using these observations, we can re-formulate Equation (4.7) for the  $(n_r)$ -colored shadow:

$$|(P,gl)|_{(n_r)} = \sum_{\eta \in \text{adm}(P,gl,(n_r))} \prod_{i=1}^{k} \begin{vmatrix} n_r & m^i & m^i \\ n_r & m^i & m^i \end{vmatrix} \prod_{j=1}^{l} \begin{vmatrix} n_r & m_1^j & m_2^j \\ n_r & m_3^j & m_4^j \end{vmatrix}^2$$
(4.12)



(a) A surface-coloring by  $m \in I_r$  of a shadow corresponding to a pair of S—moves.



(b) A surface-coloring by  $m_i \in I_r$  of a shadow corresponding to a pair of A-moves.

Figure 4.8 Surface-colored shadows.

We remark that the notation of Equation (4.12) is chosen out of convenience. The construction of the invariant may introduce dependencies between surface-colors and hence between entries of the quantum 6j-symbols. For example, if an S-piece with region colored by  $m^i$  is glued to an A-piece along the boundary circle adjacent to a region colored by  $m^j$ , the regions combine to form a single region with color  $m^i = m^j$ . We choose to omit these additional details since they do not change the overall result of Lemma 4.4.5.

By Lemma 4.4.6, the quantum 6j-symbols of the form  $(n_r, m_1, m_2, n_r, m_3, m_4)$  are real-valued. This means

$$\prod_{j=1}^{l} \left| \begin{array}{ccc} n_r & m_1^j & m_2^j \\ n_r & m_3^j & m_4^j \end{array} \right|^2$$

is non-negative and implies that the sign of the summand of Equation (4.12) is determined by the quantum 6j-symbols associated to the S-pieces

$$\prod_{i=1}^{k} \left| \begin{array}{ccc} n_r & m^i & m^i \\ n_r & m^i & m^i \end{array} \right|.$$
(4.13)

By Lemma 4.4.7, the sign of each factor in Expression (4.13) is independent of the surface-colorings  $m^i$ , for  $i \in \{1, ..., k\}$ , of the S-pieces.

Therefore, the sign of  $|(P,gl)|_{(n_r)}^{\eta}$  is independent of the surface-coloring  $\eta$ . From this, we

can conclude

$$||(P,gl)|_{(n_r)}| = \left| \sum_{\eta \in adm(P,gl,n_r)} |(P,gl)|_{(n_r)}^{\eta} \right|$$

$$= \sum_{\eta \in adm(P,gl,n_r)} ||(P,gl)|_{(n_r)}^{\eta}|. \tag{4.14}$$

In fact, since the number of S-pieces k is even, every summand of Equation (4.12) is non-negative, though Equation (4.14) is sufficient for our purposes.

We can bound the sum in Equation (4.14) below by the absolute value of a single state  $|(P, gl)|_{(n_r)}^{\eta}$ . In particular, we consider the bound obtained from the surface-coloring  $\eta = (n_r)$ . This gives us the inequality

$$\liminf_{r \to \infty} \frac{4\pi}{r} \log ||(P, gl)|_{(n_r)}| \ge \lim_{r \to \infty} \frac{4\pi}{r} \log \left| \left| \begin{array}{ccc} n_r & n_r & n_r \\ n_r & n_r & n_r \end{array} \right|^{k+2l} \right|$$

$$= 2(k+2l)v_{oct},$$

where the equality is due to Equation (4.4) in Lemma 4.3.4. This means the growth rate of the shadow state sum invariant is bounded below by the simplicial volume  $v_{tet}||M_L(k,l)|| = 2(k+2l)v_{oct}$ , establishing the lemma.

We can now prove Theorem 1.4.1.

Proof of Theorem 1.4.1. Fix a root of unity  $q = e^{\frac{2\pi\sqrt{-1}}{r}}$ . Let  $M = \Sigma_g \times S^1$  be a trivial  $S^1$ -bundle over an orientable closed surface  $\Sigma_g$ , and let  $L \subset M$  be a 2k + 2l component link such that  $M_L(k,l) \in \mathcal{M}$ . Suppose L is colored by  $\gamma \in I_r^{2k+2l}$ , and consider the  $I_r$ -colored shadow  $(P, gl, \gamma)$  associated to  $M_L(k, l)$ .

We begin by formulating  $TV_r(M_L(k,l);q)$  in terms of the shadow state sum invariant. By Proposition 2.3.9 and Theorem 4.3.15, the Turaev–Viro invariant of  $M_L(k,l)$  is given by

$$TV_r(M_L(k,l);q) = \sum_{\gamma \in I_r^{2k+2l}} |RT_r(M,L,\gamma)|^2$$
$$= \sum_{\gamma \in I_r^{2k+2l}} |C_r|(P,gl)|_{\gamma}|^2.$$

We start with the upper bound, which is proven analogously to the upper bound in Lemma 4.4.5. Let  $B'_r := (\#I_r)^{2k+2l}$  be the number of link colorings. Both  $|C_r|$  and  $B'_r$  grow at most polynomially with r, so we obtain the following bound. See Theorem 3.3 of [18] where  $C_r$  is written as a product of terms which grow at most polynomially.

$$\limsup_{r \to \infty} \frac{2\pi}{r} \log |TV_r(M_L(k,l);q)| = \limsup_{r \to \infty} \frac{2\pi}{r} \log \left| \sum_{\gamma \in I_r^{2k+2l}} ||(P,gl)|_{\gamma}|^2 \right|$$

$$\leq 2 \limsup_{r \to \infty} \max_{\gamma \in I_r^{2k+2l}} \frac{2\pi}{r} \log ||(P,gl)|_{\gamma}|.$$

Since  $|(P, gl)|_{\gamma}$  is a product of k + 2l quantum 6j-symbols, we obtain the following bound using Theorem 4.3.1.

$$\limsup_{r \to \infty} \frac{2\pi}{r} \log |TV_r(M_L(k,l);q)| \le 2(k+2l)v_{oct}.$$

We now focus on the lower bound. Since all summands are positive, we can bound the absolute value of the sum below by the absolute value of an individual summand. In particular, we consider the bound obtained from the summand corresponding to the  $I_r$ coloring  $\gamma = (n_r)$ . This gives us the following inequality:

$$\lim_{r \to \infty} \inf \frac{2\pi}{r} \log |TV_r(M_L(k,l);q)| \ge \lim_{r \to \infty} \inf \frac{2\pi}{r} \log \left| |C_r|(P,gl)|_{(n_r)} \right|^2 \\
= \lim_{r \to \infty} \frac{4\pi}{r} \log \left| |(P,gl)|_{(n_r)} \right| ,$$

where equality holds since the limit exists, by Lemma 4.4.5, which is equal to the limit inferior and because  $|C_r|$  grows at most polynomially. Applying Lemma 4.4.5, we obtain the lower bound

$$\liminf_{r \to \infty} \frac{2\pi}{r} \log |TV_r(M_L(k,l);q)| \ge 2(k+2l)v_{oct}.$$

Therefore, we can conclude that

$$\lim_{r \to \infty} \frac{2\pi}{r} \log |TV_r(M_L(k, l); q)| = 2(k + 2l)v_{oct} = v_{tet}||M_L(k, l)||.$$

#### CHAPTER 5

# q-HYPERBOLIC KNOTS IN $S^3$

This chapter is based on joint work with Kalfagianni in a preprint submitted for publication [44].

In this chapter, we utilize Dehn surgery methods in combination with recent results toward the Turaev–Viro invariant volume conjecture to construct the first known infinite families of knots in  $S^3$  satisfying Conjecture 1.5.1. Due to the deep connection between the Exponential Growth Conjecture and the AMU conjecture, these result in new families of mapping classes acting on surfaces of any genus and one boundary component satisfying Conjecture 1.5.6.

# 5.1 Introduction

As in Chapters 3 and 4, we consider the Turaev–Viro invariants  $TV_r(M;q)$  of a compact 3-manifold M parameterized by an integer  $r \geq 3$  depending on the 2r-th root of unity  $q = e^{\frac{2\pi\sqrt{-1}}{r}}$ .

Recall from Subsection 2.3.3, a compact 3-manifold M with empty or toroidal boundary with lTV(M) > 0 is called q-hyperbolic. We will say that a knot K is q-hyperbolic if the complement  $M_K := \overline{S^3 \setminus n(K)}$  is q-hyperbolic, where n(K) is a tubular neighborhood of K.

The purpose of this chapter is to give constructions of the first infinite families of q-hyperbolic knots in the 3-sphere. The only hyperbolic knot complement in the 3-sphere for which the asymptotic behavior of the Turaev–Viro invariants has been explicitly understood is the figure-eight knot complement [25]. On the other hand, the volume conjecture of [16] has been proved for all hyperbolic 3-manifolds that are obtained by Dehn filling the figure eight knot complement [64, 87]. Our constructions combine these results, with a result of [23] about the behavior of the Turaev–Viro invariants under Dehn-filling, and with several Dehn surgery techniques, to produce these families. These results also have new applications to the conjecture of [5].

Given a knot K, let  $\mu, \lambda$  denote a set of canonical generators for  $H_1(\partial(n(K)))$ . For a

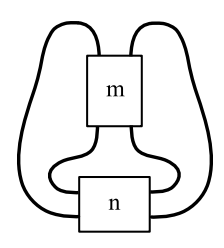


Figure 5.1 A double twist knot D(m, n) diagram with m vertical half-twists and n horizontal half-twists.

simple closed curve s on  $\partial(n(K))$ , we denote by  $[s] = p\mu + q\lambda$  its class in  $H_1(\partial(n(K)))$ , where p,q are relatively prime integers. Recall that s is completely determined, up to isotopy, by the fraction  $p/q \in \mathbb{Q} \cup \{\infty\}$ . We will use  $M_K(p/q)$  to denote the 3-manifold obtained by Dehn-filling  $M_K$  along the slope s determined by p/q.

For  $m, n \in \mathbb{Z}$ , let the double twist knot D(m, n) with m vertical half-twists and n horizontal half-twists be as in Figure 5.1. For example, D(2, -2) is the figure-eight knot and D(2, 2) is the left-handed trefoil.

Remark 5.1.1. We note that the notation for the double twist knots D(m, n) follows the convention of Boden–Curtis [12]. In particular, for m > 0, the associated vertical half-twists correspond to over-crossings with slope +1, and for n > 0, the associated horizontal half-twists correspond to over-crossings with slope -1. This convention is meant to be consistent with the actual operation of applying a half-twist to either horizontal or vertical strands, and we refer the reader to Section 2.5 of [12] for further details. In the two above examples, under this convention,  $4_1 = D(2, -2)$  is an alternating projection and  $3_1 = D(2, 2)$  is a non-alternating projection which may be modified to a 3-crossing alternating projection under Reidemeister moves and ambient isotopy.

The first result we establish is the following, which was initially stated in Chapter 1.

**Theorem 1.5.2.** For any integer  $n \neq 0, -1$ , the following are true:

1. The knots  $D_n := D(2n, -3)$  and  $D'_n := D(2n, -2)$  are q-hyperbolic.

- 2. The 3-manifolds  $M_n := M_{D_n}(4n+1)$  and  $M'_n := M_{D'_n}(1)$  are hyperbolic and q-hyperbolic.
- 3. We have

$$lTV(M_{D_n}) \ge vol(M_n)$$
, and  $lTV(M_{D'_n}) \ge vol(M'_n)$ .

Using Theorem 1.5.2, we may conclude that many low-crossing knots are q-hyperbolic. We refer to Tables 5.1 and 5.2 in Section 5.5.

A slope p/q is called non-characterizing for a knot  $K \subset S^3$  if there is a knot K' that is not equivalent to K and such that  $M_K(p/q)$  is homeomorphic to  $M_{K'}(p/q)$ . In the articles, [2, 1, 3], the authors give constructions of knots that admit infinitely many non-characterizing slopes. Combining their techniques and results with Theorem 1.5.2, we are able to construct new infinite families of q-hyperbolic knots.

# **Theorem 1.5.3.** There is an an infinite set of knots K such that:

- 1. Every knot in K is q-hyperbolic.
- 2. For every  $K \in \mathcal{K}$ ,  $M_K(-7)$  is homeomorphic to  $M_{4_1}(-7/2)$  and it is q-hyperbolic.
- 3. No two knots in K are equivalent.

To apply the methods of [1] one needs to start with a knot  $K_0$  that admits an "annulus presentation". Then, for any non-zero  $n \in \mathbb{N}$ , one applies a certain operation called an "n-fold annulus twist" repeatedly to generate a family of knots  $\mathcal{K}$ , so that for any  $K \in \mathcal{K}$  we have  $M_K(n) \cong M_{K_0}(n)$ . The method of the proof of Theorem 1.5.3 is as follows: First we show that the six-crossing knot  $6_2 = D_{-2} = D(-4, -3)$  is q-hyperbolic and that the 3-manifold  $M_{6_2}(-7)$ , obtained by (-7)-surgery on  $6_2$ , is homeomorphic to  $M_{4_1}(-7/2)$  and is q-hyperbolic. Then we verify that the knot  $6_2$  has an "annulus presentation" to which we apply a "-7-fold annulus twist" inductively, to generate a family of knots  $\mathcal{K}$ . In this case, the annulus presentation of  $6_2$  is nice in a certain sense, and we are able to argue that the resulting knots have mutually distinct Alexander polynomials. We refer the reader to

Section 5.3 and, in particular, to Remark 5.3.7, for details. The annulus twisting technique also applies to each of the knots  $D'_n := D(2n, -2)$  to produce families of q-hyperbolic knots. However, in this case we don't know whether the resulting knots are necessarily distinct. We have the following:

**Theorem 1.5.5.** For any |n| > 1, let  $D'_n := D(2n, -2)$ . There is a sequence of q-hyperbolic knots  $\{K_n^i\}_{i\in\mathbb{N}}$  such that for any  $i\in\mathbb{N}$  we have the following:

- 1. The knot  $K_n^i$  is q-hyperbolic.
- 2. The 3-manifold  $M_{K_n^i}(1)$  is homeomorphic to  $M_{D_n^i}(1)$  and it is q-hyperbolic.

Finally, the knots D(2n, -3) are fibered when  $n \leq -1$  and the monodromies of their fibrations provide explicit families of mapping classes acting on surfaces with a single boundary component that satisfy the AMU conjecture, as we will see in Theorem 1.5.7. These are the first examples known to satisfy this conjecture that are constructed as monodromies of fibered knots in  $S^3$ . The examples of [22] are coming from monodromies of fibered links of multiple components, while the examples [24] come from monodromies of fibered knots in closed q-hyperbolic 3-manifolds. In fact, the constructions presented here provide a framework for further examples to be discovered, as any fibered knot in  $S^3$  which can be shown to share a surgery with  $4_1$  has a monodromy satisfying the AMU conjecture.

The chapter is organized as follows: We give a proof of Theorem 1.5.2 in Section 5.2. In Section 5.3, first we recall the definitions and results from [2, 1, 3] relevant here, and then we prove Theorems 1.5.3 and 1.5.5. We apply our results to the conjecture of [5] in Section 5.4. Finally, Section 5.5 we summarize knots up to 15 crossings that can be shown to be q-hyperbolic using Theorem 1.5.2, as well as a non-ehaustive list of manifolds which can be shown experimentally to share surgeries with the figure-eight knot complement.

#### 5.2 q-hyperbolic double twist knots

In this section, we will show the q-hyperbolicity of two families of knots in  $S^3$  which share hyperbolic Dehn surgeries with the figure-eight knot.

Suppose M is a compact 3-manifold with empty or toroidal boundary. If M is hyperbolic, by Mostow rigidity the volume of a hyperbolic metric is a topological invariant of M denoted by vol(M). If M is disconnected, the total volume is the sum of volumes over all connected components. Recall from Subsection 2.1.1 that M admits a unique decomposition along tori into manifolds with toroidal boundary that are Seifert fibered spaces or hyperbolic. Also recall that by Theorem 2.1.9, the simplicial volume of a 3-manifold with toroidal boundary decreases under Dehn-filling. That is, if M is a 3-manifold with toroidal boundary, and M' is obtained by Dehn-filling some components of  $\partial M$ , then ||M'|| < ||M||.

The asymptotics of the Turaev–Viro invariants have an analogous property, as shown by Detcherry-Kalfagianni [23].

**Theorem 5.2.1** ([23], Corollary 5.3). Let M be a compact oriented 3-manifold with toroidal boundary  $\partial M = \bigsqcup_{i=1}^n T_i^2$  and let M' be a manifold obtained from M by Dehn-filling some of the boundary components. Then

$$lTV(M') \le lTV(M)$$
.

In particular, if M' is q-hyperbolic then M is q-hyperbolic.

Let K be a knot in the 3-sphere with complement  $M_K$ . Recall that isotopy classes of simple closed curves on  $\partial M_K$  are in one to one correspondence with slopes  $p/q \in \mathbb{Q} \cup \{1/0\}$ . Slopes of the form p/1 will be denoted by p. Given a slope p/q, let  $M_K(p/q)$  denote the 3-manifold obtained by p/q-surgery along K (i.e.  $M_K(p/q)$  is obtained by a Dehn-filling of  $M_K$  along the simple closed curve of slope p/q on  $\partial M_K$ ). If K is hyperbolic and  $M_K(p/q)$  is not hyperbolic, we say that p/q is an exceptional slope of K.

Let  $M_{4_1}$  denote the complement of figure-eight knot  $4_1$ . The following is well known:

**Proposition 5.2.2.** The set of the exceptional slopes of the knot figure-eight knot is  $E_{4_1} := \{0, 1/0, \pm 1, \pm 2, \pm 3, \pm 4\}$ . Thus for any  $p/q \notin E_{4_1}$  the 3-manifold  $M_{4_1}(p/q)$  is hyperbolic.

The asymptotics of the Turaev–Viro invariants of hyperbolic manifolds obtained by surgery on the figure eight knot are well understood. Ohtsuki [64] proved that hyperbolic

manifolds obtained by integral surgeries on  $4_1$  satisfy the volume conjecture, and the result was extended to rational surgeries by Wong and Yang [87].

**Theorem 5.2.3** ([64, 87]). For any non-exceptional slope p/q of the knot  $4_1$  we have

$$lTV(M_{4_1}(p/q)) = vol(M_{4_1}(p/q)),$$

and hence, in particular,  $M_{4_1}(p/q)$  is q-hyperbolic.

Next we construct two families of q-hyperbolic double twist knots parametrized by an integer n, which we denote by  $D_n := D(2n, -3)$  and  $D'_n := D(2n, -2)$ .

**Theorem 1.5.2.** For any integer  $n \neq 0, -1$ , the following are true:

- 1. The knots  $D_n := D(2n, -3)$  and  $D'_n := D(2n, -2)$  are q-hyperbolic.
- 2. The 3-manifolds  $M_n := M_{D_n}(4n+1)$  and  $M'_n := M_{D'_n}(1)$  are hyperbolic and q-hyperbolic.
- 3. We have

$$lTV(M_{D_n}) \ge vol(M_n)$$
, and  $lTV(M_{D'_n}) \ge vol(M'_n)$ .

We will need the following lemma.

### **Lemma 5.2.4.** For any $n \in \mathbb{Z}$ we have the following:

- 1. The 3-manifold  $M_{4_1}((-4n-1)/n)$  is homeomorphic to  $M_{D_n}(4n+1)$ .
- 2. The 3-manifold  $M_{4_1}(-1/n)$  is homeomorphic to  $M_{D'_n}(1)$ .

*Proof.* For n=0 both (1) and (2) are trivially true: For, both  $D_0, D_0'$  are the trivial knot and we have:  $M_{4_1}(1/0) \cong M_{D_0}(1) = M_{D_0'}(1) \cong S^3$ .

Next suppose that  $n \neq 0$ . Part (1) follows from the fact that the 3-manifold  $M_{4_1}(-(4n+1)/n)$  is related to  $M_{D_n}(4n+1)$  by the sequence of Kirby-Rolfsen-Rourke calculus which is well known to preserve 3-manifolds up to homeomorphism. See for example [72, Chapter

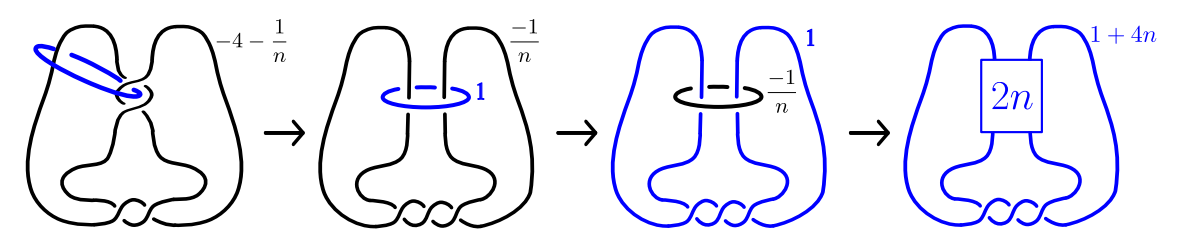


Figure 5.2 Kirby-Rolfsen-Rourke calculus moves showing that  $M_{4_1}((-4n-1)/n)$  is homeomorphic to  $M_{D_n}(4n+1)$ .

- 9]. The sequence of moves required is shown in Figure 5.2. To describe the moves required, let us recall that, as is customary in the Kirby-Rolfsen-Rourke calculus, one indicates the 3-manifold M obtained by Dehn-filling along a link L in  $S^3$  by a diagram of L with each component labeled by the surgery slope used for the component known as a surgery presentation. For components where the surgery coefficient is 1/0, we will omit the label (such surgery is called  $\infty$ -surgery and it produces back  $S^3$ ).
  - The 3-manifold  $M_{4_1}(-(4n+1)/n)$  has a surgery diagram consisting of a knot diagram for  $4_1$  labeled by (-4n-1)/n = -4 1/n. In the leftmost panel of Figure 5.2, we have inserted an unknotted component U, shown in blue, on which the surgery coefficient is  $1/0 = \infty$  and such that it has linking number  $\pm 2$  with the figure-eight knot component. That is  $|lk(U, 4_1)| = 2$ . A -1-twist along U produces produces the second surgery diagram in the sequence. Note that the surgery coefficient of the component corresponding to  $4_1$  has now changed to  $-(4n+1)/n + (lk(U, 4_1))^2 = -1/n$ . This operation is also known as a blow up.
  - The surgery diagram shown in the third panel of Figure 5.2 is obtained by that of the second panel by ambient isotopy that interchanges the two components of the underlying link.
  - Finally, performing n-twists on the component labelled by -1/n gives the rightmost panel of Figure 5.2, which represents a surgery diagram of  $M_{D_n}(4n+1)$ . The operation of performing this (-1/n)-surgery on an unknotted component is also known as a blow down.

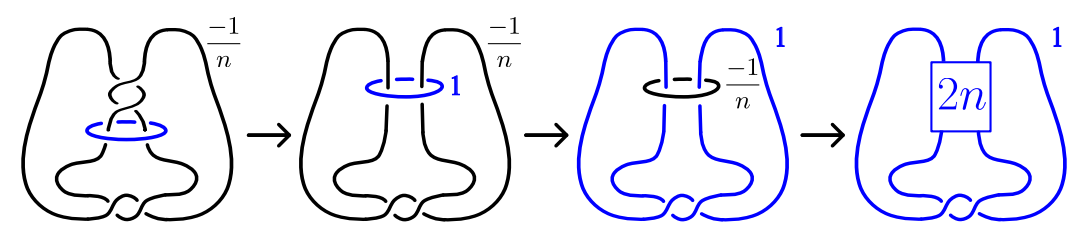


Figure 5.3 Kirby-Rolfsen-Rourke calculus moves showing that  $M_{4_1}(-1/n)$  is homeomorphic to  $M_{D'_n}(1)$ .

A similar sequence of Kirby-Rolfsen-Rourke calculus moves, shown in Figure 5.3, in proves that  $M_{4_1}(-1/n)$  is homeomorphic  $M_{D'_n}(1)$ . Note that this time the inserted unknotted component U, drawn in blue in the leftmost panel of Figure 5.3, has zero linking number with  $4_1$ . That is,  $lk(U, 4_1) = 0$ . In this case, the surgery coefficient of the component corresponding to  $4_1$  is unchanged under the blow up operation since  $-1/n + (lk(U, 4_1))^2 = -1/n$ .

We are now ready to give the proof of Theorem 1.5.2:

Proof of Theorem 1.5.2. By Lemma 5.2.4, for any  $n \in \mathbb{Z}$ , the 3-manifolds  $M_n := M_{D_n}(4n+1)$  is obtained by (-(4n+1)/n)-surgery along the knot  $4_1$ . Since  $n \neq 0, -1$ , by Proposition 5.2.2, the slope -(4n+1)/n is not exceptional for  $4_1$ . Hence  $M_n$  is hyperbolic. Similarly, since  $N_n := M_{D'_n}(1)$  is also obtained by a (-1/n)-surgery along  $4_1$ , it is hyperbolic for  $n \neq 0, \pm 1$ . By Theorem 5.2.3, we conclude that the manifolds  $M_{D_n}(4n+1)$  and  $M_{D'_n}(1)$  are q-hyperbolic for  $n \neq \pm 1$ .

Theorem 5.2.1 implies that the growth rates of the Turaev–Viro invariants of the unfilled twist knot complements  $M_{D_n}$  and  $M_{D'_n}$  are bounded below by the growth rates of  $M_n$  and  $N_n$  respectively. That is we have

$$0 < lTV(M_n) \le lTV(M_{D_n})$$
 and  $0 < lTV(M'_n) \le lTV(M_{D'_n})$ .

Hence, by their definitions, the double twist knots  $D_n$  and  $D'_n$  are also q-hyperbolic, concluding the proof.

# 5.3 Non-characterizing slopes and q-hyperbolicity

A slope p/q is called non-characterizing for a knot  $K \subset S^3$  if there is a knot K' that is not equivalent to K and such that  $M_K(p/q)$  is homeomorphic to  $M_{K'}(p/q)$ . For the viewpoint of this chapter, non-characteristic slopes are useful in the following sense: If we know that  $M_K(p/q)$  is q-hyperbolic then, arguing as in the proof Theorem 1.5.2, we conclude that

$$0 < lTV(M_K(p/q)) = lTV(M_{K'}(p/q)) \le lTV(M_{K'}),$$

and hence K' is a q-hyperbolic knot.

In the articles, [2, 1, 3], the authors provide constructions of knots that admit many non-characterizing slopes. The techniques of these papers apply to many double twist knots to conclude that they admit non-characterizing slopes. On the other hand, these knots can be seen to be q-hyperbolic by Theorem 1.5.2. Using this approach, one starts with a double twist knot, say K, to which both the techniques of [2, 1, 3] and Theorem 1.5.2 apply and builds a family of q-hyperbolic knots that have a common surgery with K.

To illustrate this, we note that the knot  $6_2$  is isotopic to the double twist knot D(-4, -3); we will write  $6_2 = D(-4, -3)$ . See Section 5.5 for more details. By Theorem 1.5.2,  $M_{6_2}(-7) \cong M_{4_1}(-7/2)$  and  $6_2$  is q-hyperbolic. We will use the approach discussed above to prove the following theorem stated in Section 1.5:

### **Theorem 1.5.3.** There is an an infinite set of knots K with the following properties:

- 1. Every knot in K is q-hyperbolic.
- 2. For every  $K \in \mathcal{K}$ ,  $M_K(-7)$  is homeomorphic to  $M_{6_2}(-7)$  and it is q-hyperbolic.
- 3. No two knots in K are equivalent.

In order to prove Theorem 1.5.3 and to discuss further applications of the techniques of [2, 1, 3] in constructions of q-hyperbolic knots, we need some preparation.

## 5.3.1 Annulus presentations and twists

We begin by recalling the notion of an *annulus presentation* of a knot and the operation of an *annulus twist* for knots admitting annulus presentations. The latter operation takes a surgery presentation along a particular class of knots and returns a possibly different knot which shares a surgery with the original knot.

**Definition 5.3.1.** We will say that a knot  $K \subset S^3$  admits an annulus presentation if it can be constructed in the following way:

- Start with standardly embedded annulus  $A \subset \mathbb{R}^2 \cup \{\infty\} \subset S^3$  together with an an unknotted curve c that is disjoint from A that bounds a disc  $\Sigma$  whose interior intersects  $\partial A$  twice; once for each component of  $\partial A$ . Consider c as a framed knot with framing  $\pm 1$ .
- Consider an embedded band  $b: I \times I \to S^3$  such that
  - (i)  $b(I \times I) \cap \partial A = b(\partial I \times I)$ ,
  - (ii)  $b(I \times I) \cap \text{int} A \text{ consists of ribbon singularities}$ ,
  - (iii)  $A \cup b(I \times I)$  is an immersed orientable surface, and
  - (iv)  $b(I \times I) \cap c = \emptyset$ ,

where I = [0, 1]. See the right hand side panel of Figure 5.4 for an illustration of an annulus presentation (A, b, c).

• Performing the  $\pm 1$  surgery on c (i.e blowing down along c) transforms the curve  $(\partial A \setminus b(\partial I \times I)) \cup b(I \times \partial I)$  into a knot that is isotopic to K in  $S^3$ .

Remark 5.3.2. We note that the definition of annulus presentation differs slightly across the literature. Namely, in [3], the authors use a more general defintion of annulus presentation that allows the annulus A to be any embedding. They define a *special* annulus presentation equivalently to the above definition except that the presentation includes the single full

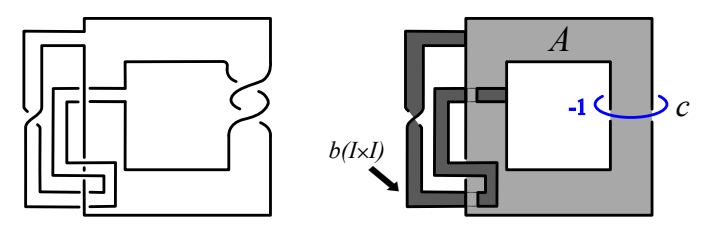


Figure 5.4 Annulus presentation of the knot  $6_2$  in  $S^3$ .

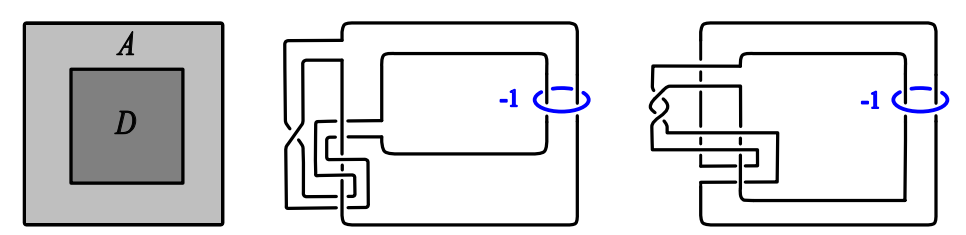


Figure 5.5 **Left:** One of the two connected components, D, of  $\mathbb{R}^2 \cup \{\infty\} \setminus \text{int} A$ . **Middle:** Simple annulus presentation of the knot  $6_2$ . **Right:** Non-simple annulus presentation of the knot  $5_2$ .

crossing (either positive or negative) in the Hopf band resulting from surgery along the  $(\pm 1)$ -framed unknotted component c. Here we use the definition given by Abe–Jong–Omae–Takeuchi [2] and Abe–Jong–Luecke–Osoinach [1]. Note that in [2], the authors use the term band presentation rather than annulus presentation.

To continue, note that given an annulus presentation (A, b, c), the complement of the annulus  $A \subset \mathbb{R}^2 \cup \{\infty\}$  consists of two disk components D and D'. Take D to the component corresponding to the finite region in  $\mathbb{R}^2$  (see leftmost panel of Figure 5.5) and assume that  $\infty \in D'$ .

**Definition 5.3.3.** The annulus presentation (A, b, c) is called *simple* if we have  $b(I \times I) \cap$  int  $D = \emptyset$ .

The middle panel of Figure 5.5 illustrates a simple annulus presentation of the knot  $6_2$  while the rightmost panel illustrates a non-simple annulus presentation for the knot  $5_2$ .

The following lemma of [2] gives a family of knots which admit annulus presentations. In particular, the double twist knots  $D'_n = D(2n, -2)$ , including those listed in Table 5.2, satisfy the assumptions of Lemma 5.3.4.

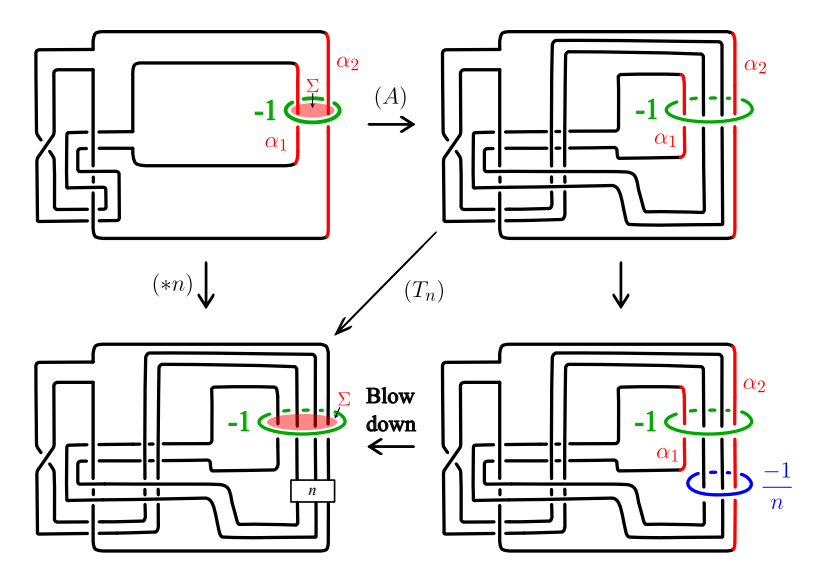


Figure 5.6 **Top row:** Simple annulus presentation of  $6_2$  and the annulus twist (A). **Bottom row:** Introduction of (-1/n)-framed component and blow down.

**Lemma 5.3.4** ([2], Lemma 2.2). If K is a knot with unknotting number one, then K admits an annulus presentation.

Abe and Tagami [3] give a tabluation of all prime knots with 8 or fewer crossings admitting an annulus presentation (see Table 1 of [3]).

We now define an operation known as an n-fold annulus twist. We refer the reader to [1, 2] for further details of this construction. This operation can be applied to a knot K with an annulus presentation (A, b, c), and surgery slope given by an integer  $n \in \mathbb{Z}$ , to produce another knot K', with annulus presentation (A, b', c), so that the 3-manifold  $M_K(n) \cong M_{K'}(n)$ .

**Definition 5.3.5.** Let K be a knot with annulus presentation (A, b, c) with  $\partial A = l_1 \sqcup l_2$ , and let  $n \in \mathbb{Z}$ . We define the n-fold annulus twist operation, denoted by (\*n), as follows:

1. First apply an annulus twist (A). This involves performing Dehn surgery on  $l_1$  and  $l_2$  along slopes 1 and -1, respectively, and gives rise to a homeomorphism of the complement  $M_{l_1 \sqcup l_2}$ . An example is illustrated in the top row of Figure 5.6. Note that in the leftmost panel we have two vertical arcs  $\alpha_1, \alpha_2 \subset \partial A$  that intersect the interior of a disk  $\Sigma$  bounded by the -1 framed unknot c exactly twice. After the operation (A)

is applied, the disk  $\Sigma$  is intersected by four vertical arcs, two of which are between  $\alpha_1$  and  $\alpha_2$ .

- 2. Apply the operation  $(T_n)$ , which is defined by
  - (i) adding another (-1/n)-framed unknot engulfing all but  $\alpha_1$  of the vertical arcs going through c. An illustration is given in the rightmost panel of the second row of Figure 5.6.
  - (ii) blowing down along the (-1/n)-framed component, as shown in the leftmost panel of the second row of Figure 5.6.

An important property of the n-fold annulus twist operation is the following result of Abe-Jong-Luecke-Osoinach [1].

**Theorem 5.3.6** ([1], Theorem 3.10). Let K be a knot with an annulus presentation and K' be the knot obtained by the n-fold twist (\*n). Then the 3-manifold  $M_K(n)$  is homeomorphic to  $M_{K'}(n)$ . That is we have

$$M_K(n) \cong M_{K'}(n).$$

A proof of Theorem 5.3.6 for the knot  $K = 6_2$  is given in Figure 5.7, which is summarized as follows:

- (i) First we blow up around the *n*-framed component, which changes its framing to 0 and introduces a (-1/n)-framed component as shown in the middle panel of the first row.
- (ii) After introducing 1 and −1-framed components (in red) in the right most panel of the first row, we slide the 1-framed component across the −1-framed component to get the right most panel of the second row. Note that the 1 and −1-framed components (in red) in the right most panel of the second row correspond to the boundary components of the annulus A and give the surgery description for the move (A).

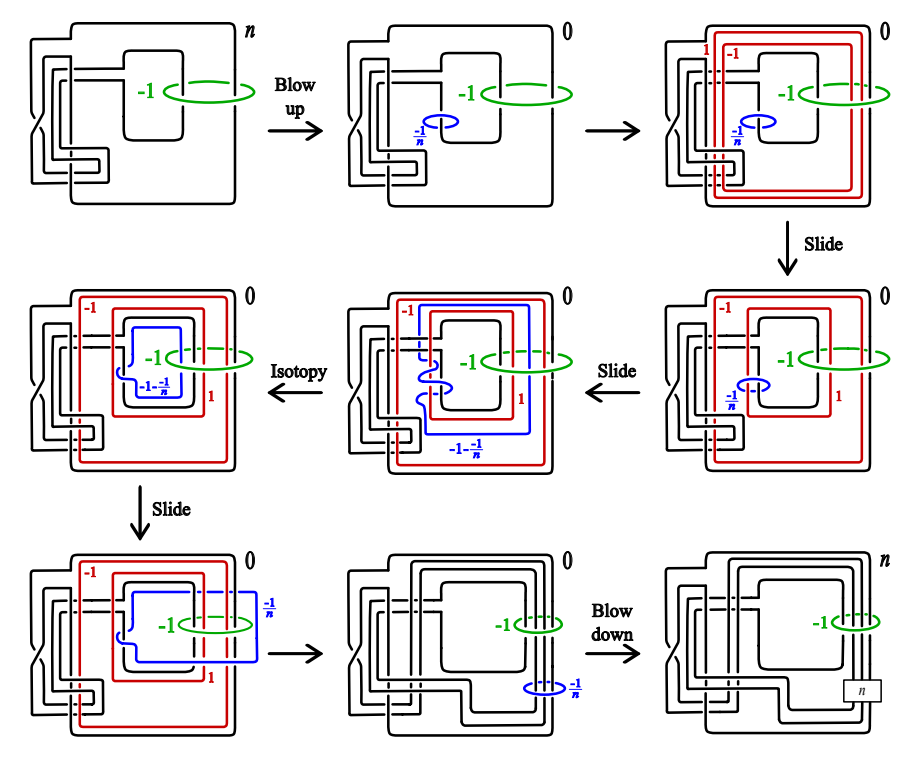


Figure 5.7 A proof that  $M_K(n) \cong M_{K'}(n)$  for  $K = 6_2$  starting with an annulus presentation of K in the top-left and ending with an annulus presentation of K' = (\*n)K in the bottom-right.

- (iii) Next we slide the (-1/n)-framed component across both the 1-framed component (in red) and the -1-framed component (in green) to get the left most panel of the third row.
- (iv) To get from the left most panel to the middle panel of the third row, we perform surgery on the red 1 and -1-framed components, corresponding to the annulus twist (A), and isotope the (-1/n)-framed component. Finally, we blow down, which introduces n full positive twists and changes the framing from 0 to n. This isotopy and blow down correspond to the operation  $(T_n)$ . Hence in the sequence of operations in third row contains an (A) move and a  $(T_n)$  move.

**Remark 5.3.7.** If a knot K admits an annulus presentation and a knot K' is obtained from K by an n-fold annulus twist (\*n), then, in general, K' can be far more complicated than K. However, if K admits a simple annulus presentation, then the annulus presentation of

K' is also simple and is not quite as complicated.

Since the *n*-fold annulus twist operation on a knot produces another knot which also admits an annulus presentation, this operation can be iterated. Indeed, Theorem 5.3.6 implies that for any knot K which admits an annulus presentation and any integer  $n \neq 0$ , there is a set  $K = \{K_i\}_{i \in \mathbb{N}}$  of knots such that

...
$$M_{K_i}(n) \cong M_{K_{i-1}}(n) \cong \cdots \cong M_{K_1}(n) \cong M_K(n)$$
.

In general, we don't know that the knots  $K_i$  are necessarily distinct, so the set  $\mathcal{K}$  may be finite. However, we will see in the proof of Theorem 1.5.3 that in the case of  $6_2$ , iterating the twist operation produces an infinite sequence of mutually distinct knots.

#### 5.3.2 Applications to q-hyperbolicity

In order to prove Theorem 1.5.3, we recall some definitions from Section 3.3.1 of [1]. There the authors use the surgery description of the infinite cyclic covering  $\tilde{E}(K)$  of the exterior E(K) of a knot K to dinstinguish knots obtained by applying the operation (\*n) iteratively, provided that the annulus presentation of the knot to begin with is "good" in the sense of Definition 5.3.8 below.

Let K be a knot with a simple annulus presentation (A, b, c). If we ignore the (-1)-framed loop c, the knot  $U := (\partial A \setminus b(\partial I \times I)) \cup b(I \times \partial I)$  is trivial in  $S^3$ . Consider the link  $U \cup c$  in  $S^3$ . Let D be the disk bounded by U and let  $\Sigma$  be the disk bounded by c. We may isotope  $U \cup c$  so that D is a flat disk contained in  $\mathbb{R}^2 \subset (\mathbb{R}^2 \cup \{\infty\})$  by shrinking the band  $b(I \times I)$ ; denote this isotopy by  $\phi$ . Fix orientations on U and c and cut along and cut the complement of U in  $S^3$  along D. This gives a solid cylinder  $D \times [-1, 1]$ . We will denote the two copies of D resulting from this cutting by  $D_{-1}$  and  $D_1$ . The cutting separates the oriented loop c into a set A oriented arcs with endpoints on  $D_{\pm 1}$ , and the endpoints of each arc  $\alpha \in A$  may be labelled by "+" (resp. "-") according to whether the algebraic intersection number of  $\alpha$  with the disk it lies on is positive (resp. negative). This categorizes  $\alpha$  as one of four

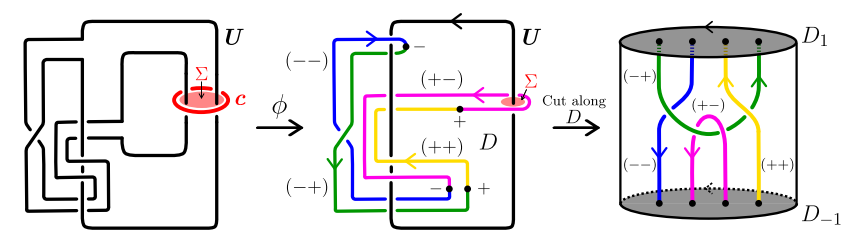


Figure 5.8 The isotopy  $\phi$  applied to the simple annulus presentation of  $6_2$ . In the collar  $D \times [-1, 1]$ , the (+-) arc (in pink) and the (-+) arc (in green) have linking number -1 relative to  $D_{-1} \sqcup D_1$ .

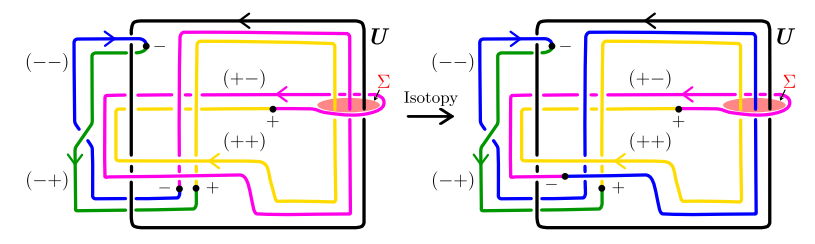


Figure 5.9 **Left:** The isotopy  $\phi$  applied to the simple annulus presentation of  $(A)6_2$ . In this form, Part (2) of Definition 5.3.8 fails. **Right:** Good annulus presentation of  $(A)6_2$ .

types: (++), (--), (+-), and (-+). An illustration of the process for the  $6_2$  knot is shown in Figure 5.8. We refer the reader to [1, Section 3.3.1] for further details of this construction. We need the following definition of [1].

**Definition 5.3.8.** ([1, Definition 3.14]) A simple annulus presentation (A, b, c) is good if  $b(I \times \partial I) \cap intA \neq \emptyset$  and the set of arcs  $\mathcal{A}$  in  $D \times [-1, 1]$  obtained by cutting along D satisfies the following up to isotopy.

- (1)  $\mathcal{A}$  contains exactly one (+-) arc and exactly one (-+) arc, and the linking number of these arcs rel $(D_{-1} \sqcup D_1)$  is  $\pm 1$ .
- (2) For  $\alpha \in \mathcal{A}$ , if  $\alpha \cap \operatorname{int}\Sigma \neq \emptyset$ , then  $\alpha$  is of type (++) (resp. (--)) and the sign of each intersection point in  $\alpha \cap \Sigma$  is + (resp. -).

To illustrate and motivate Definition 5.3.8, we apply the isotopy  $\phi$  shown in Figure 5.8 for the simple annulus presentation of  $6_2$  to the simple annulus presentation obtained by applying the annulus twist (A) shown in the top row of Figure 5.6. The left panel of Figure

5.9 shows the result of applying  $\phi$  to  $(A)6_2$ . However, since there is a (+-) arc intersecting the interior of  $\Sigma$ , it does not satisfy Part (2) of Definition 5.3.8.

To remedy this, we apply an isotopy to move the (-) intersection point between the disk D and the (+-) and (--) arcs, as shown in the right panel of Figure 5.9. This isotopy moves this intersection through  $\Sigma$  and results in a diagram satisfying Part (2) of Defintion 5.3.8. In particular, since the only arcs intersecting int $\Sigma$  are of type (++) and (--), the diagram in the right panel of Figure 5.9 corresponds to a good annulus presentation. After this isotopy, further applications of the annulus twist (A) leave the (+-) and (-+) arcs fixed since they are now disjoint from int $\Sigma$ .

The importance of having a good annulus presentation for a knot K lies in the fact that, as shown in [1], the number of intersection points between (++) arcs and int $\Sigma$  determines the degree of its Alexander polynomial. As Figure 5.9 illustrates, each annulus twist increases the number of such intersections with int $\Sigma$ , hence increasing the degree of the Alexander polynomial.

The following lemma of [1] will be used in the proof of Theorem 1.5.3.

**Lemma 5.3.9** ([1], Lemma 3.12). Let  $n \in \mathbb{Z}$  and suppose the knot K admits a good annulus presentation. Let K' be the knot obtained by applying the operation (\*n) to K. Then, we have the following:

- 1. The knot K' also admits a good annulus presentation.
- 2. If  $\Delta_K(t)$  and  $\Delta_{K'}(t)$  denotes the Alexander polynomial of K and K' respectively, then  $deg\Delta_K(t) < deg\Delta_{K'}(t)$ .

**Remark 5.3.10.** As shown in [1], if a knot K admits a good annulus presentation, then its Alexander polynomial  $\Delta_K(t)$  is monic.

We may now prove Theorem 1.5.3.

Proof of Theorem 1.5.3. As noted earlier the knot  $K_0 := 6_2$  admits a simple annulus presentation. We will consider  $K_0$  with framing -7 and apply the sequence of moves in Figure 5.7 to obtain a knot  $K_1$  with simple annulus presentation and such that  $M_{K_1}(-7) \cong M_{6_2}(-7) \cong M_{4_1}(-7/2)$ . See Theorem 5.3.6. Since as discussed earlier  $M_{6_2}(-7)$  is q-hyperbolic, we obtain that  $K_1$  is q-hyperbolic and  $M_{K_1}(-7)$  is q-hyperbolic. Now we can repeat the process for the knot  $K_1$ , and apply Theorem 5.3.6 again to obtain a knot  $K_2$  with simple annulus presentation and such that  $M_{K_2}(-7) \cong M_{K_1}(-7)$ . Inductively, we create a set  $\mathcal{K} = \{K_i\}_{i \in \mathbb{N}}$  of knots with simple annulus presentations such that

...
$$M_{K_i}(-7) \cong M_{K_{i-1}}(-7) \cong \cdots \cong M_{K_1}(-7) \cong M_{6_2}(-7) \cong M_{4_1}(-7/2).$$

By construction, each  $K_i$  and  $M_{K_i}(-7)$  are q-hyperbolic, hence the collection  $\mathcal{K}$  satisfies parts (1)-(2) of the statement of the theorem.

We now claim that the knots  $K_i \in \mathcal{K}$  are distinct. Let U be the trivial knot in  $S^3$  obtained by ignoring the (-1)-framed loop c in the simple annulus presentation of  $K_0$  (see the middle panel of Figure 5.5). Let D be the disk bounded by U, and let  $\Sigma$  be the disk bounded by c. Figure 5.8 gives the isotopy that flattens D so that it is contained in  $\mathbb{R}^2 \subset (\mathbb{R}^2 \cup \{\infty\})$ . Let  $D_{-1} = D \times \{-1\}$  and  $D_1 = D^2 \times \{1\}$  be copies of D in the bundle  $D^2 \times [-1,1]$ obtained by cutting along D. Note that the resulting set of oriented arcs  $\mathcal{A}$  shown in the right panel of Figure 5.8 contains exactly one (+-) arc and exactly one (-+) arc. Relative to  $D_{-1} \sqcup D_1 \subset D \times [-1,1]$ , the (+-) arc (in pink) links with the (-+) arc (in green) with linking number  $\pm 1$ . Moreover,  $\alpha \cap \Sigma = \emptyset$  for any arc  $\alpha \in \mathcal{A}$ . By Definition 5.3.8,  $K_0$  admits a good annulus presentation.

By Lemma 5.3.9, every  $K_i \in \mathcal{K}$  admits a good annulus presentation, and the Alexander polynomials of this family satisfy

$$\deg \Delta_{K_0}(t) < \deg \Delta_{K_1}(t) < \dots < \deg \Delta_{K_{i-1}}(t) < \deg \Delta_{K_i}(t) < \dots$$

This establishes part (3) of the statement of the theorem.

The above argument applies to any q-hyperbolic knot which admits a good annulus presentation and an integer q-hyperbolic Dehn-filling. For any such knot, analogously to  $6_2$ , one may apply the same procedure to produce an infinite family of distinct q-hyperbolic knots with homeomorphic n-surgeries. For instance, the method can be applied to the knot  $8_{20}$ . See section 5.5 for more details. Hence we have the following:

**Theorem 1.5.4.** Suppose that K is knot that admits a good annulus presentation and such that  $M_K(n)$  is q-hyperbolic for some  $n \in \mathbb{Z} \setminus \{0\}$ . Then there is an infinite family  $\{K_i\}_{i \in \mathbb{N}}$  of distinct q-hyperbolic knots, such that  $M_{K_i}(n) \cong M_K(n)$ , for any  $i \in \mathbb{N}$ .

We now turn our attention to the q-hyperbolic knots  $D'_n = D(2n, -2)$  and their q-hyperbolic fillings  $D'_n(1)$ . It is known that these double twist knots have unknotting number 1, hence admit an annulus presentation by Lemma 5.3.4. This gives rise to the following theorem.

**Theorem 1.5.5.** For any |n| > 1 let  $D'_n := D(2n, -2)$ . There is a sequence of q-hyperbolic knots  $\{K_n^i\}_{i\in\mathbb{N}}$  such that for any  $i\in\mathbb{N}$  we have the following:

- 1. The knot  $K_n^i$  is q-hyperbolic.
- 2. The 3-manifold  $M_{K_n^i}(1)$  is homeomorphic to  $M_{D_n^i}(1)$  and it is q-hyperbolic.

Proof. Fix |n| > 1. The double twist knot  $D'_n := D(2n, -2)$  has unknotting number 1 and hence by Lemma 5.3.4, it admits an annulus presentation. Let  $K_n^0 := D'_n$ . By Theorem 5.3.6 there is a sequence  $\{K_n^i\}_{i\in\mathbb{N}}$  such that

...
$$M_{K_n^i}(1) \cong M_{K_n^{i-1}}(1) \cong \cdots \cong M_{K_n^1}(1) \cong M_{D_n'}(1).$$

Since  $D'_n(1)$  is q-hyperbolic, by Theorem 1.5.2, each manifold  $K^i_n(1)$  is q-hyperbolic. Furthermore, by Theorem 5.2.1, each knot  $K^i_n$  is also q-hyperbolic.

**Remark 5.3.11.** We note that the knots considered in Theorem 1.5.5 are obtained by iteratively applying 1-fold annulus twists. While each knot  $D'_n$  admits an annulus presentation,

they do not have monic Alexander polynomials. Indeed, for  $n \in \mathbb{Z}$ , we have

$$\Delta_{D'_n}(t) \doteq nt - (2n+1) + nt^{-1},\tag{5.1}$$

where  $\doteq$  is taken up to multiplication by  $\pm t^k$ . By Remark 5.3.10, for |n| > 1, the knot  $D'_n$  does not admit a good annulus presentation. This means the knots resulting from 1-fold annulus twists may not be distinct from  $D'_n$ , so the resulting sequence  $\{K_i^n\}_{i\in\mathbb{N}}$  may only be a finite family of distinct q-hyperbolic knots.

# 5.4 An application to quantum representations

In this section, we discuss an application to a conjecture of Andersen, Masbaum, and Ueno known as the AMU conjecture [5] on quantum representations of mapping class groups of surfaces.

Let  $\Sigma_{g,n}$  be a compact oriented surface of genus g with n boundary components, and let  $\operatorname{Mod}(\Sigma_{g,n})$  denote its mapping class group, the group of orientation-preserving homeomorphisms of  $\Sigma_{g,n}$  fixing the boundary pointwise defined in Subsection 2.4.1. The SO(3)-Witten-Reshetikhin-Turaev TQFTs [70, 78] provide families of finite dimensional projective representations of  $\operatorname{Mod}(\Sigma_{g,n})$ .

Fix an odd integer  $r \geq 3$ , which we refer to as the *level*, and let  $I_r = \{0, 2, ..., r-3\}$  be the set of non-negative even integers less than r-2. Fix a primitive 2rth root of unity  $\zeta_{2r}$  and a coloring c of the components of  $\partial \Sigma_{g,n}$  by elements of  $I_r$ . Using the skein-theoretic framework of Blanchet, Habegger, Masbaum, and Vogel [11], this gives a finite dimensional  $\mathbb{C}$ -vector space  $RT_r(\Sigma_{g,n},c)$  and a respresentation

$$\rho_{r,c}: \operatorname{Mod}(\Sigma_{g,n}) \to \mathbb{P}\operatorname{Aut}(RT_r(\Sigma_{g,n},c)),$$

called the SO(3)-quantum representation of  $Mod(\Sigma_{g,n})$  at level r.

The Nielsen-Thurston classification implies that mapping classes  $\gamma \in \text{Mod}(\Sigma_{g,n})$  are either periodic, reducible, or pseudo-Anosov, and the geometry of the mapping torus  $M_{\gamma} = \Sigma_{g,n} \times I/(x \sim \gamma(x))$  of  $\gamma$  is determined by this classification. The AMU conjecture [5] relates the Nielsen-Thurston classification of mapping classes to their quantum representations.

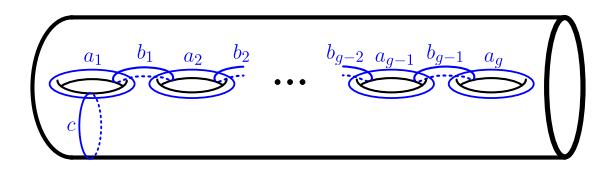


Figure 5.10 The curves  $c, a_1, b_1, \dots, b_{g-1}, a_g$  on  $\Sigma_{g,1}$ .

Conjecture 1.5.6 (AMU Conjecture, [5]). Let  $\phi \in Mod(\Sigma_{g,n})$  be a pseudo-Anasov mapping class. Then for any big enough level r, there is a choice of coloring c of the components of  $\partial \Sigma_{g,n}$  such that  $\rho_{r,c}(\phi)$  has infinite order.

**Remark 5.4.1.** Note that if a mapping class  $\phi \in \operatorname{Mod}(\Sigma_{g,n})$  satisfies the AMU conjecture, then any mapping class that is conjugate of a power of  $\phi$  also satisfies the conjecture

For a simple closed curve  $a \subset \Sigma_{g,n}$  let  $\tau_a \in \operatorname{Mod}(\Sigma_{g,n})$  denote the mapping class represented by a Dehn twist along a and  $\tau_a^{-1}$  denote the inverse mapping class.

On the surface of genus g and with one boundary component  $\Sigma_{g,1}$ , consider the simple closed curves  $c, a_1, b_1, \dots, b_{g-1}, a_g$  shown in Figure 5.10 and the mapping classes

$$\phi_g = \tau_c \tau_{a_1} \tau_{b_1}^{-1} \tau_{a_2} \cdots \tau_{b_{g-1}}^{-1} \tau_{a_g}, \text{ and } \phi_g' = \tau_c^{-1} \tau_{a_1}^{-1} \tau_{b_1} \tau_{a_2}^{-1} \cdots \tau_{b_{g-1}} \tau_{a_g}^{-1}.$$

**Theorem 1.5.7.** For  $g \ge 1$ , the mapping classes  $\phi_g, \phi'_g \in Mod(\Sigma_{g,1})$  are pseudo-Anosov and they satisfy the AMU conjecture.

Given  $\phi \in \text{Mod}(\Sigma_{g,1})$ , the mapping torus

$$T_{\phi} = \Sigma_{g,1} \times [-1,1]/_{(x,1) \sim (\phi(x),-1)}$$

is a 3-manifold which fibers over  $S^1$  with fiber  $\Sigma_{g,1}$  and monodromy  $\phi$ . By Theorem 2.4.6, if  $T_{\phi}$  is q-hyperbolic, then  $\phi$  satisfies the AMU conjecture. To prove Theorem 1.5.7, we will show that each of  $T_{\phi_g}$  and  $T_{\phi'_g}$  is homeomorphic to the complement of a q-hyperbolic double twist knot.

#### 5.4.1 Fibered double twist knots

. The knot D(m,n) is the two-bridge knot associated with the rational number

$$\frac{n}{mn-1} = [m, -n] = \frac{1}{m - \frac{1}{n}}.$$

In general, we define the continued fraction expansion (CFE) by

$$[a_1, a_2, \dots, a_k] := \frac{1}{a_1 + \frac{1}{a_2 + \frac{1}{a_3 + \dots + \frac{1}{a_k}}}}.$$

We note that a CFE for a rational number is not unique, hence a two-bridge knot can have multiple associated CFEs. The following properties of double twist knots will useful:

- D(m,n) = D(n,m) are equivalent knots.
- Suppose D(m,n) has an associated CFE  $[a_1,\ldots,a_k]$ . Its mirror image  $D^*(m,n)$  is equivalent to D(-m,-n), and the CFE of the mirror image is  $[-a_1,\ldots,-a_k]$ .

We recall the following well known lemma that can be found, for example, in [33].

**Lemma 5.4.2.** A two-bridge knot is fibered if and only if it has a CFE of the form  $[a_1, \ldots, a_k]$  such that  $|a_i| = 2$  for  $i = 1, \ldots, k$  and k is even.

As shown in [33], every fibered two-bridge knot can be identified with the boundary of the Murasugi sum of a sequence of right and left Hopf bands determined by the entries in its CFE. The monodromy of the left (resp. right) Hopf band is the left (resp. right) Dehn twist, and the monodromy of a fibered two-bridge knot with CFE  $[a_1, \ldots, a_k]$  (with  $|a_i| = 2$ ) is given by the product of k Dehn twists corresponding to each Hopf band in the Murasugi sum. In this case, the resulting fiber is the surface of genus  $\frac{k}{2}$  with one boundary component.

**Proposition 5.4.3.** For any integer g > 0, the double twist knot  $D(3, 2g) \subset S^3$  is fibered with monodromy  $\phi_g \in Mod(\Sigma_{g,1})$ .

Proof. Let  $n \le -1$  be an integer, and set g := -n. By the properties of twist knots, we have  $D(2n, -3) = D^*(3, 2g)$ . The knot D(3, 2g) is the two-bridge knot associated to [3, -2g] = -1

 $\frac{-2g}{-6g+1}$ . By Lemma 5.4.2, D(2n, -3) is fibered if and only if D(3, 2g) has a CFE of the form  $[a_1, \ldots, a_k]$  with  $|a_i| = 2$ . We will show that D(3, 2g) has a CFE  $[2, 2, -2, 2, \ldots, -2, 2]$  of length 2g.

We note this CFE alternates sign beginning with the second term. We assume

$$\frac{-2g}{-6g+1} = [2, 2, -2, 2, \dots, (-1)^{2g-1}2, (-1)^{2g}2] = \frac{1}{2+A_q},$$
(5.2)

where  $A_g := [2, -2, 2, \dots, (-1)^{2g-1}2, (-1)^{2g}2]$  of length 2g - 1, and proceed by induction. For D(3, 2(g+1)), we have

$$[2, 2, -2, \dots, (-1)^{2g+2}2] = \frac{1}{2 + \frac{1}{-2 + A_g}}$$

$$= \frac{-2(g+1)}{-6(g+1) + 1}$$

$$= [3, -2(g+1)],$$

where the second line follows from the identity  $A_g = [3, -2g] - 2$ . This establishes the claim, which implies that the double twist knot D(2n, -3) is fibered for  $n \le -1$ .

Following [33], the knot D(3,2g) can be identified with the boundary of the Murasugi sum of 2g Hopf bands. The monodromy is then a product of left and right Dehn twists corresponding to the sign of each entry of the CFE  $[2,2,-2,2,\ldots,(-1)^{2g-1}2,(-1)^{2g}2]$ . These Dehn twists correspond to the collection of curves on  $\Sigma_{g,1}$  shown in Figure 5.10, and the monodromy  $\phi_g = \tau_c \tau_{a_1} \tau_{b_1}^{-1} \tau_{a_1} \cdots \tau_{b_{g-1}}^{-1} \tau_{a_g}$ .

## 5.4.2 Proof of Theorem 1.5.7

By Proposition 5.4.3, the knot D(3,2g), for g > 0, is fibered. Since the knots D(3,2g) are hyperbolic (see for example [29]), by the work of Thurston the mapping class  $\phi_g$  is pseudo-Anosov [74]. By Theorem 1.5.2, these knots are q-hyperbolic. The mirror image

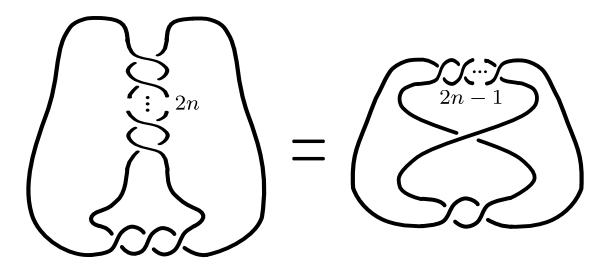


Figure 5.11 Alternating diagram of D(-2n, -3) realizing the even crossing knots of Table 5.1.

n	-4	-3	-2	-1	1	2	3
$D_n$	$10_{2}$	82	$6_2$	$4_1$	$5_2$	$7_3$	$9_{3}$

Table 5.1 Low-crossing knots  $D_n = D(2n, -3)$ .

 $D(-2g, -3) = D^*(3, 2g)$  is also hyperbolic, q-hyperbolic and fibers with monodromy  $\phi'_g = \tau_c^{-1}\tau_{a_1}^{-1}\tau_{b_1}\tau_{a_1}^{-1}\cdots\tau_{b_{g-1}}\tau_{a_1}^{-1}$ . Hence, by [22, Theorem 1.2],  $\phi_g$  and  $\phi'_g$  satisfy the conclusion of the AMU conjecture.

#### 5.5 Low crossing knots and low volume 3-manifolds

Tables 5.1 and 5.2 give the twist knots  $D_n = D(2n, -3)$  and  $D'_n = D(2n, -2)$  up to 10 crossings, respectively. By Lemma 5.2.4, all of these share surgeries with  $4_1$ .

We identify these knots by giving an alternating projection realizing the crossing numbers in conjunction with Rolfsen's tabulation of low-crossing knots [72]. We note that for the knot D(2n, -3), the resulting diagram with 2n + 3 crossings corresponding to Figure 5.1 is alternating when  $n \geq 1$ , allowing us to identify the odd crossing knots of Table 5.1. To identify the even crossing knots of Table 5.1, we see in Figure 5.11 that, after applying Reidemeister moves, we obtain an alternating diagram for D(-2n, -3) with 2n+2 crossings.

Similarly, the original diagram for D(2n, -2) is also alternating with 2n + 2 crossings for  $n \ge 1$ , allowing us to identify the even crossing knots of Table 5.2. Figure 5.12 gives an alternating diagram for D(-2n, -2) with 2n + 1 crossings, realizing the odd crossing knots of Table 5.2.

By Proposition 5.4.3, for  $n \leq -1$  the knot D(2n, -3) is fibered with genus |n|. By Table 5.1, for n = -4, -3, -2, -1, the knot D(2n, -3) is identified as the corresponding

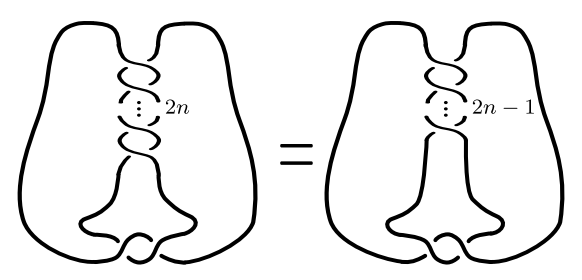


Figure 5.12 Alternating diagram of D(-2n, -2) realizing the odd crossing knots of Table 5.2.

n	-4	-3	-2	-1	1	2	3	4
$D'_n$	$9_{2}$	$7_2$	$5_2$	$3_1$	$4_1$	$6_{1}$	81	$10_{1}$

Table 5.2 Low-crossing knots  $D'_n = D(2n, -2)$ .

knot shown in the table. Indeed the knots  $10_2$ ,  $8_2$ ,  $6_2$ , and  $4_1$  are well known to be fibered of genus, 4, 3, 2, and 1, respectively [57].

**Remark 5.5.1.** The manifold  $M_{4_1}(-5)$ , which is homeomorphic to  $M_{5_2}(5)$  by Lemma 5.2.4 and Table 5.1, is known as the Meyerhoff manifold. It is the second-smallest volume closed orientable hyperbolic 3-manifold, with volume approximately 0.9814.

Futer, Purcell, and Schleimer recently wrote a software package [31], in conjunction with forthcoming work [32], for testing the cosmetic surgery conjecture. At our request, they extended the code to allow for testing whether pairs of cusped 3-manifolds have common Dehn fillings as well as identifying those fillings. Running the code for knots up to 12 crossings, as well as on SnapPy's census of the 1267 hyperbolic knot complements that can be triangulated with fewer than 10 tetrahedra [20], he verified the data given in Tables 5.1 and 5.2 and identified many additional knots which share surgeries with 4<sub>1</sub>.

Tables 5.3 and 5.4 list all the knot complements from the SnapPy census of hyperbolic cusped 3-manifolds that admit triangulations with at most nine tetrahedra and have shared Dehn fillings with the complement of  $4_1$ . The information on the tables is recorded as follows: Column 1 presents the knot K with the notation used in the SnapPy census while Column 2 gives the approximate volume of  $M_K$ . Column 3 gives the surgery slopes a/b, p/q, with

K	$vol(M_K)$	Slopes $a/b$ , $p/q$	$\operatorname{vol}(M_K(a/b))$	Knot
$K2_1$	2.029883	-	-	$4_1$
$K3_2$	2.828122	5, -5	0.981369	$5_2$
		1, 1/2	1.398509	
$K4_1$	3.163963	1, -1/2	1.398509	61
$K4_2$	3.331744	1, 1/3	1.731983	$7_2$
$K5_2$	3.427205	1, -1/3	1.731983	81
$K5_3$	3.486660	1, 1/4	1.858138	$9_{2}$
$K5_9$	4.056860	-2, 2/3	1.737124	$10_{132}$
$K5_{12}$	4.124903	3, 3/2	1.440699	820
$K5_{13}$	4.124903	1, 1/3	1.731983	$11n_{38}$
$K5_{19}$	4.400833	-7, -7/2	1.649610	$6_{2}$
$K5_{20}$	4.592126	9, -9/2	1.752092	$7_3$
$K6_1$	3.526196	1, -1/4	1.858138	$10_{1}$
$K6_2$	3.553820	1, 1/5	1.918602	$11a_{247}$
$K6_8$	4.293750	-3, 3/5	1.921026	
$K6_9$	4.307917	-2, 2/5	1.919520	
$K6_{23}$	4.935243	-11, -11/3	1.876053	82
$K6_{24}$	4.994856	13, -13/3	1.903695	$9_{3}$
$K6_{37}$	5.413307	7, 7/3	1.805827	$15n_{41127}$
$K7_1$	3.573883	1, -1/5	1.918602	$12a_{803}$
$K7_2$	3.588914	1, 1/6	1.952062	$13a_{3143}$
$K7_{10}$	4.354670	-4, 4/7	1.973762	
$K7_{11}$	4.359783	-3, 3/7	1.973161	
$K7_{41}$	4.933530	-5, 5/4	1.873482	
$K7_{44}$	4.993457	7, 7/5	1.932061	
$K7_{45}$	5.114841	-15, -15/4	1.946574	$10_{2}$
$K7_{46}$	5.140207	17, -17/4	1.957888	$11a_{364}$
$K7_{95}$	5.860539	11, 11/2	1.822675	$10_{128}$
$K7_{96}$	5.860539	13, 13/3	1.903695	$11n_{57}$
$K7_{98}$	5.904086	14, 14/3	1.915331	$12n_{243}$
$K7_{129}$	6.922634	-7, 7/3	1.805827	

Table 5.3 Knots in the SnapPy census of cusped hyperbolic 3-manifolds that share surgeries with  $4_1$ .

 $M_K(a/b) \cong M_{4_1}(p/q)$  and Column 4 gives the approximate volume of that manifold. All of these knots, many of which are twisted torus knots, have known diagrams, but they may be complicated and require hundreds of crossings. Using the tables of [13, 15, 14], we may identify some of the examples from the knot tables. Note that since since  $4_1$  is amphicheiral, we have  $M_{4_1}(-p/q) \cong M_{4_1}(p/q)$ . Hence the slopes p/q in the tables can be, equivalently, be replaced with its negative.

The following applies to all the knots in Tables 5.3 and 5.4:

**Proposition 5.5.2.** Suppose that K is a hyperbolic knot in  $S^3$  such that  $M_K$  admits a triangulation with t tetrahedra. Suppose, moreover, that  $M_K(a/b) \cong M_{4_1}(p/q)$ , for some slopes  $a/b, p/q \in \mathbb{Q}$ , where p/q is a non-exceptional slope of  $4_1$ . Then we have

$$\operatorname{vol}(M_K(a/b)) \le lTV(M_K) \le v_{\operatorname{oct}} \cdot t$$

where  $v_{\rm oct} \approx 3.6638$  is the volume of the ideal regular octahedron.

*Proof.* The upper bound follows at once from [9, Corollary 3.9].

By Theorem 5.2.3,  $\operatorname{vol}(M_{4_1}(p/q)) = lTV(M_{4_1}(p/q))$  and, by assumption,  $M_K(a/b) \cong M_{4_1}(p/q)$ . Combining these with Theorem 5.2.1, leads to the lower bound of  $lTV(M_K)$ .  $\square$ 

Remark 5.5.3. It is known that the lowest volume hyperbolic knots are  $4_1$ ,  $5_2$ ,  $6_1$ , and the (-2,3,7)-pretzel knot. In [16], Chen and Yang give computational evidence for the Turaev–Viro invariant volume conjecture for each of these knots. By Lemma 5.2.4,  $5_2$  and  $6_1$  share surgeries with  $4_1$ , hence are q-hyperbolic by Theorem 1.5.2. However, the (-2,3,7)-pretzel knot was shown not to share any surgeries with  $4_1$  using the code of Futer–Purcell–Schleimer [31]. Similarly the knot  $6_3$  was shown not to share any surgeries with  $4_1$ , making it the only hyperbolic knot with up to six crossings for which q-hyperbolicity cannot be decided with the methods of this paper.

**Remark 5.5.4.** As we see in Table 5.3, the knot  $K5_{12} = 8_{20}$  shares a surgery with  $4_1$ . In particular,  $M_{4_1}(3/2) \cong M_{8_{20}}(3)$ . This is a closed manifold of volume  $\approx 1.440699$ . In

addition, as shown in [1],  $8_{20}$  admits a good annulus presentation. This means an analogous version of Theorem 1.5.3 also holds for  $8_{20}$ .

Remark 5.5.5. Table 5.3 includes the knots  $8_{20}$ ,  $10_{132}$ ,  $11n_{38}$ , and  $11n_{57}$ . According to KnotInfo [57], the complements  $M_{8_{20}}$ ,  $M_{10_{132}}$ ,  $M_{11n_{38}}$ , and  $M_{11n_{57}}$  are also fibered, so their associated monodromies (as well as powers of conjugates of those mapping classes) satisfy he AMU conjecture.

K	$\operatorname{vol}(M_K)$	Slopes $a/b$ , $p/q$	$\operatorname{vol}(M_K(a/b))$	Knot
$K8_1$	3.60046726278	1, -1/6	1.9520620754135	$14a_{12741}$
$K8_2$	3.6095391745	1, 1/7	1.9724601973306	$15a_{54894}$
$K8_9$	4.3790606712	-5, 5/9	1.9957717794010	
$K8_{10}$	4.38145643736	-4, 4/9	1.9954776244141	
$K8_{61}$	5.07001608898	9, 9/7	1.9788631982608	
$K8_{62}$	5.0827080657	11, 11/8	1.9914466741922	
$K8_{64}$	5.1955903246	-19, 19/5	1.9776430099735	$12a_{722}$
$K8_{65}$	5.2086109485	-21, 21/5	1.983357467405	$13a_{4874}$
$K8_{96}$	5.75222662008	11, 11/5	1.9478817102192	
$K8_{105}$	5.8281487245	-16, 16/7	1.9891579197851	
$K8_{133}$	6.1411744018	22, 22/5	1.9859441335531	
$K8_{135}$	6.1504206159	23, 23/5	1.9883610027459	T(7,9,6,-6,5,-1)
$K8_{143}$	6.2597017011	-13, 13/4	1.9334036965515	
$K8_{145}$	6.27237250941	1, 1/2	1.3985088841508	$14n_{18212}$
$K8_{268}$	7.26711903086	9, 9/4	1.9026876676640	
$K9_1$	3.61679304740	-1, -1/7	1.9724601973306	
$K9_2$	3.62268440821	1, 1/8	1.9857927453641	
$K9_8$	4.3912243457	-6, 6/11	2.0069885249369	
$K9_9$	4.39253386353	5, 5/11	2.0068241855029	
$K9_{83}$	5.1043901461	13, 13/10	2.004926648441	
$K9_{85}$	5.1089909300	-15, 15/11	2.0095023855854	
$K9_{93}$	5.23864536794	23, -23/6	1.9940644235057	$14a_{12197}$
$K9_{94}$	5.24618858374	25, -25/6	1.9973474789782	$15a_{85258}$
$K9_{152}$	5.8653629974	20, 20/9	2.004886373798	
$K9_{155}$	5.8812168764	-25, 25/11	2.0133867882020	
$K9_{242}$	6.2152290434	31, 31/7	2.007727892627	
$K9_{244}$	6.21858163948	-32, 32/7	2.0085996110216	
$K9_{282}$	6.5328202770	-21, 21/4	1.9754820965797	
$K9_{296}$	6.6272713527	27, 27/5	1.9965186652378	
$K9_{299}$	6.6445653099	19, 19/3	1.9565702867106	
$K9_{435}$	7.2356793751	-3, 3/4	1.8634426716184	

Table 5.4 Knots in the SnapPy census of cusped hyperbolic 3-manifolds that share surgeries with  $4_1$ .

#### **BIBLIOGRAPHY**

- [1] T. Abe, I. D. Jong, J. Luecke, and J. Osoinach. Infinitely many knots admitting the same integer surgery and a four-dimensional extension. *Int. Math. Res. Not. IMRN*, 2015(22):11667–11693, 2015.
- [2] T. Abe, I. D. Jong, Y. Omae, and M. Takeuchi. Annulus twist and diffeomorphic 4-manifolds. *Math. Proc. Cambridge Philos. Soc.*, 155(2):219–235, 2013.
- [3] T. Abe and K. Tagami. Knots with infinitely many non-characterizing slopes. *Kodai Math. J.*, 44(3):395–421, 2021.
- [4] I. Agol. Small 3-manifolds of large genus. Geom. Dedicata, 102:53–64, 2003.
- [5] J. E. Andersen, G. Masbaum, and K. Ueno. Topological quantum field theory and the Nielsen-Thurston classification of M(0,4). *Math Proc. Cambridge Philos. Soc.*, 141:477–488, 2006.
- [6] M. Atiyah. Topological quantum field theories. Inst. Hautes Études Sci. Publ. Math., 68:175–186 (1989), 1988.
- [7] X. Bao and F. Bonahon. Hyperideal polyhedra in hyperbolic 3-space. *Bull. Soc. Math. France*, 130(3):457–491, 2002.
- [8] G. Belletti. The maximum volume of hyperbolic polyhedra. Trans. Amer. Math. Soc., 374(2):1125–1153, 2021.
- [9] G. Belletti, R. Detcherry, E. Kalfagianni, and T. Yang. Growth of quantum 6*j*-symbols and applications to the volume conjecture. *J. Differential Geom.*, 120(2):199–229, 2022.
- [10] R. Benedetti and C. Petronio. On Roberts' proof of the Turaev-Walker theorem. *J. Knot Theory Ramifications*, 5(4):427–439, 1996.
- [11] C. Blanchet, N. Habegger, G. Masbaum, and P. Vogel. Topological quantum field theories derived from the Kauffman bracket. *Topology*, 34(4):883–927, 1995.
- [12] H. Boden and C. Curtis. The  $SL(2,\mathbb{C})$  Casson invariant for Dehn surgeries on two-bridge knots. Algebraic & Geometric Topology, 12(4):2095-2126, 2012.
- [13] P. J. Callahan, J. C. Dean, and J. R. Weeks. The simplest hyperbolic knots. *J. Knot Theory Ramifications*, 8(3):279–297, 1999.
- [14] A. Champanerkar, I. Kofman, and T. Mullen. The 500 simplest hyperbolic knots. *J. Knot Theory Ramifications*, 23(12):1450055, 34, 2014.
- [15] A. Champanerkar, I. Kofman, and E. Patterson. The next simplest hyperbolic knots. J. Knot Theory Ramifications, 13(7):965–987, 2004.
- [16] Q. Chen and T. Yang. Volume conjectures for the Reshetikhin-Turaev and the Turaev-Viro invariants. *Quantum Topol.*, 9(3):419–460, 2018.

- [17] F. Costantino. 6j-symbols, hyperbolic structures and the volume conjecture. Geom. Topol., 11:1831–1854, 2007.
- [18] F. Costantino. Coloured Jones invariants of links and the volume conjecture. J. Lond. Math. Soc. (2), 76(1):1–15, 2007.
- [19] F. Costantino and D. Thurston. 3-manifolds efficiently bound 4-manifolds. *J. Topol.*, 1(3):703–745, 2008.
- [20] M. Culler, N. M. Dunfield, M. Goerner, and J. R. Weeks. SnapPy, a computer program for studying the geometry and topology of 3-manifolds. Available at http://snappy.computop.org (08/02/2023).
- [21] R. Detcherry. Growth of Turaev-Viro invariants and cabling. *J. Knot Theory Ramifications*, 28(14):1950041, 8, 2019.
- [22] R. Detcherry and E. Kalfagianni. Quantum representations and monodromies of fibered links. Adv. Math., 351:676–701, 2019.
- [23] R. Detcherry and E. Kalfagianni. Gromov norm and Turaev-Viro invariants of 3-manifolds. Ann. Sci. Éc. Norm. Supér. (4), 53(6):1363–1391, 2020.
- [24] R. Detcherry and E. Kalfagianni. Cosets of monodromies and quantum representations. *Indiana Univ. Math. J.*, 71(3):1101–1129, 2022.
- [25] R. Detcherry, E. Kalfagianni, and T. Yang. Turaev-Viro invariants, colored Jones polynomials, and volume. *Quantum Topol.*, 9(4):775–813, 2018.
- [26] T. Dimofte and S. Gukov. Quantum field theory and the volume conjecture. In *Interactions between hyperbolic geometry, quantum topology and number theory*, volume 541 of *Contemp. Math.*, pages 41–67. Amer. Math. Soc., Providence, RI, 2011.
- [27] B. Farb and D. Margalit. A primer on mapping class groups, volume 49 of Princeton Mathematical Series. Princeton University Press, Princeton, NJ, 2012.
- [28] R. Fenn and C. Rourke. On kirby's calculus of links. Topology, 18(1):1–15, 1979.
- [29] D. Futer and F. Guéritaud. Angled decompositions of arborescent link complements. *Proc. Lond. Math. Soc.* (3), 98(2):325–364, 2009.
- [30] D. Futer, E. Kalfagianni, and J. Purcell. Guts of surfaces and the colored Jones polynomial, volume 2069 of Lecture Notes in Mathematics. Springer, Heidelberg, 2013.
- [31] D. Futer, J. S. Purcell, and S. Schleimer. Excluding cosmetic surgeries using hyperbolic geometry. Code available at http://github.com/saulsch/Cosmetic.git.
- [32] D. Futer, J. S. Purcell, and S. Schleimer. Excluding cosmetic surgeries using hyperbolic geometry. *In Preparation*, 2023.
- [33] D. Gabai and W. H. Kazez. Pseudo-anosov maps and surgery on fibred 2-bridge knots. Topology and its Applications, 37(1):93–100, 1990.

- [34] M. Gromov. Volume and bounded cohomology. Inst. Hautes Études Sci. Publ. Math., 56:5–99 (1983), 1982.
- [35] A. Hatcher. Notes on Basic 3-Manifold Topology. Unpublished notes, 2001.
- [36] A. Hatcher, P. Lochak, and L. Schneps. On the Teichmüller tower of mapping class groups. *J. Reine Angew. Math.*, 521:1–24, 2000.
- [37] A. Hatcher and W. Thurston. A presentation for the mapping class group of a closed orientable surface. *Topology*, 19(3):221–237, 1980.
- [38] J. Hempel. 3-Manifolds. Princeton University Press, Princeton, N. J.; University of Tokyo Press, Tokyo, 1976. Ann. of Math. Studies, No. 86.
- [39] K. H. Hofmann and G. Betsch, editors. Geschlossene Flächen in dreidimensionalen Mannigfaltigkeiten [19–29], pages 147–159. De Gruyter, Berlin, New York, 2005.
- [40] W. H. Jaco and P. B. Shalen. Seifert fibered spaces in 3-manifolds. *Mem. Amer. Math. Soc.*, 21(220):viii+192, 1979.
- [41] K. Johannson. Homotopy equivalences of 3-manifolds with boundaries, volume 761 of Lecture Notes in Mathematics. Springer, Berlin, 1979.
- [42] V. F. R. Jones. A polynomial invariant for knots via von Neumann algebras. *Bulletin* (New Series) of the American Mathematical Society, 12(1):103 111, 1985.
- [43] V. F. R. Jones. Hecke algebra representations of braid groups and link polynomials. *Annals of Mathematics*, 126(2):335–388, 1987.
- [44] E. Kalfagianni and J. M. Melby. Constructions of q-hyperbolic knots, 2023.
- [45] R. M. Kashaev. Quantum dilogarithm as a 6j-symbol. Modern Phys. Lett. A, 9(40):3757-3768, 1994.
- [46] R. M. Kashaev. A link invariant from quantum dilogarithm. Modern Phys. Lett. A, 10(19):1409-1418, 1995.
- [47] R. M. Kashaev. The hyperbolic volume of knots from the quantum dilogarithm. *Lett. Math. Phys.*, 39(3):269–275, 1997.
- [48] L. H. Kauffman. State models and the Jones polynomial. *Topology*, 26(3):395–407, 1987.
- [49] R. Kirby. A calculus for framed links in  $s^3$ . Invent Math, 45:35–56, 1978.
- [50] A. N. Kirillov and N. Y. Reshetikhin. Representations of the algebra  $U_q(sl(2))$ , q-orthogonal polynomials and invariants of links. In *Infinite-dimensional Lie algebras and groups (Luminy-Marseille, 1988)*, volume 7 of *Adv. Ser. Math. Phys.*, pages 285–339. World Sci. Publ., Teaneck, NJ, 1989.

- [51] S. Kumar. Fundamental shadow links realized as links in  $S^3$ . Algebraic & Geometric Topology, 21(6):3153–3198, 2021.
- [52] S. Kumar and J. M. Melby. Asymptotic additivity of the Turaev-Viro invariants for a family of 3-manifolds. J. Lond. Math. Soc. (2), 106(4):3043–3068, 2022.
- [53] S. Kumar and J. M. Melby. Turaev–Viro invariants and cabling operations. *International Journal of Mathematics*, 34(09):2350065, 2023.
- [54] W. B. R. Lickorish. A representation of orientable combinatorial 3-manifolds. *Annals of Mathematics*, 76(3):531–540, 1962.
- [55] W. B. R. Lickorish. The skein method for three-manifold invariants. *J. Knot Theory Ramifications*, 2(2):171–194, 1993.
- [56] W. B. R. Lickorish. An Introduction to Knot Theory. Graduate Texts in Mathematics. Springer, New York, NY, 1 edition, 1997.
- [57] C. Livingston and A. H. Moore. Knotinfo: Table of knot invariants. URL: knotinfo. math.indiana.edu, March 2023.
- [58] B. Martelli. An Introduction to Geometric Topology. CreateSpace Independent Publishing Platform, 2016.
- [59] J. Milnor. A unique decomposition theorem for 3-manifolds. American Journal of Mathematics, 84(1):1–7, 1962.
- [60] H. R. Morton. The coloured Jones function and Alexander polynomial for torus knots. Math. Proc. Cambridge Philos. Soc., 117(1):129–135, 1995.
- [61] G. D. Mostow. Quasi-conformal mappings in *n*-space and the rigidity of hyperbolic space forms. *Inst. Hautes Études Sci. Publ. Math.*, 34:53–104, 1968.
- [62] H. Murakami. An introduction to the volume conjecture. In *Interactions between hyper-bolic geometry, quantum topology and number theory*, volume 541 of *Contemp. Math.*, pages 1–40. Amer. Math. Soc., Providence, RI, 2011.
- [63] H. Murakami and J. Murakami. The colored Jones polynomials and the simplicial volume of a knot. *Acta Math.*, 186(1):85–104, 2001.
- [64] T. Ohtsuki. On the asymptotic expansion of the quantum su(2) invariant at  $q = exp(4\pi/n)$  for closed hyperbolic 3-manifolds obtained by integral surgery along the figure-eight knot. Algebraic & Geometric Topology, 2018.
- [65] G. Perelman. The entropy formula for the Ricci flow and its geometric applications.  $arXiv\ preprint\ available\ at\ arXiv:math/0211159,\ 2002.$
- [66] G. Perelman. Finite extinction time for the solutions to the Ricci flow on certain three-manifolds. arXiv preprint available at arXiv:math/0307245, 2003.

- [67] G. Perelman. Ricci flow with surgery on three-manifolds. arXiv preprint available at arXiv:math/0303109, 2003.
- [68] G. Prasad. Strong rigidity of Q-rank 1 lattices. Invent. Math., 21:255–286, 1973.
- [69] V. V. Prasolov and A. B. Sossinsky. Knots, links, braids and 3-manifolds, volume 154 of Translations of Mathematical Monographs. American Mathematical Society, Providence, RI, 1997. An introduction to the new invariants in low-dimensional topology, Translated from the Russian manuscript by Sossinsky [Sosinskii].
- [70] N. Reshetikhin and V. G. Turaev. Invariants of 3-manifolds via link polynomials and quantum groups. *Invent. Math.*, 103(3):547–597, 1991.
- [71] J. Roberts. Skein theory and Turaev-Viro invariants. Topology, 34(4):771–787, 1995.
- [72] D. Rolfsen. Knots and Links. American Mathematical Society, 2003.
- [73] J. Schultens. *Introduction to 3-manifolds*, volume 151 of *Graduate Studies in Mathematics*. American Mathematical Society, Providence, RI, 2014.
- [74] W. P. Thurston. The geometry and topology of three-manifolds. Princeton University Math Department Notes, 1979.
- [75] W. P. Thurston. Three-dimensional manifolds, Kleinian groups and hyperbolic geometry. *Bull. Amer. Math. Soc.* (N.S.), 6(3):357–381, 1982.
- [76] W. P. Thurston. On the geometry and dynamics of diffeomorphisms of surfaces. *Bulletin* (New Series) of the American Mathematical Society, 19(2):417 431, 1988.
- [77] V. G. Turaev. Shadow links and face models of statistical mechanics. *J. Differential Geom.*, 36(1):35–74, 1992.
- [78] V. G. Turaev. Quantum invariants of knots and 3-manifolds, volume 18 of De Gruyter Studies in Mathematics. Walter de Gruyter & Co., Berlin, 1994.
- [79] V. G. Turaev and O. Y. Viro. State sum invariants of 3-manifolds and quantum 6j-symbols. *Topology*, 31(4):865–902, 1992.
- [80] A. H. Wallace. Modifications and cobounding manifolds. Canadian Journal of Mathematics, 12:503–528, 1960.
- [81] E. Witten. Topological quantum field theory. Communications in Mathematical Physics, 117(3):353-386, 1988.
- [82] E. Witten. Quantum field theory and the Jones polynomial. Communications in Mathematical Physics, 121(3):351 399, 1989.
- [83] K. H. Wong. Asymptotics of some quantum invariants of the Whitehead chains. arXiv preprint at arXiv:1912.10638, 2019.

- [84] K. H. Wong. Volume conjecture, geometric decomposition and deformation of hyperbolic structures. arXiv preprint at arXiv:1912.11779, 2020.
- [85] K. H. Wong and T. Yang. Relative Reshetikhin-Turaev invariants, hyperbolic cone metrics and discrete Fourier transforms I. arXiv preprint at arXiv:2008.05045, 2020.
- [86] K. H. Wong and T. Yang. Relative Reshetikhin-Turaev invariants, hyperbolic cone metrics and discrete Fourier transforms II. arXiv preprint at arXiv:2009.07046, 2020.
- [87] K. H. Wong and T. Yang. On the volume conjecture for hyperbolic dehn-filled 3-manifolds along the figure-eight knot, 2022.

# APPENDIX: FURTHER DETAILS ON LINEAR OPERATORS OF CHAPTER 3

In this appendix we provide further details regarding the matrices  $R_m$  and  $S_m$  which are ultimately unnecessary to the argument for Theorem 1.3.1 in Chapter 3. That being said, the following analysis provides a more explicit picture of the behavior of the linear operators  $RT_r(C_{p,q})$ , and we feel it may be of use to someone studying Question 3.5.1 stated in Section 3.5. Here we use much of the notation introduced in Section 3.4, especially from Lemmas 3.4.7 and 3.4.8.

Let  $R_m$  be the matrix defined in Section 3.4, that is, the  $(m \times m)$ -matrix with columns corresponding to the vectors  $\{\tilde{f}_l|l=0,\ldots,m-1\}$ , and let  $S_m$  be the  $(m \times m+1)$ -matrix obtained by appending the vector  $\tilde{f}_m$  to  $R_m$ .

As we saw in Lemmas 3.4.7 and 3.4.8 and the proof of Lemma 3.4.5, col(m+1) of  $S_m$ , corresponding to  $\tilde{f}_m$ , either corresponds to  $col(l^*+1)$ , in which case it has a single nonzero entry, or it has exactly two nonzero entries. The following lemmas give an explicit characterization of this column.

**Lemma .0.6.** Suppose r = 2m + 1 is coprime to q and r > q + 6. Define

$$i_{\pm} := \begin{cases} \frac{q}{2} \pm 1 & \text{if } q \text{ is even} \\ m - \frac{q - 1 \mp 2}{2} & \text{if } q \text{ is odd.} \end{cases}$$
 (3)

Then rows  $row(i_{\pm})$  of  $R_m$  have exactly one nonzero entry and all other rows have exactly two nonzero entries. Furthermore, suppose these nonzero entries lie in  $col(l_{\pm})$  of  $R_m$ , respectively. Then  $l_- \neq l_+$  and for  $q \geq 8$ ,  $col(l_{\pm}) \neq col(l^* + 1)$ . Finally,  $col(l_-) = col(1)$  if and only if q = 4 and  $col(l_-) = col(l^* + 1)$  if and only if q = 6.

*Proof.* Assume r > q + 6. We first assume  $l^* < m$  and consider the cases where q is even and odd separately. Both cases make heavy use of the  $g_l^{\pm}$ ,  $h_l^{\pm}$  notation introduced in Lemma 3.4.9, arguing that there can be at most one solution to each equation in Lemma 3.4.9 Part (ii).

#### Case 1:

Suppose q is even. Let  $i_- = \frac{q}{2} - 1$  and  $i_+ = \frac{q}{2} + 1$ . Each case uses a nearly identical argument, so we will limit ourselves to Case (1). Here,

$$l_1 + l_2 = \frac{q + (k_1 + k_2)r - 2}{q} = 1 + \frac{(k_1 + k_2)r - 2}{q},$$

which is integral if and only if  $(k_1 + k_2)r - 2 = qn$  for some  $n \in \mathbb{Z}$ ,  $n \ge 0$ . Similarly,

$$l_1 - l_2 = \frac{(k_1 - k_2)r \mp 2}{q},$$

which is integral if and only if  $(k_1 - k_2)r \mp 2 = qn'$  for some  $n' \in \mathbb{Z}$ ,  $n' \geq 0$ . So

$$l_1 + l_2 = l_1 - l_2 + 2l_2 = n' + 1 + \frac{2k_2r - 2 \pm 2}{q}.$$

Taking the top sign, we have that

$$l_1 + l_2 = n' + 1 + \frac{2k_2r}{q},$$

which is integral if an only if  $2k_2 = qn''$  for some integral  $n'' \ge 0$ . However, n'' = 0 implies  $l_2 \notin \mathbb{Z}$ , so  $n'' \ge 1$ . This means  $l_1 + l_2 \ge 3 + r > 2m$ , which is a contradiction. For the bottom sign,  $l_1 + l_2 \in \mathbb{Z}$  if and only if  $2(k_2r - 2) = qn'''$  for some integral  $n''' \ge 0$ . However, n''' = 0 implies  $l_2 \notin \mathbb{Z}$ , so  $n''' \ge 1$ . Then

$$l_2 = 1 + \frac{1 + n'''}{2},$$

so n''' must be odd. Since  $k_1r + k_2r - 2 = qn$ , we have  $2k_1r = q(2n - n''')$  and thus  $k_1$  is some nontrivial multiple of  $\frac{q}{2}$ . This implies that  $l_1 > m - 1$ , which is a contradiction.

Cases (2) - (6) follow similarly. Thus  $row(i_{-})$  and  $row(i_{+})$  each have exactly one nonzero entry. Let  $l_{\pm}$  be the corresponding column index of the nonzero entry in  $row(i_{\pm})$ . If q > 6, row(1) and row(2) must each have two nonzero entries, so neither of  $col(l_{\pm})$  coincide with col(1) or  $col(l^* + 1)$ .

Now suppose that  $i_- = g_l^{\pm}$ . One checks that this implies that  $i_+ \notin \{g_l^{\pm}, g_l^{\mp}, h_l^{\pm}, h_l^{\mp}\}$ . Similarly, if  $i_- = h_l^{\pm}$ , this implies that  $i_+ \notin \{g_l^{\pm}, g_l^{\mp}, h_l^{\pm}, h_l^{\mp}\}$ . Thus  $l_- \neq l_+$ . Finally, note that q=4 if and only if  $i_-=1$  and  $i_+=3$ , and by Lemma 3.4.7 Part (ii),  $col(l_-)=col(1)$ . Similarly, q=6 if and only if  $i_-=2$  and  $i_+=4$ , and by uniqueness of  $l^*$  in Lemma 3.4.7 Part (ii) and since  $l_-\neq l_+$ ,  $col(l_-)=col(l^*+1)$ .

#### Case 2:

Suppose q is odd. Let  $i_{-} = m - \frac{q+1}{2}$  and  $i_{+} = m - \frac{q-3}{2}$ . Each case uses a nearly identical argument, so we will again limit ourselves to Case (1). Here

$$l_1 + l_2 = \frac{2m + 3 - q + (k_1 + k_2)r}{q} = \frac{(1 + k_1 + k_2)r + 2}{q} - 1,$$

which is integral if and only if  $(k_1 + k_2)r - 2 = qn$  for some  $n \in \mathbb{Z}$ ,  $n \ge 0$ . Similarly,

$$l_1 - l_2 = \frac{(k_1 - k_2)r \mp 2}{q},$$

which is integral if and only if  $(k_1 - k_2)r \mp 2 = qn'$  for some  $n' \in \mathbb{Z}$ ,  $n' \ge 0$ . So

$$l_1 + l_2 = l_1 - l_2 + 2l_2 = n' - 1 + \frac{(2k_2r + 1)r + 2 \pm 2}{q}.$$

Taking the bottom sign, we have that

$$l_1 + l_2 = n' + 1 + \frac{2k_2r}{q},$$

which is integral if an only if  $2k_2+1=qn''$  for some integral  $n''\geq 1$ . This means  $l_1+l_2>2m$ , which is a contradiction. For the top sign,  $l_1+l_2\in\mathbb{Z}$  if an only if  $(2k_2+1)r+4=qn'''$  for some integral  $n'''\geq 1$ . Then

$$l_2 = \frac{n''' - 1}{2},$$

so n''' must be odd. Since  $(1 + k_1 + k_2)r + 2 = qn$ , we have  $(1 + 2k_1)r = q(2n - n''')$  and thus  $1 + 2k_1$  is some nontrivial multiple of q. This implies that  $l_1 > m - 1$ , which is a contradiction.

Cases (2)-(6) follow similarly. Thus  $row(i_{-})$  and  $row(i_{+})$  each have exactly one nonzero entry. Let  $l_{\pm}$  be the corresponding column index of the nonzero entry in  $row(i_{\pm})$ . By the same argument as part (i),  $l_{-} \neq l_{+}$ . Finally, since  $m > \frac{q+5}{2}$ ,  $i_{-} > 2$ . By Lemma 3.4.7 part (ii), neither of  $col(l_{\pm})$  coincide with col(1) or  $col(l^{*}+1)$ .

Finally, we must address the case where  $l^* = m$ . We see in the argument of Lemma 3.4.5 that this case corresponds to when col(1) is the only column of  $R_m$  with exactly one nonzero entry. This means that, by Lemma 3.4.7,  $R_m$  has 2m-1 nonzero entries in total. However, since r > q+6 implies that there exists  $row(i_{\pm})$ , each with a single nonzero entry, and every other row has no more than two nonzero entries, there are at most 2m-2 nonzero entries in  $R_m$ , giving us a contradiction.

Lemma .0.6, along with Lemmas 3.4.7 and 3.4.8, imply the following.

Corollary .0.7. Suppose r = 2m + 1 is coprime to q and r > q + 6. Then there are exactly two nonzero entries in col(m + 1) of  $S_m$ . Moreover, they lie in rows  $row(i_{\pm})$ .

*Proof.* Since the first m columns of  $S_m$  are identical to  $R_m$ , and r > q + 6, col(m + 1) of  $S_m$  must have exactly two nonzero entries. Otherwise, we reach the same contradiction as the case  $l^* = m$  addressed in the argument of Lemma .0.6.

These nonzero entries must lie in rows  $row(i_{\pm})$ . This is because every other row of  $R_m$  has exactly two nonzero entries by Lemma .0.6 and, by Lemma 3.4.8 Part (i), none of these corresponding rows of  $S_m$  can have a third nonzero entry in col(m+1).

The proof of Theorem 1.3.1 utilized the inveritibity of  $RT_r(C_{p,q})$  established in Theorem 1.3.4, which in turn used the fact that  $R_m$  is a change of basis (see Proposition 3.4.2). It was important to the argument to present the matrix  $R_m^{-1}$  in order to bound its operator norm polynomially.

That being said, Lemma .0.6 and Corollary .0.7, in combination with Lemmas 3.4.7 and 3.4.8, provide a method for algorithmically verifying the nonsingularity of  $R_m$  directly using a procedure reminiscent of the argument of Lemma 3.4.5. We state an alternative proof of the first part of Proposition 3.4.2 for the interested reader, noting importantly that the following does not establish any sort of bound on the operator norm  $|||R_m^{-1}|||$ . The primary benefit of this argument is its explicit algorithmic verification of the nonsingularity of  $R_m$ , rather than the more abstract argument given in Subsection 3.4.2.

**Proposition .0.8.** Let r = 2m + 1 be coprime to q, and suppose r > q + 6. Then  $R_m$  is nonsingular.

*Proof.* It suffices to show that for  $m > \frac{q+5}{2}$ ,  $R_m$  is nonsingular, as  $R_m$  corresponds to the basis transformation  $\tilde{F}_m \to \{e_1, \ldots, e_m\}$ . To establish nonsingularity, we will show that  $det R_m \neq 0$ . Note that by Lemma 3.4.7 Part (ii), every nonzero entry of  $R_m$  is a root of unity.

Let  $R := R_m$ . Consider the following cofactor expansion procedures for computing det R. Here, we abuse notation slightly by referring to row/column indices of the original matrix R when expanding along rows of minors of R.

The following procedures depend on both the parity of m and on the value of  $q \mod 4$ . In particular, if  $q \equiv 0 \mod 4$ , then  $i_{\pm}$  are odd, and if  $q \equiv 2 \mod 4$ , then  $i_{\pm}$  are even. Analogously, if  $q \equiv 1 \mod 4$ , the  $i_{\pm}$  have the opposite parity than m, and if  $q \equiv 3 \mod 4$ , the  $i_{\pm}$  have the same parity as m. We consider each case separately.

Case:  $q \equiv 0 \mod 4$ :

- (1) Expand along  $row(i_{-})$  to obtain the  $R_{i_{-}}$ -minor.
- (2) Expand along  $row(i_{-}-2)$  to obtain the  $(R_{i_{-}})_{i_{-}-2}$ -minor. Continue iteratively by expanding along rows  $i_{-}-4, i_{-}-6, \ldots, 3, 1$ .
- (3) Expand iteratively along rows  $i_+, i_+ + 2, \dots, m-1$  if m is even and along rows  $i_+, i_+ + 2, \dots, m$  if m is odd.
- (4) Expand iteratively along rows  $m, m-2, \ldots, 4, 2$  if m is even and along rows  $m-1, m-3, \ldots, 4, 2$  if m is odd.

Case:  $q \equiv 1 \mod 4$ :

(1) Expand along  $row(i_{-})$  to obtain the  $R_{i_{-}}$ -minor.

- (2) Expand along  $row(i_{-}-2)$  to obtain the  $(R_{i_{-}})_{i_{-}-2}$ -minor. Continue iteratively by expanding along rows  $i_{-}-4, i_{-}-6, \ldots, 4, 2$  if m is odd and along rows  $i_{-}-4, i_{-}-6, \ldots, 3, 1$  if m is even.
- (3) Expand iteratively along rows  $i_+, i_+ + 2, \dots, m-1$
- (4) Expand iteratively along rows  $m, \ldots, 4, 2$  if m is even and along rows  $m, \ldots, 3, 1$  if m is odd.

Case:  $q \equiv 2 \mod 4$ :

- (1) Expand along  $row(i_{-})$  to obtain the  $R_{i_{-}}$ -minor.
- (2) Expand along  $row(i_{-}-2)$  to obtain the  $(R_{i_{-}})_{i_{-}-2}$ -minor. Continue iteratively by expanding along rows  $i_{-}-4, i_{-}-6, \ldots, 4, 2$ .
- (3) Expand iteratively along rows  $i_+, i_+ + 2, ..., m$  if m is even and along rows  $i_+, i_+ + 2, ..., m 1$  if m is odd.
- (4) Expand iteratively along rows  $m-1, m-3, \ldots, 3, 1$  if m is even and along rows  $m-2, m-4, \ldots, 3, 1$  if m is odd.

Case:  $q \equiv 3 \mod 4$ :

- (1) Expand along  $row(i_{-})$  to obtain the  $R_{i_{-}}$ -minor.
- (2) Expand along  $row(i_{-}-2)$  to obtain the  $(R_{i_{-}})_{i_{-}-2}$ -minor. Continue iteratively by expanding along rows  $i_{-}-4, i_{-}-6, \ldots, 3, 1$  if m is odd and along rows  $i_{-}-4, i_{-}-6, \ldots, 4, 2$  if m is even.
- (3) Expand iteratively along rows  $i_+, i_+ + 2, \dots, m$
- (4) Expand iteratively along rows  $m-1,\ldots,4,2$  if m is odd and along rows  $m-1,\ldots,3,1$  if m is even.

We argue that each row expansion in these procedures contributes a single nonzero factor to the total determinant of R. We include the argument for  $q \equiv 0 \mod 4$ . The other three cases are analogous.

Indeed, Lemma .0.6 implies that Step (1) contributes a nonzero factor to detR and subsequently, the clearing of  $row(i_{-})$  and  $col(l_{-})$  clears one of the two nonzero entries in  $row(i_{-}-2)$ . By Lemma .0.6,  $row(i_{-}-2)$  is now one of two rows with a single nonzero entry. By the same argument, each iteration of Step (2) contributes a nonzero factor to the determinant and clears one of the two nonzero entries two rows up. Since  $i_{-}$  is odd, all rows cleared have odd index in R, and Step (2) terminates when we expand along row(1).

In a similar way, Lemma .0.6 and Lemma 3.4.8 Part (ii) imply that each iteration in Step (3) contributes a nonzero factor to the determinant and terminates at row(m-1) if m is even and row(m) if m is odd. All odd-index rows of R have been cleared in Steps (1) - (3), and Lemma 3.4.8 Part (ii) implies that Step (4) iterates across every even-index row of R. Each iteration of Step (4) contributes a nonzero factor to the determinant and clears one of the two nonzero entries two rows up. Step (4) terminates when we expand along the unique row (corresponding to row(2) of R) in the  $(1 \times 1)$ -minor  $[D_{l^*}]$ , due to Lemma 3.4.7 Part (ii).

Thus  $R = R_m$  has nonzero determinant, hence nonsingular.